Oil - Water Flushing of Pipelines

Performing and analysing experiments on a 1:12 diameter scale, to study flushing dynamics and to increase future flushing efficiency

V.C. Klaassens

Delft University of Technology

TNO

Master Thesis

Oil - Water Flushing of Pipelines

Performing and analysing experiments on a 1:12 diameter scale, to study flushing dynamics and to increase future flushing efficiency

V.C. Klaassens (4098811)

Track: Energy, Flow & Process Technology

Supervisor: dr.ir. A.T. van Nimwegen (TNO)

Professor: prof.dr.ir. R.A.W.M. Henkes (TU Delft)

February 2022

Abstract

Due to the energy transition an increasing number of oil pipelines will be decommissioned in the foreseeable future. As a part of the decommissioning process, the oil needs to be flushed from the pipelines. Some models to predict the required water velocity to flush oil from pipelines are available, but these are limited in accuracy, and data to validate these models is lacking. The aim of this MSc research project is to gain a better understanding of the oil flushing process in pipelines using water, and to provide validation data for the existing models. Thereto lab experiments were carried out in the flow loop of TNO in Rijswijk. The length of the measurement section is 5.65 meter, the diameter is 56 mm.

The experiments are performed by filling the experimental pipe section with oil and subsequently flushing it using four pipe volumes of water. The first set of experiments, for a pipe inclination of 0° to -5°, was performed with superficial flushing velocities ranging from 0.05 m/s to 1.5 m/s, for two different types of oil. Data were collected using a mass flow meter system and a video capturing system. These data were subsequently analysed using the software tool MATLAB. The first set of experiments was also modelled in the multi-phase flow modelling tool OLGA. A second set of experiments was performed to find the transition point between stratified and mixed flow, which is relevant for the flushing efficiency, by varying the inclination in a range of 0° to -90° relative to the horizontal plane, using a superficial water velocity of 0.1 m/s. In addition to the mass flow measurements, data were collected with a video system during all sets of experiments, and subsequently processed to determine the phase distribution throughout the pipe during, and after the flushing process.

It was established that the flushing efficiency is proportional to the superficial water velocity. For both types of oil, for inclinations between 0° and -5°, a superficial water velocity of 0.35 m/s suffices to flush all oil when flushing four pipe volumes of water. For all considered inclinations and pipe geometries for and both oil types, the bulk($\geq$ 95%) of the oil is removed from the pipe for a flushing velocity of 0.25 m/s. In a horizontal orientation, the lighter and less viscous Fuchs Renolin DTA7 oil is flushed more efficiently from the pipe compared to the Mobil Velocite No.10 oil. This effect diminishes for downward inclined orientations and is reversed for an inclination of -5°.

In OLGA it is possible to easily vary for example the geometry of the pipeline and show the effect on the two-phase flow. Discrepancies were shown however when the flow was evaluated around the 0° inclination angle. Small deviations from this angle of inclination gave significantly different results.

For the 0° to 90° range of inclination, and a superficial velocity of 0.1 m/s, the transition zone between stratified and mixed flow was established to be in a range of 7.5° to 20° relative to the horizontal plane. Either decreasing or increasing the inclination angle from this point is beneficial to the flushing process.

Apart from the increased understanding of the flushing process summarised in the preceding paragraphs, the data collected on the flushing process under various sets of conditions can be used to validate models for predicting oil flushing processes.

Acknowledgements

Before starting off this report, I would like to express my gratitude to the people who have supported me these last 10 months conducting this research into "Oil-Water Flushing". It was nice to see in practice some of the many theories from the books that have to be worked through for the study of mechanical engineering.

First and foremost, I wish to thank my supervisors dr.ir. A.T. van Nimwegen (TNO) and Prof.dr.ir. R.A.W.M. Henkes (TU Delft) for their invaluable support and suggestions on this research. Through every progress meeting I gained more insights and direction, it was instructive and challenging to discuss the matters at hand, even when many of these meetings were online. Furthermore, your prompt support on short notice was always highly appreciated!

I'd like to thank the colleagues at TNO for providing an insight into the interesting research that is done at TNO, in so many fields of engineering. Although the total amount of hours in office was limited due to the pandemic, it certainly inspired me to be in an environment with so many bright people. Thank you Hajo Pereboom for the overall support during the project, and for asking critical questions to make sure every experiment would bring the most and most worthwhile data. I also owe the photo on the cover of this report to you. Thank you, Stefan Belfroid for your instructions with OLGA, but above all by challenging me to think deeper about the drivers behind the problems I was trying to answer.

My gratitude is also due to TU Delft PhD candidate Qi An for assisting me in performing measurements, even while you were busy with your own research.

I also would like to mention the wonderful people in the TNO lab in Rijswijk. Engineering without application would be missing the mark, and the people connecting the two are invaluable. Thanks for helping me with the setup, but also for making me smile throughout the process.

Last, but certainly not least, I want to mention the people who have been there for me in the background, supporting me through the whole process. Working from home certainly was challenging and would have been difficult without my awesome roommates.

Special thanks and appreciation to my girlfriend and family, who have been there for me providing encouragement, company, and the welcome distraction!

Vincent Klaassens
Delft, February 2022

Contents

Nomenclature

α	Holdup ratio	[−]
$\dot{m}$	Mass flow rate	[kg/s]
μ	Dynamic viscosity	[kg/(m · s]
ϕ	Angle of inclination	[]
ρ	Density	[kg/m^3]
υ	Kinematic viscosity	[cST]
A	Area	[m^2]
D	Diameter	[m]
Fr	Froude number	[−]
g	Gravitational constant	[9 81m/s^2]
H	Height	[m]
Q	Volumetric flow rate	[m^3/s]
r	Radius	[m]
S	Slip ratio	[−]
T	Temperature	[°C]
U	Velocity	[m/s]
U_{B}	Benjamin bubble velocity	[m/s]
U_{E}	Effective bubble velocity	[m/s]
U_{S}	Superficial velocity	[m/s]
U_{T}	Taylor bubble velocity	[m/s]
V	Volume	[L]
VI	Viscosity index	[−]

1 | Introduction

Relevance of this Research

Anyone who opens the news is confronted with items about climate change, especially after the recent developments at the 2021 United Nations Climate Change Conference in Glasgow. NGO's and governments are pushing more and more for a greener future, one in which fossil fuels will have a smaller global footprint. In the report "Net zero by 2050", the International Energy Agency calls for new investments in oil to be discontinued[1], which means quite a shift in policy compared to previous years.

These trends have as a consequence that in the foreseeable future an increasing number of oil pipelines will have to be decommissioned as they will no longer be used. In order to properly decommission these pipelines they need to be purged of their contents. Some simulation models exist, but they are limited in detail and lack thorough validation. Continued research is needed to make the process efficient.

Current Approach to Pipeline Flushing

The current way to remove the contents from oil and gas pipelines is to flush them with seawater. This is fed into the pipelines at high flow rates and high volume levels to ensure that no residual oil remains. However, reliable data on the quantity of water actually needed and the required flow rate for each specific situation are limited. This leads to inefficiencies in the cleaning process, with much excess water that needs to be treated afterwards, while high-power pumps are needed to perform the rinse. Clean-up of pipelines remains paramount, since leaving residual oil in the pipelines would create an environmental risk.

Organising the Project

The Dutch Organisation for Applied Scientific Research, TNO, has constructed an experimental facility to study the flushing of oil from pipelines. Experiments on an approximately 1:12 diameter scale, relative to typical subsea oil pipelines, were carried out and subsequently analysed to better understand the flushing dynamics. This thesis delves deeper into this subject, providing additional experimental data using an oil with different properties, as well as modelling the experiments and comparing the experimental and modelling data sets. Furthermore, novel experiments were carried out to investigate the flushing efficiency for pipe angles ranging from 0° to 90°. The study findings and data are intended to make the flushing process more efficient, both in terms of time and costs.

Timeline

This research project on oil pipeline cleaning is part of a larger investigation. The experimental setup was built up and experiments with a first oil were conducted in Phase I, which spanned from the end of 2020 until the spring of 2021. Phase II and III are described in this thesis.

Phase II was carried out in the summer of 2021. Experiments were carried out by the author as an introduction to the experimental setup and the project as a whole. This was done under the supervision of dr.ir. A.T. van Nimwegen who analysed this set of data. The oil used in Phase II was Renolin DTA7 produced by Fuchs.

Phase III of the flushing project lasted from fall 2021 to late winter 2022. The data gathering and subsequent analysis from this phase is part of this thesis. The experiments in Phase III were carried out with Mobil's Velocite No. 10 oil, which is more dense and more viscous than the oil used in Phase II.

Application Field

Figure 1.1 gives an example of a typical subsea pipeline network. The majority of the pipelines lie on the bottom of the sea and follow the contours of the seabed. Inclinations are generally mild, with sporadic bends and the occasional connection with more complex geometries. In normal operations, the oil enters the pipeline from the well at temperatures of around 100 °C, which is significantly higher than the temperature at the seafloor. The temperatures of the seafloor in the North Sea, for example, vary between 4 °C and 15 °C, depending on the season and the measured depth[2]. As this temperature shift has a large influences on parameters like the viscosity, the variation of the viscosity will be of particular interest in this study.

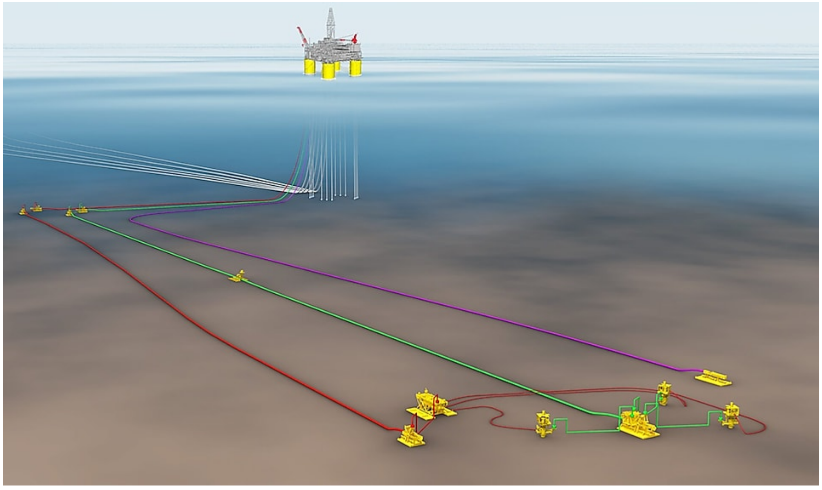

Figure 1.1: Example of subsea pipeline infrastructures[3].

Project Goal and Scope

Several sets of oil pipeline cleaning experiments have been carried out in the past. Questions originating from these earlier experiments, along with questions raised by operators in the industry have been incorporated into the project's scope:

- During flushing operations: What is the distribution of oil and water along the pipeline as a function of time and space?
- How long would it take to remove the oil from the pipeline, and how much water is used in the flushing process?
- In a range of angles of inclination between 0° and 90° relative to the horizontal plane, where does the transition point between stratified and dispersed flow lie?
- What is the influence of a variation in inclination, superficial water velocity and different types of oil on the efficiency of the flushing process? The flushing efficiency is determined by the ratio between the volume of oil that remains after flushing divided by the volume of oil that was originally in the pipe.
- How do experimental results collected from the physical setup compare to modelling results using the multiphase modelling tool OLGA?

Structure of this Report

Chapter 2 contains a brief summary of the literature research that was performed prior to performing the experiments. Chapter 3 gives an introduction to the experimental setup, including the three separate data acquisition and modelling systems. The methods used to conduct the experiments and analyse the data are also detailed in this chapter. Chapter 4 and 5 present the results of the experimental work and the modelling data, respectively. Interpretation of these results is also given in these chapters. Chapter 6 takes a more casual approach addressing interesting results and setup features, as well as the questions raised in the project goal and scope. Conclusions and recommendations for future research are described in chapter 7.

2 | Literature Summary and Background Information

This chapter contains a concise version of the literature research that was performed before the work on the experimental setup commenced. The purpose of this chapter is to give a short description of some basic definitions on two phase flow, shortly introduce some well known classical experiments, after which it ends with findings by earlier studies on the subject of flushing and general two phase oil-water flow.

2.1 Definitions Regarding Two Phase Flows

Flows are often specified as a mass flow rate $\dot{m}$, a volumetric flow rate, or even as a molar flow rate. The volumetric flow rate Q_w is equal to the mass flow rate $\dot{m}_w$ divided by the density ρ_w:

$$Q_w = \frac{\dot{m}_w}{\rho_w} \tag{2.1}$$

Superficial flow velocity

The superficial flow velocity is a term that is used extensively in this report, as it is very useful to determine the velocity of a fluid in a multiphase flow system.

The superficial velocity of a fluid is the hypothetical velocity of the fluid, when it would be the only fluid present in a pipe. Other phases or particles present in the pipe are disregarded. In the case of a multiphase flow system, the velocity of the fluid is not the same as the superficial flow velocity, as other phases are present.

In the case of oil-water flushing, the superficial water velocity is very useful as it describes the flow of water through the system when the flow of the other phase, the oil, is not always known. The actual velocity of each of the phases is hard to find as it varies from place to place and from time to time. The formula for the superficial velocity for water(U_{Sw}) and oil(U_{So}) can be seen in equation 2.2 and 2.3, where A is the surface area of a cross section of the pipe.

$$U_{Sw} = \frac{Q_w}{A} = \frac{\dot{m}_w}{\rho_w \cdot A} \tag{2.2}$$

$$U_{So} = \frac{Q_o}{A} = \frac{\dot{m}_o}{\rho_o \cdot A} \tag{2.3}$$

Holdup

One of the most important parameters to design and operate oil-water flow systems is the holdup. In multiphase flow, each fluid moves at a different speed due to different densities and viscosities, with the heavier phase moving slower, or being more held up, than the lighter phase. Holdup is defined as the ratio of the domain occupied by water or oil to the total domain occupied by the multi-phase flow mixture.

The holdup is a key dimensionless quantity for determining numerous other important parameters like the density and viscosity of mixtures and the relative averaged velocity of each phase. Moreover, after predicting the holdup from the expected flow rates, the holdup is very important for predicting flow pattern transitions, heat transfer, pressure drop and corrosion rates in oil–water flow. In general, in multiphase flows, each phase flows at a different velocity. As a result, the in-situ volume fraction (holdup) of each phase is different from its input fraction.

Based on the previous experimental studies, the holdup behaviours are strongly affected by oil–water flow patterns and inclination angle of the pipes.(see for example Mukherjeeet al.(1981)[4] and Vigneaux et al.(1988)[5])

Shown in equations 2.4 and 2.5 are the holdup fractions for a two-phase flow of water α_w and oil α_o. The sum of the holdup of all the fluids combined equals one. A_w and A_o represent the area in a cross section that the water and oil take up respectively.

$$\alpha_w = \frac{A_w}{A} \tag{2.4}$$

$$\alpha_o = \frac{A_o}{A} \tag{2.5}$$

In positively inclined sections where gravity plays a large role, generally the holdup becomes larger than the quality for the heavier phase. This will be reversed in sections where there is a decline.

Slip Ratio
The slip ratio is a ratio that indicates whether the phases are moving at different velocities relative to each other. When the slip ratio is equal to one, the phases are flowing at the same velocity. A value less than one means that the phase in the denominator is flowing faster. A slip ratio greater than one says that the phase which is represented in the nominator is flowing faster. The equation for the slip ratio can be found in equation 2.6.

$$S = \frac{U_{\mathrm{w}}}{U_{\mathrm{o}}} = \frac{A_{\mathrm{o}}}{A_{\mathrm{w}}} \cdot \frac{U_{\mathrm{sw}}}{U_{\mathrm{so}}} \tag{2.6}$$

Viscosity
Viscosity is the internal resistance to deformation in a fluid and is one of the governing properties of a fluid. Viscosity corresponds to the "thickness" of a fluid, where for example honey has a higher viscosity than water, and is therefore more "thick". Viscosity quantifies the internal frictional force between adjacent layers of fluid in relative motion. An example is fluid flow through a tube, where in a viscous fluid the flow will have a higher flow velocity in the middle of the tube because of the shear stress with the tube wall.

In general fluid viscosity is divided into two main categories: dynamic viscosity and kinematic viscosity.

Dynamic viscosity ($Pa \cdot s$) is directly proportional to the shear stress in the fluid. The kinematic viscosity (υ), shown in equation 2.7, is equal to the dynamic viscosity divided by the mass density of the fluid.

$$\upsilon = \frac{\mu}{\rho} \tag{2.7}$$

Viscosity is sometimes noted in centiPoise, being 1/100 Poise. Poise relates to Pascal seconds in the following way: $1cP = 0.01P = 0.001Pa \cdot s = 1mPa \cdot s$. Water with a temperature of 20 °C has a viscosity of 1 cP. The kinematic viscosity seen in equation 2.7 is equal to the dynamic viscosity divided by the density of the fluid and has a dimension of $\frac{(length)^2}{time}$, where the dynamic viscosity has a dimension of $\frac{force \cdot time}{area}$.

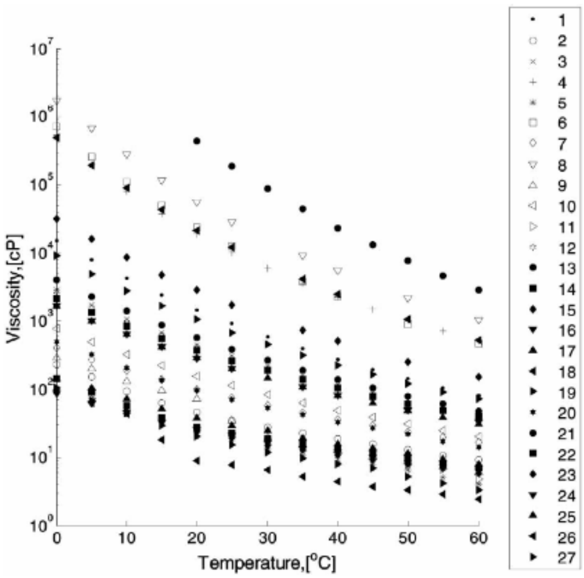

Figure 2.1: Effect of temperature on viscosity of 27 crude oil samples[6].

As can be seen in figure 2.1, the viscosity can increase by an order of magnitude when decreasing the temperature by a few tenths of degrees. When performing experiments, and when determining the viscosity, the temperature should be taken into account.

2.2 Classical Experiments - Taylor and Benjamin Bubbles

2.2.1 Taylor Bubbles

Sir Geoffrey Ingram Taylor was a British physicist and mathematician, and a major figure in fluid dynamics and wave theory. He is the figurative father of many theorems and experiments, of which two well applicable to the field of oil-water flushing, are displayed in the coming section.

In his well known paper from 1950, Taylor discusses the shape of small air bubbles rising in a fluid, and studies the rise velocity of these bubbles. The second part of the paper deals with the rise velocity of bubbles confined in a vertically oriented cylinder.[7]

During experiments photographs were taken of the rising bubbles. These bubbles showed that a large part of the top part of the bubbles is always spherical in shape. Theoretical research confirmed this, but looking into the rise velocity, something noteworthy was found. The experiments agree better with the arbitrary assumption that flow over the forward part of the bubble is the same as that calculated for a sphere moving in a frictionless liquid, than with calculations based on the pressure distribution measured over the surface of a solid of nearly the same shape as the bubble. It can be noted, however, that the flow of the liquid near the front of a bubble is expected to be more like a truly irrotational one than the liquid flow near a solid body, because in the latter case a boundary layer would necessarily be present, whereas in the former case the air in the bubble would cause no appreciable drag.

$$U = \frac{2}{3}\sqrt{g \cdot r} \tag{2.8}$$

The closeness with which the observed points fit the line of the equation 2.8 is remarkable, where U is the rise velocity, g is the gravitational acceleration and R is the radius of curvature of the bubble. The experimental points show almost no scatter proving a constant rise velocity. This suggests that the flow near the front of a bubble must be very close to the theoretical flow near the front of a complete sphere in an inviscid fluid indeed.

It was observed that large bubbles in water assume a form which is very near to the lenticular(lens shaped) volume contained between a sphere and a horizontal plane cutting it above its centre. The pressure distribution over the spherical surface was found experimentally to be approximately the same as that calculated for a complete sphere moving in an ideal fluid. This pressure, together with the hydrostatic pressure due to gravity, leads to a uniform surface pressure when the velocity of rise, U, is like the one shown in equation 2.8.

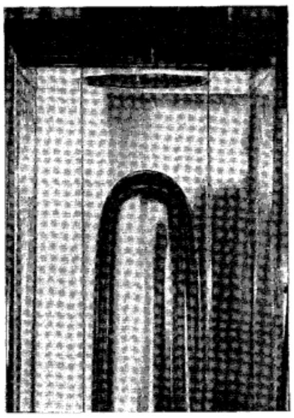

Figure 2.2: Taylor bubble from the original experiments[7].

It is not possible to accurately define the shape of the wake of this bubble. However, when considering a tube that is being emptied from the bottom, this wake is not present, because the lower end of the bubble does not have a surface. The tube is just open to the atmosphere at its lower end, so it is possible to solve this problem. A picture of the actual experiment is shown in figure 2.2. A rough approximate calculation for the rise velocity of the bubble in an emptying cylinder then becomes equal to equation 2.9, where g is again the gravitational acceleration and r is the radius of the tube. This equation fits well with the experimental data where a factor of 0.466 to 0.49 was found which is remarkably close to the rough theory leading to a value of 0.464. Even before Taylor, Dumitrescu also found an analytical way to solve this problem, obtaining the expression given in 2.10 for the dimensionless bubble velocity.

$$U = 0.464\sqrt{g \cdot r} \tag{2.9}$$

$$Fr = \frac{U}{\sqrt{gD}} = 0.352 \tag{2.10}$$

2.2.2 Gravity Currents and the Benjamin Bubble

A classical experiment for horizontal flow, which is quite similar to the Taylor bubble for vertical flow, is the Benjamin bubble experiment. In 1967 Benjamin published a study on the properties of steady gravity currents and simple extensions of it like the classical theory about hydraulic jumps.[8] The first three parts of his paper are of most interest for the present study and will be elaborated upon. A gravity current consists of a wedge of heavy fluid (e.g. salt water, cold air) intruding into an expanse of lighter fluid. If the effects of viscosity and mixing of fluids at the interface are ignored, the hydrodynamical problem is formally the same as that for a cavity(bubble) advancing along the upper boundary of a liquid, which is now known as a Benjamin bubble.

Von Karman used Bernoulli's theorem to derive that the propagation velocity of a gravity current can be written as equation 2.11, where g is the gravitational acceleration and H is the asymptotic height of the interface above the bottom.

$$U^2 = 2 \cdot g \cdot H \cdot \frac{\rho_1 - \rho_2}{\rho_2} \tag{2.11}$$

To derive the equation for the Benjamin bubble, it should be considered that the flow up to the forward stagnation point is hardly disturbed by the breaking process which, as experimental observation shows, generates intensive turbulence only on the rearward side of the head wave. Hence the pressure in the cavity, relative to the pressure on the horizontal boundary far upstream is given by $p_c = \frac{1}{2} \cdot \rho \cdot U^2$. When a path is considered that is started at the boundary far upstream and finally reaches the free surface through the wake region where the flow is almost parallel, the pressure variation is simply hydrostatic. This means that the pressure in the cavity is $\rho \cdot g \cdot H$, corresponding to the net fall H between the starting and end points. Then, equating the two expressions for the pressure in the cave, equation 2.12 is obtained, which is equivalent to the result that Von Karman has found.

In the second part of the 1967 paper by Benjamin the flow-force balance is set up and the possible states of steady flow between horizontal boundaries are examined under the assumption that the interface becomes horizontal far downstream. In the absence of dissipation only one flow is possible, where the asymptotic level of the interface is halfway the plane boundaries.

$$U = \sqrt{2 \cdot g \cdot H} \tag{2.12}$$

In part three of Benjamin's paper the flow in a circular cross section pipe is shown and also the agreement between theory and experiments is presented. A very important equation that is derived is the one for the propagation velocity of the advancing air-filled cavity formed when liquid flows freely out from one end of a horizontal tube, as described in equation 2.13. The cross-section of the tube is taken to be circular, with radius R, and the flow is assumed to be uniform far upstream and far downstream.

$$U = 0.767 \cdot \sqrt{g \cdot R} \tag{2.13}$$

Figure 2.3: Benjamin bubble[8].

Figure 2.3 shows the structure of the Benjamin bubble. Benjamin first derived the dimensionless bubble velocity, or the Froude number, in a 2D channel, as defined in equation 2.14. Here U is the bubble velocity, g the gravitational acceleration and H the channel height. For a 3D pipe the equation turns into equation 2.15, where D is the pipe diameter. Both these equations were confirmed by experimental results by Benjamin.

$$Fr = \frac{U}{\sqrt{gH}} = 0.5 \tag{2.14}$$

$$Fr = \frac{U}{\sqrt{gD}} = 0.542 \tag{2.15}$$

2.2.3 Relating the Benjamin and Taylor Bubbles to Flushing

The classical experiments as described in the previous section deal with systems of two fluids which are immiscible and most importantly, have different densities. This is very similar to fluid-fluid displacement in the case of oil evacuation in pipelines. Because oil and water are immiscible there is a finite interfacial tension between the two phases, which is the reason why mixing on a molecular level will not take place. To be able to predict how the flow would develop for a certain flow rate, first the initial static case is examined. I.e. determining the bubble velocity when one fluid is propagating along the other fluid.

In this case the effective bubble velocity, seen in equation 2.18, is calculated[9] by using the Taylor bubble velocity, seen in equation 2.16, and combining this with the Benjamin bubble velocity, which is shown in equation 2.17. Using the Taylor bubble, which represents a pipe that is placed vertically, and the Benjamin bubble, which represents a tube that is oriented horizontally, the effective bubble velocity is obtained by combining the two with the orientation of the pipe. The inclination of the pipe is brought into the equation by multiplying the Taylor bubble velocity and the Benjamin bubble velocity using the sine and cosine of the inclination ϕ, respectively.

$$U_{\mathrm{T}} = 0.496 \cdot \sqrt{\frac{\rho_{\mathrm{w}} - \rho_{\mathrm{o}}}{\rho_{\mathrm{w}}} \cdot g \cdot R} \tag{2.16}$$

$$U_{\mathrm{B}} = 0.767 \cdot \sqrt{\frac{\rho_{\mathrm{w}} - \rho_{\mathrm{o}}}{\rho_{\mathrm{w}}} \cdot g \cdot R} \tag{2.17}$$

$$U_{\mathrm{E}} = U_{\mathrm{T}} \cdot sin(\phi) + U_{\mathrm{B}} \cdot cos(\phi) \tag{2.18}$$

The effective bubble velocity in equation 2.18 only holds for the case in which the two phases do not mix. In the practice of oil-water flushing, this is not always the case however. In relation to flushing, the effective bubble velocity is the velocity that the water flow rate needs to achieve to overcome the oil bubble velocity in order to flush the oil out. To ensure that no oil is trapped in the system the water flow velocity should be sufficiently high, taking into consideration the inclination of each section of pipe. For upward inclined flow all oil is flushed directly from the system for all flow velocities because of the density difference, where the oil phase just floats on the water phase.

2.3 Literature Regarding Flushing and other Two-Phase Flows

2.3.1 Effect of Geometry and Velocity on Flushing

The geometry and orientation of the setup significantly affect he effective bubble velocity, as can already be seen in the equation of the effective bubble velocity (equation 2.18),

Kazemihatami(2013)[10] performed experiments to determine the required superficial liquid velocity of the water to flush oil from different pipe geometries. The geometries consisted of a straight pipe, horizontal and slightly inclined, and an M-shaped jumper pipe. The conclusion was that the minimum velocity to remove the oil from a horizontally oriented tube was 0.384 m/s, as well as for the special M-shaped jumper. This is an interesting result because the M-shaped jumper contains downward vertical sections. Using the effective bubble velocity theory, the minimally required velocity is higher in vertically downward oriented pipes relative to horizontally oriented pipes.

The conclusions from Phase I of the TNO flushing study also does not agree with the conclusion made by Kazemihatami. As equation 2.18 predicts, TNO found that flushing in horizontal pipes is more effective compared to downward inclinations. This is because at low flow rates the water can flow underneath the oil in such a way that a fixed amount of oil can remain in the pipe. When looking at more complex geometries, such as U- and V-shaped geometries, the oil and water flow will mix, with the result that more oil is removed than in slightly downward inclined sections. The small bubbles that are created have a lower terminal velocity than the value calculated with the effective bubble velocity 2.18, which makes these bubbles easier to flush.

Although using slightly different parameters than in the study by TNO, the study by Folde (2017)[11] gave similar results. Folde found that a water velocity of 0.3113 m/s was required to displace 98.6% of the oil after flushing 2.2 pipe volumes of water for a horizontal orientation. These researchers also investigated the reverse of this experiment, by using oil to displace water. In this case a higher velocity was needed, 0.4222 m/s of oil for a displacement of 98.0% of water after 2 volumes displaced.

All considered studies agree that increasing the water flow velocity is beneficial to the flushing process.

2.3.2 Effect of Density, Viscosity and Interfacial Tension on Oil-Water Flushing

Although the effects of other parameters like the density, viscosity and surface tension are generally lower than the flushing velocity, these other parameters also influence the flushing process.

Folde (2017)[11] concluded that a density ratio, between the oil and water, closer to 1, is beneficial to the flushing process. In other words, an oil with a density of 900 kg/m^3 flushes more easily than an oil with a density of 800 kg/m^3. This is in agreement with the theory of the effective bubble velocity, as seen in equation 2.18.

A sensitivity analysis on the viscosity was also performed in the same study using the dynamic pipeline simulation tool Ledaflow. A result from this analysis was that the viscosity does not significantly affect the flushing process, unless the viscosity of the displacing fluid is significantly increased. Only when increasing the oil viscosity 50 times an increase in the displacement efficiency of 5 % was seen. The Ledaflow simulation was generally in agreement with performed experiments in the same study.

The interfacial tension between the oil and water was also examined in the sensitivity analysis with Ledaflow by Folde (2017)[11]. An increase in interfacial tension led to a reduction in the displacement efficiency, and hence reducing the surface tension increases the flushing efficiency. This suggests that if one is able to reduce the interfacial tension between the liquids, a more successful fluid removal will be obtained. This is similar to what would be expected when adding soap to an oily solution. The soap lowers the interfacial surface tension, allowing droplets to become smaller, which are more easily flushed.

A last conclusion for the specific case of oil-water flushing by Folde (2017)[11] is that the presence of gas is detrimental to the flushing process.

2.3.3 Effect of Density, Viscosity and Surface Tension on General Oil-Water Flow

Although experiments on general oil-water flow do not always apply to flushing processes, some useful conclusions can be made from these studies.

Amundsen (2011)[12] performed experiments on two phase oil water flow in pipes with an inclination of -10°to +10°, in which he found that both the velocity and the inclination have a large effect on the flow profiles in the pipeline. In his experiments, the flow velocity had a larger effect on the turbulence profiles than the inclination. Another effect found by Amundsen is that in the case of two phase oil-water flow with constant liquid volumetric flow rate, the larger the water cut(∼50%), the larger the effect of pipe inclination on the velocity and turbulence profiles, compared to a water cut of ∼25%, which is probably because of the higher average density. Also, the larger the water cut(∼50%), the larger the effect of pipe inclination on the velocity and turbulence profiles.

This significant effect of the velocity and the density ratio of the fluids on the flushing found by Amundsen (2011) can be linked to Achmed et al.(2018)[13] where it was found that a fluid with a higher momentum entrains a fluid with a lower momentum more effectively.

Kroes et al.(2013)[14] examined the effect of the salinity of water in two phase flow with oil. The mixture of high salinity water and oil showed more separation than that of low salinity water and oil, and thus has a negative effect on flushing. The higher the salinity of the water, the more pronounced this effect becomes. The higher the salinity, the stronger the effects of gravity compared to the inertial forces, hampering the flushing process. For higher velocities, the inertial forces become more dominant and the buoyancy forces have a smaller effect. This outcome is interesting in the case of oil-water flushing, because flushing experiments are often done with fresh water, whereas the actual flushing of oil pipelines is done with saline sea water.

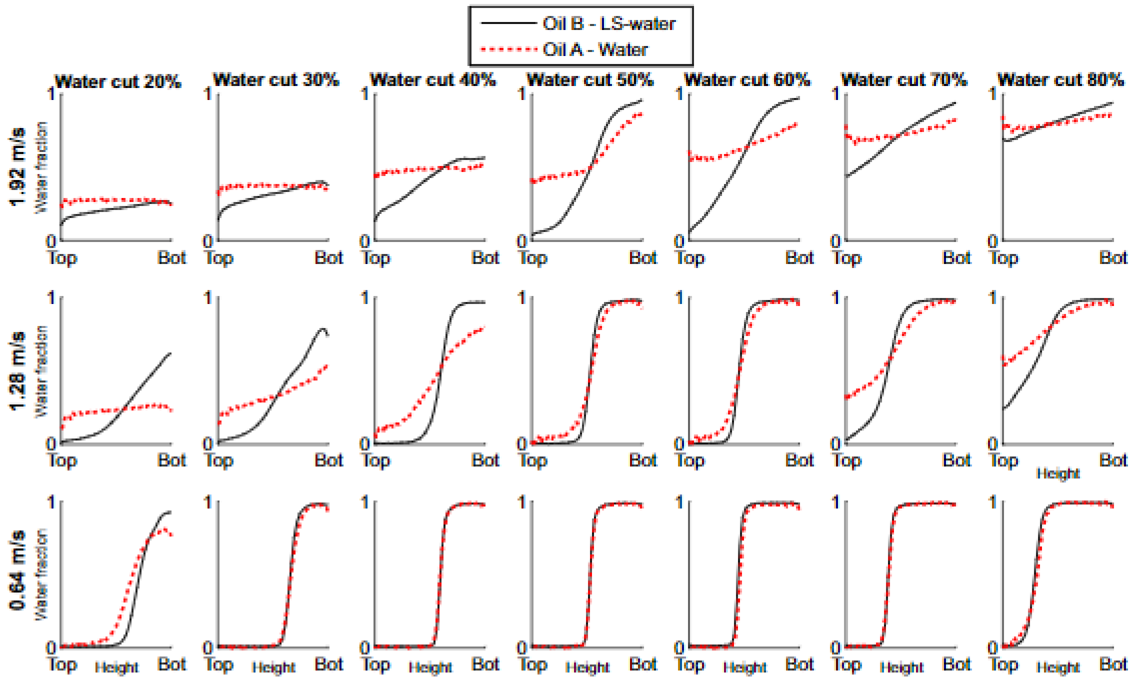

Figure 2.4: Comparison between the concentration distributions of high viscous oil A - low salinity water and low viscous oil B - water along a vertical transverse through the pipe[14].

Kroes et al.(2013)[14] also performed experiments in which they studied the effect of different viscosity of the oil on oil-water flows. A comparison between the concentration distributions for two different oils can be seen in figure 2.4. According to Kroes et al.(2013), higher oil viscosities make turbulent dispersive forces more prominent causing less separation to occur. This corresponds with their observations in experiments: the differences in the amount of dispersion of the two phases between experiments with different flow rates are most significant in the high velocity experiments, for which the dispersive forces are most prominent. This would suggest that in the case of the oil-water flushing, an oil with a higher viscosity would flush more effectively since separation generally does not work in favour of the flushing process.

A remark that is also made by Kroes et al.(2013)[14] is that the choice for a substitute oil to be used in experiments instead of crude oil should be made very carefully. The density, viscosity and surface tension of the substitute oil should match crude oil as much as possible, since otherwise the experiments will give non-representative results[14].

2.4 Measurement Techniques

Determining the flow conditions and properties of the flow in specific locations in the pipe can be cumbersome. This section is a summary of the different types of measurement techniques used in previous research, followed by the techniques that have been used in the study found later in this report.

The problem of determining the holdup in the pipe can be approached in different ways. An example of an approach applied in previous studies is employing the difference in electrical conductivity between oil and water. This can be done using conductivity probes like Kazemihatami (2013)[10] and Folde (2017)[11] did. Electrodes are placed around the pipe containing the oil and water flow and the average conductance of the contents of the tube is measured. The advantage of placing the electrodes this way is that they do not interfere with the flow in the pipe. Calibration is performed beforehand by filling a small section of the pipe with known quantities of oil and water, and measuring the resulting conductance. This test is performed with the liquids being stationary, which is obviously not the case during an experiment. This makes calibration troublesome while still not giving very accurate results. Another method is using X- or Gamma rays. Amundsen (2011)[12], Kroes et al.(2013)[14] and Rodriguez et al.(2006)[15] used these techniques for determining the holdup in the pipe. This technique is much more accurate than using electrodes around the pipe, but the capital costs make employing this technique harder.

Photo cameras have also been used to study the flow. Going back to the classical experiments of Taylor and Benjamin, cameras in combination with a chequered background were used to look at the flow and its development over time. In the study of Ibarra et al.(2018) the dynamics of liquid-liquid flows were studied using two-line planar laser-induced fluorescence and particle velocimetry. This technique proved to be very useful in displaying the characteristics of the flow, down to little eddies in the flow, but might be less useful to assign a value to the holdup in the pipe on a more macroscopic scale. Other uses of cameras have mainly been limited to verification by visual observation[10][11][16]; not in connection with software tools.

The TNO setup, which is the basis of the present study, uses a different approach in determining the flow characteristics. Both mass flow meters and camera images are used to determine the volume fractions of oil and water. In the post-processing, the holdup will be automatically determined from the images supplied by the camera. This is done by considering the difference in colour between the oil and the water. The measurement procedures are discussed in more detail in chapter 3.

3| Flow Facility Setup, Data Acquisition and Methods

This chapter contains all information regarding the experimental & modelling setup used in this thesis. It also describes the handling operations to perform the experiments. The chapter starts with a section explaining how the setup is build up, its capabilities and properties, and what types of measurement equipment are used. The chapter proceeds by specifying the properties of the used fluids. Next, the experimental procedures are described and a list of all performed experiments is provided. The reproducibility of the experiments is also discussed. The data processing and analysis is set forth in the final part of this chapter.

3.1 Experimental Setup

3.1.1 Mechanical Composition Flow Loop

This section describes the flow loop used in the experiments of Phase II and III of this research as mentioned in the introduction. Figure 3.1 displays the complete setup, figure 3.2 shows a schematic version of the same setup. The setup consists of two parts: one for the storage and pressurisation of the water and the oil, and the measurement section, also referred to as the experimental pipe section. The total setup is largely automated for operating ease, reproducibility and safety reasons.

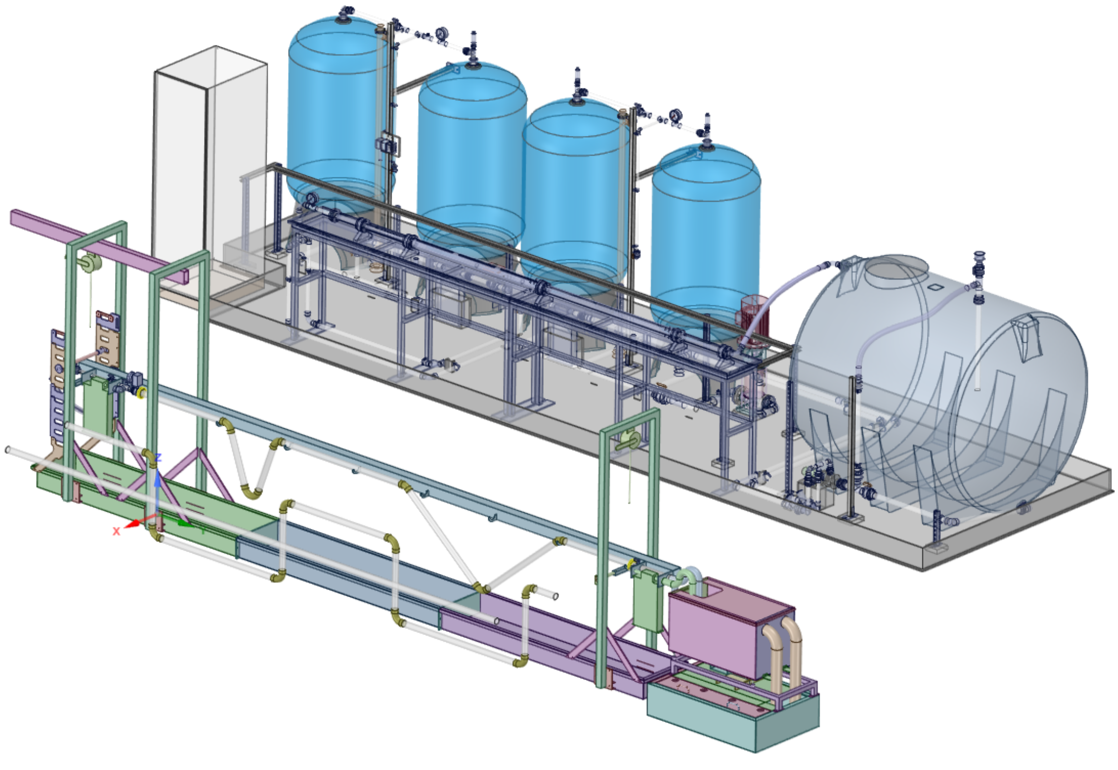

Figure 3.1: Overview of the Flow Loop.[17]

Supportive Section

The supportive section is shown on the top half of figure 3.1. This supportive section provides a constant stream of water under a certain pressure and flow rate such that experiments can be performed in the measurement section, shown in the lower half of figure 3.1. The supportive section mainly consists of large blue tanks and the circulation loop. After passing through the measurement section, the water and oil are pumped into the large 5000 liter tank, seen on the far left of figure 3.1. This tank serves as the separator of the mixture of oil and water produced by each experiment. From the bottom of this separator tank water is pumped to the relatively smaller 1000 liter buffer tanks, depicted to the left of the separator tank. Only two of these tanks were used, to reduce the total amount of water in the setup.

These two buffer tanks feed the circulation loop, shown in the schematic overview. This circulation allows the feed pump to run while the pneumatic valve on/off on route to the measurement pipe section is still closed. This circulation loop is fitted with a valve that opens at a fixed pressure, which can be manually adjusted to achieve a certain pressure in the loop while the circulation loop pump is running. The desired flow and pressure for the downstream measurement section are controlled by the pump rpm, and the orifice size of the flow control valve. Both these values are adjusted remotely from the control panel located on the left of figure 3.2.

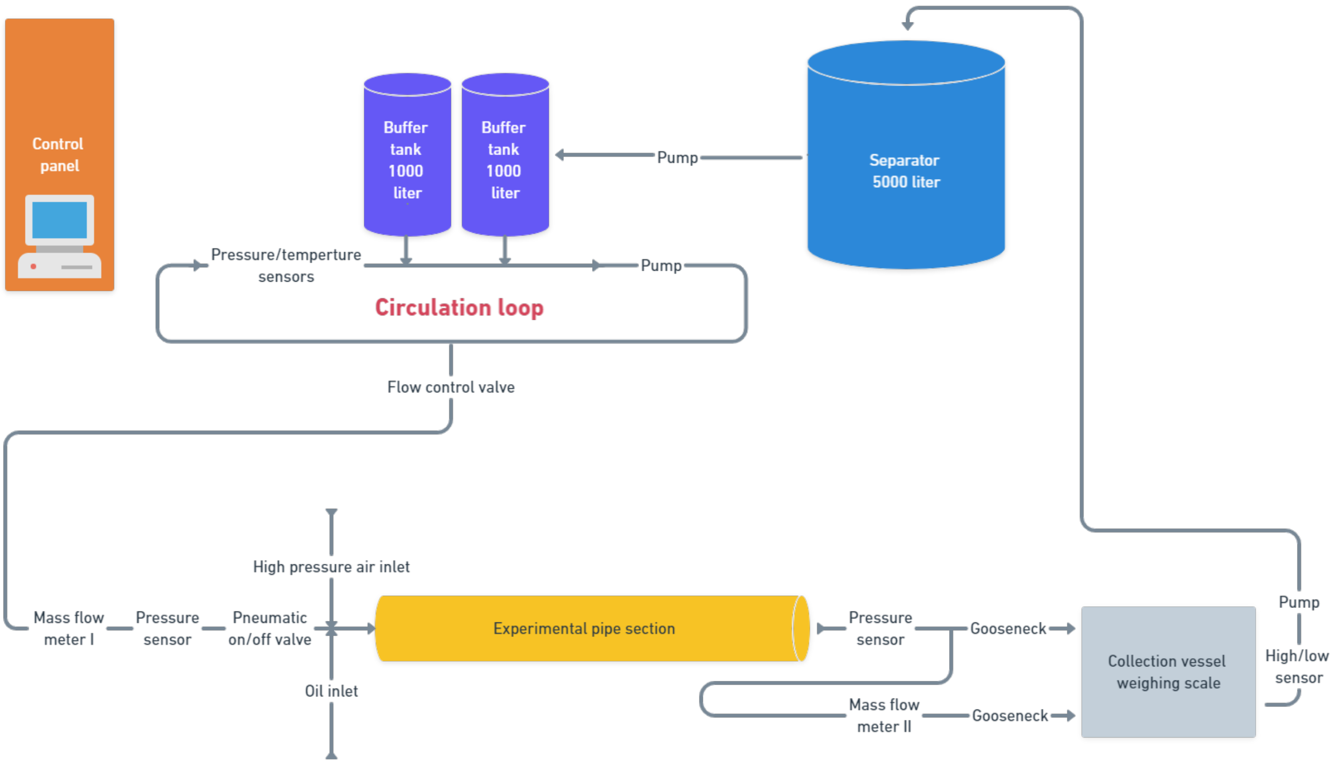

Figure 3.2: Schematic overview of the Flow Loop.

Measurement Section

The flow provided by the supportive section is fed to the measurement section via a connecting pipe. Between this feeding pipe and the measurement section, a pneumatic on/off valve is placed. In contrast to the flow control valve at the beginning of this feeding pipe which can take on values in the range from 0% to 100%, the pneumatic valve can only be in two positions, fully open or fully closed. When the timer on the control panel is started, this valve automatically opens to provide the measurement section with the set flow of water, and will automatically close when the timer reaches its set value. The detailed actions for operating the setup are briefly described in section 3.4, and described in detail in section A.1. A mass flow meter is mounted upstream of the measurement section, shown in figure 3.1 as the green box on the left part of the lower section. The same type of mass flow meter is situated downstream of the measurement section. Between this first mass flow meter and the measurement pipe section, two inlets are situated, one to provide compressed air, and one which is used to fill the measurement pipe section with oil prior to an experiment.

The measurement pipe section in which the flushing dynamics are studied consists of a polycarbonate pipe with a length of 5.65 meter, an inner diameter of 56 mm and a wall thickness of 2 mm. The volume of this straight pipe section including connections amounts to roughly 14.5 liters. The orientation of the measurement pipe section can be varied between approximately -5°and +5°, with step sizes of approximately 1°, as can be seen in table 3.1.

Step	1	2	3	4	5	6	7	8	9	10	11
Angle in degrees °	-4.6	-3.7	-2.8	-1.8	-0.9	0.0	0.9	1.8	2.8	3.7	4.6

Table 3.1: Angles of orientation of the measurement pipe section.

(a) Low, medium and high variations of goosenecks.

(b) Gooseneck used in experiments.

Figure 3.3: Preventing unwanted flow to and from the pipe section.

After travelling through the measurement pipe section, the mixture of water and oil is finally fed into a collection vessel, located at the lower right of figure 3.1. The collection vessel is continually weighed during each experiment, and is subsequently drained. Right after the measurement section, a two way valve is placed. One of its outlets leads to the mass flow meter, and empties into the collection vessel. The other outlet bypasses the mass flow meter, and is used when the measurement section is emptied, or during the process of filling the pipe with oil. This makes sure that the mass flow meter is filled only with water prior to an experiment. Both streams are connected to a gooseneck(figure 3.3b), to prevent unwanted flow in or out of the measurement section. During Phase II, the effect of different gooseneck heights on the flow was studied, of which the results are shown in section 6.1.3.

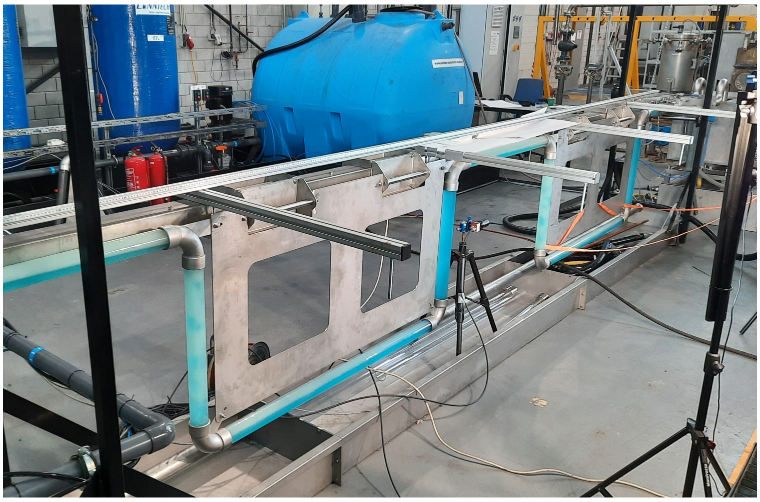

Figure 3.4: U-sections installed in the experimental setup.

The straight pipe is not the only geometrical configuration used in the experiments. Figure 3.1 displays a pipe with two V shapes, with in front of the setup a pipe with two U-sections. A picture of these U-sections installed in the experimental setup can be seen in figure 3.4. These U-sections can be rotated around their length axis, as also seen in this figure. By rotating, the two vertical sections of the U-shape are tilted to an angle of 0° to 90° with respect to the horizontal plane, allowing for more steeper angle variation experiments to be performed. Figure 3.5 shows this operation in action. The measurement procedure for these experiments is shown in section 3.4.

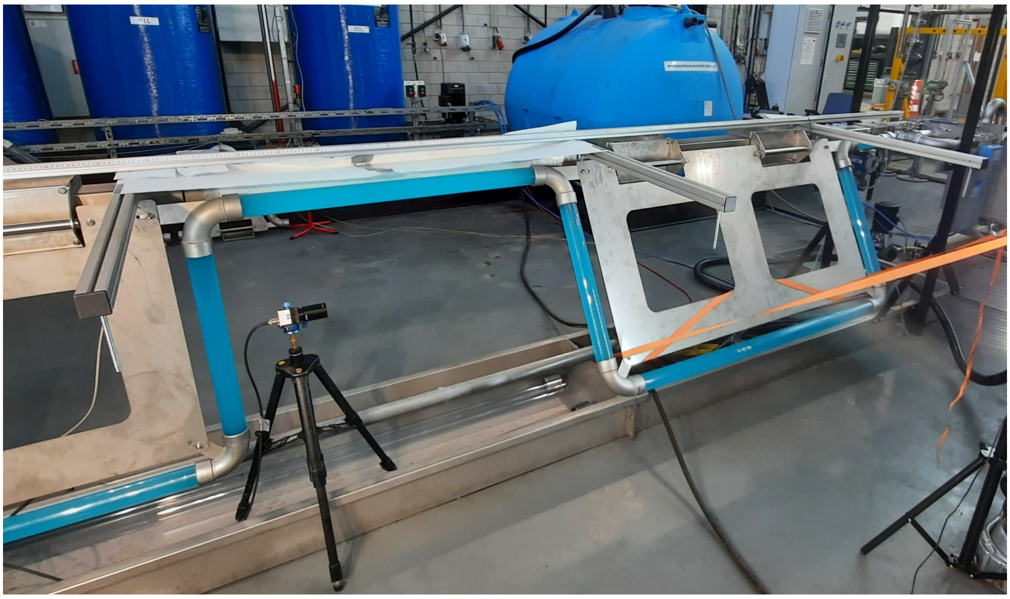

Figure 3.5: U-section 0° to 90° angle variation.

3.1.2 Sensors and Data Acquisition

To measure the temperature of the water that is fed into the experimental section, two PT100 temperature sensors are used with a range of −50 °C to 300 °C. They are situated just upstream and downstream of the circulation loop pump respectively. Temperature sensors are also used to record the ambient temperature in the lab hall. During the analysis of the data, the viscosity and density are corrected for using the recorded temperature.

To monitor the pressure in the system, an ATM118639 pressure meter is used in the circulating loop, just in front of the flow control valve. Its range is from 0 to 8 bara. To measure the pressure drop over the measurement section two IDP25-T22B05E-M1L1 pressure differential sensors are used, with a range of 0 to 2.5 bar. These measure the pressure in the pipe with respect to the ambient pressure.

The weight of the contents of the collection vessel is measured with a HBM PW12C load cell with a range of 0 to 300 kg. A ruler was placed in the collection vessel to measure the liquid level.

The mass flow through the experimental section is measured using two Rheonik RHM20 Coriolis mass flow meters, with an application range of 2.5 to 300 kg/min. The majority of the experiments was performed on the lower end of this range, from approximately 7 kg/min to 55kg/min. Between the experiments the section was flushed with a significantly higher flow rate, at around 220 kg/min.

The fact that in this project cameras are used, to not only record the flow dynamics, but also to analyse the footage with a MATLAB script, sets this study apart from others. This is done as an extra way to determine the holdup of the pipe section by using two 30 fps colour cameras with a horizontal resolution of 2464 pixels. The vertical resolution was adjusted to the part of the pipe section that was in the picture, to reduce file size. The two cameras are pointed to the measurement section like can be seen in the schematic top view in figure 3.6. The cameras are placed as far apart as possible, but also far enough from either end to prevent any possible end effects on screen. After a consideration, 50 cm was chosen for the horizontal length of the pipe section in picture to have a sufficient resolution, but no significant holdup fluctuations resulting from interface waves.

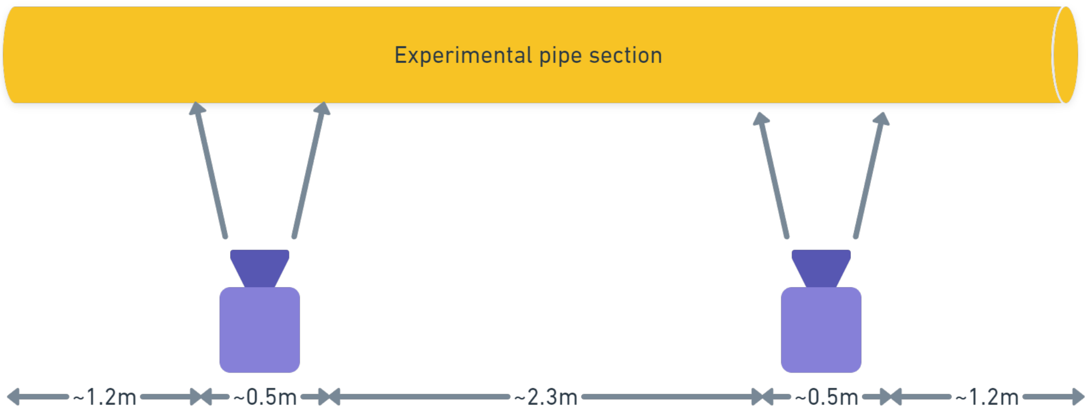

Figure 3.6: Schematic setup cameras.

Cameras are also used in the U-section, 0° to 90° angle variation experiment to determine the holdup in the pipe section. In this case, one of the cameras is positioned in such a way that it covers the horizontal pipe section between the two U-sections (for reference see figure 3.4). The other camera, pointed at the first vertical section of the second U-section(figure 3.5), is not used for further data analysing purposes, but is merely used as an observation device.

The data coming from all the individual sensors is aggregated by a data acquisition system by the company Dewetron. The data recording on the Dewetron is triggered by starting the video recording in the software tool Coreview. This synchronises the video and the pressure and temperature data. The Dewetron collects the data streams at a uniform sample frequency of 10,000 Hz, after which it combines and stores the data in one location.

3.2 Fluid Properties

During the three phases of the flushing experiments study, 3 different oils were used to study the effect of viscosity on the flushing process. The oils were mainly selected based on their viscosity at room temperature, but also keeping in mind their vapour pressure for safety reasons. For Phase II, Fuchs Renolin DTA7 was selected, for Phase III Mobil Velocite No. 10 oil was used.

The water used in the setup is regular tap water with a hardness of around 8.5 to 10.4 dH[18][19]. A density of 998.6 kg/m3 is taken for water. Blue dye(E131) is added to this water to increase the visual contrast between the oil and water phases.

3.2.1 Verification of the Oil Properties

To verify the values provided by the suppliers of the oils, the properties of the oils were measured. This was also done to detect and quantify any changes when reusing the oil after being mixed with water in the experiments. The measurements were performed using an Anton Paar DMA 4100 M density meter at temperatures betweem 15 °C and 25 °C. The experiments were performed at temperatures of 15 °C to 20 °C.

RENOLIN DTA – demulsifying circulating, spindle and hydraulic oils

Product name	Description	Density at 15 °C kg/m³	Flash point Cleveland °C	Kinematic viscosity at 40 °C mm²/s	Kinematic viscosity at 100 °C mm²/s	Viscosity index VI	Pour-point °C	Main application area
RENOLIN DTA 2	Spindle, hydraulic and lubricating oils (machine oils) on the basis of selected base oils with additives for improved aging properties and corrosion protection. All RENOLIN DTA products are DIN 51 524-1 (HL) hydraulic oils and DIN 51 517-2 (CL) circulating oils based on mineral oil, demulsifying (water-repellent) and free of zinc. ISO 6743/4, HL, ISO 6743-6 and ISO 12925-1: CKB.	805	100	2.2	–	–	-27	For thermally-stressed bearings and hydraulic systems with peak temperatures of approx. 120°C. General lubrication without specific wear protection requirements (without AW/EP). (Refer to PI* 4-1292 for further details)
RENOLIN DTA 5		837	120	4.6	1.6	106	-40	
RENOLIN DTA 7		843	153	7.4	2.2	92	-24	
RENOLIN DTA 10		851	174	10	2.6	92	-27	
RENOLIN DTA 15		856	195	15	3.4	98	-27	
RENOLIN DTA 22		865	210	22	4.2	94	-27	
RENOLIN DTA 32		874	222	32	5.4	102	-24	
RENOLIN DTA 46		874	228	46	6.8	101	-24	
RENOLIN DTA 68		882	250	68	8.7	99	-18	
RENOLIN DTA 100		881	248	100	11.2	97	-18	
RENOLIN DTA 150		889	266	150	15.5	94	-15	
RENOLIN DTA 220		893	280	220	18.8	95	-12	
RENOLIN DTA 320		898	280	320	24.0	95	-12	
RENOLIN DTA 460		904	315	460	30.4	95	-12	
RENOLIN DTA 680		913	302	680	37.9	92	-12	

Figure 3.7: Properties Fuchs Renolin DTA oil.

Properties and Specifications

Property	NO 10
Grade	ISO 22
Copper Strip Corrosion, 3 h, 100 C, Rating, ASTM D130	1A
Copper Strip Corrosion, 3 h, 60 C, Rating, ASTM D130	
Density @ 15 C, kg/l, ASTM D4052	0.862
Flash Point, Cleveland Open Cup, °C, ASTM D92	212
Kinematic Viscosity @ 100 C, mm2/s, ASTM D445	4
Kinematic Viscosity @ 40 C, mm2/s, ASTM D445	22
Pour Point, °C, ASTM D97	-30
Rust Characteristics, Procedure A, ASTM D665	PASS
Total Acid Number, mgKOH/g, ASTM D974	0.1

Figure 3.8: Properties Mobil Velocite No. 10 oil.

Density of the Oil used in Phase II and III

The density technique used by the Anton Paar density meter is called the Pulsed Excitation method, which is based on a small U shaped tube that is oscillated. Although this technique is generally very accurate, 3 measurements where performed estimate the repeatability of the measurements. Every measurement was done with a fresh sample of oil, after stirring to get a uniform sample. A trend downwards can be seen in the measurements in table 3.2. A possible reason for this could be that the relative humidity in the measurement device changed between measurements, affecting the very sensitive oscillation tube. Since the difference between the measurements was relatively small compared to other uncertainties in the setup (see section 6.1.2), no further action have been taken to investigate the reason for this trend in measurements.

In table 3.2 and 3.3 the density of new and used DTA7 oil can be seen. The sole difference between the two samples is that one came straight from the barrel, and the other has been mixed with water during the experiments, after which the two phases were separated.

Temperature (°C)	Meas. 1	Meas. 2	Meas. 3	Average density $kg \cdot m^{-3}$	Supplier value
15 °C	831.5	831.2	831.1	831.3	843
20 °C	828.2	828.0	827.8	828.0	
25 °C	825.0	824.7	824.5	824.7	

Table 3.2: New Fuchs Renolin DTA7 oil, Meas.; Measurement.

Temperature (°C)	Measurement 1	Measurement 2	Measurement 3	Average density $kg \cdot m^{-3}$
15 °C	831.8	831.0	830.9	831.2
20 °C	828.5	827.7	827.7	828.0
25 °C	825.3	824.4	824.4	824.7

Table 3.3: Used Fuchs Renolin DTA7 oil.

In tables 3.4, 3.5 and 3.6, the density of new, used and often used Mobil Velocite No. 10 oil can be seen. After each set of experiments the produced mixture returns to the large collection tank, so it is not possible to say how often a specific molecule of oil has been through the experimental section. Therefore the terms used and heavily used have been taken here, where the term used stands for a cycle of around 10 experiments, and heavily for a total of around 90 experiments. This roughly comes down to 1 and 9 passes through the setup. A small trend upward can be seen in the density of the new versus used Mobil oil. The difference however is relatively low, so no further action has been taken based on this result.

Temperature (°C	Meas. 1	Meas. 2	Meas. 3	Average density $kg \cdot m^{-3}$	Supplier value
15 °C	848.5	848.7	848.7	848.6	862
20 °C	845.4	845.5	845.6	845.5	
25 °C	842.2	842.4	842.4	842.3	

Table 3.4: New Mobil Velocite No. 10 oil, Meas.; Measurement.

Temperature (°C	Measurement 1	Measurement 2	Measurement 3	Average density $kg \cdot m^{-3}$
15 °C	849.1	849.1	849.1	849.1
20 °C	845.9	845.9	845.9	845.9
25 °C	842.7	842.8	842.8	842.8

Table 3.5: Used Mobil Velocite No. 10 oil.

Temperature (°C	Measurement 1	Measurement 2	Measurement 3	Average density $kg \cdot m^{-3}$
15 °C	849.4	849.5	849.2	849.4
20 °C	846.2	846.3	846.1	846.2
25 °C	843.1	843.2	842.9	843.1

Table 3.6: Heavily used Mobil Velocite No. 10 oil.

Viscosity of the Oil used in Phase II and III

The viscosity of the oil samples was measured with an add-on device on the same Anton Paar DMA 4100 M machine. A cylinder inside of the device is filled with the sample after which the machine performs multiple measurements automatically. After the machine has reached a stable measurement value it calculates the average viscosity, often within 4-6 measurements. The machine pivots the cylinder to a 45° angle which makes a steel ball inside of the cylinder roll down under gravity. The time it takes for this steel ball to travel a certain distance tells of the amount of viscous drag the ball experiences. The measurements were performed twice, once with new and once with used oil.

For the DTA 7 oil the measurements were performed at a temperature of 20 °C. The results for the new DTA7 oil can be found in table 3.7, the results for used DTA7 oil in table 3.8.

	# of runs	Temperature(°C)	Density($kg \cdot m^{-3}$)	Confidence	$\mu(m \cdot pa \cdot s)$	$\nu(mm^2 \cdot s^{-1})$
Measurement I	6	20.00	828.5	0.1%	12.23	14.76
Measurement II	6	20.00	827.6	0.06%	12.1	14.62
Average		20.00	828.1		12.16	14.69

Table 3.7: New Fuchs Renolin DTA7 oil.

	# of runs	Temperature(°C)	Density($kg \cdot m^{-3}$)	Confidence	$\mu(m \cdot pa \cdot s)$	$\nu(mm^2 \cdot s^{-1})$
Measurement I	4	20.00	828.6	0.09%	12.73	15.36
Measurement II	6	20.00	827.6	0.08%	12.52	15.13
Average		20.00	828.1		12.63	15.25

Table 3.8: Used Fuchs Renolin DTA7 oil.

The intention was to measure the Mobil Velocite No. 10 oil viscosity in the same way, but this was not possible due to the high viscosity of the oil at 20 °C. Therefore measurements at 40 °C and 100 °C were performed, since the values at these temperatures were also given by the manufacturer. The results can be seen in 3.9. Unfortunately due to a technical error in the measuring machine it was not possible to repeat the measurements for used oil.

	# of runs	Temperature(°C)	Density($kg \cdot m^{-3}$)	Confidence	$\mu(m \cdot pa \cdot s)$	$\nu(mm^2 \cdot s^{-1})$
Measurement I	6	40.00	832.3	0.02%	16.07	19.31
Measurement II	4	100.00	793.9	0.06%	3.226	4.063

Table 3.9: New Mobil Velocite No. 10 oil.

Using the numbers provided by the manufacturer of the Mobil oil the viscosity index (VI) of the oil can be calculated to be 58. The viscosity index is a unit-less measure of a fluid's change in viscosity relative to temperature change. This number in turn can be used to calculate the viscosity of the oil at 20 °C. Using the measured values for the viscosity at 40 °C and 100 °C, the viscosity at 20 °C is calculated to be 44.79 $mm^2 \cdot s^{-1}$. The value for the viscosity provided by the manufacturer is 56.83 $mm^2 \cdot s^{-1}$, using the VI to calculate the viscosity at the operation temperature of 20 °C.

Effect of Recycling Oil after each Successive Set of Experiments

After reusing the oil many times, the oil was observed to be more cloudy where it was clear before. It also seemed to stick more to the pipe wall than before, see figure 3.9. Although no direct influences on the flushing process were observed, this was the reason to check the values provided by the manufacturers for the density and the viscosity, and to see whether and how these values evolved over time. As can be seen in tables 3.2 through 3.4 the density showed no significant difference between fresh oil and reused oil. The viscosity for the Fuchs Renolin DTA7 oil was 3.8% higher in the measurements for the used oil. This small increase in viscosity should not lead to major changes in the pressure gradient, which was confirmed by reviewing the pressure gradient data over the length of the pipe section. No significant change was observed looking at each 1.5 m/s superficial water velocity pass. From this result it was concluded that this thin film at the pipe wall does not affect the oil flushing in a significant way. Note however, that the oil film at the pipe wall makes it difficult to accurately determine the phase fractions from the camera images.

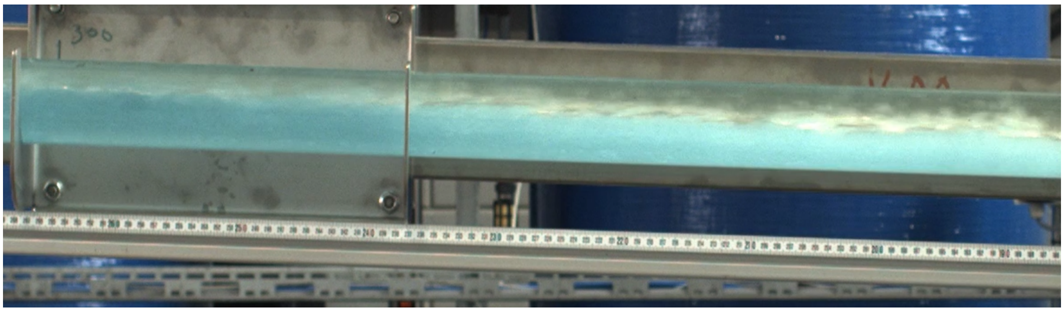

(a) Experiment performed with unused Fuchs Renolin DTA7 oil.

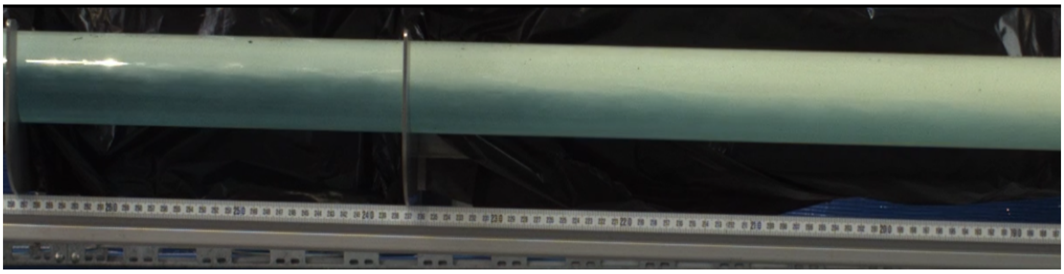

(b) Experiment performed with used Fuchs Renolin DTA7 oil.

Figure 3.9: Visual changes in oil properties after recycling from separator tank.

3.3 Experimental Matrix

In the following two sections an overview of the experiments of the phase II and phase III part of the oil flushing study can be found. The experiments using Fuchs Renolin DTA7 Oil can be found in tables 3.10 and 3.11 respectively. The experiments done with Mobil Velocite No. 10 oil can be found in tables 3.12 and 3.13. The cells containing an "x" signify an experiment taking place at the listed inclination and superficial water velocity.

3.3.1 Fuchs Renolin DTA7 Oil

Superficial Water Velocity \ Inclination	+5°	+2°	0°	-1°	-2°	-5°
0.05 m/s	x	x	x	x	x	x
0.1 m/s		x	x	x	x	x
0.2 m/s		x	x	x	x	x
0.3 m/s		x	x	x	x	x
0.6 m/s		x	x	x	x	x
1.0 m/s		x	x	x	x	x
1.5 m/s		x	x	x	x	x

Table 3.10: Experimental Matrix for Straight Pipe Angle Variation +5° to -5°.

Superficial Water Velocity \ Inclination	V (vertical)	V (horizontal)	U (vertical)
0.05 m/s	x	x	x
0.1 m/s	x	x	x
0.2 m/s	x	x	x
0.3 m/s	x	x	x
0.6 m/s	x		x
1.0 m/s	x		x
1.5 m/s	x		x

Table 3.11: Experimental Matrix for V- and U-sections.

The cells in table 3.10 in the -5° section have intentionally been left vacant apart from the 0.05 m/s superficial water velocity. This was done because at this upward angle all oil flushed almost directly, from the pipe. The same thing holds for table 3.11. The horizontal V experiments were performed between 0.05 and 0.3 m/s, since this was enough to fully evacuate the pipe of oil.

3.3.2 Mobil Velocite No. 10 Oil

The tables 3.12 and 3.13 show the experiments performed during the third phase of this study. As a follow up on phase I and II, new experiments were done on the same straight pipe, with a higher viscosity oil. This third phase decreased the step size in superficial flushing velocities in the range of 0 to 0.35 m/s. Note that there's one cross missing at 0° and 0.35 m/s. This is because at a velocity of 0.3 m/s, all oil flushed from the pipe before the 4 pipevolumes of water were used.

Superficial Water Velocity \ Inclination	0°	-1°	-2°	-5°
0.05 m/s	x	x	x	x
0.1 m/s	x	x	x	x
0.15 m/s	x	x	x	x
0.2 m/s	x	x	x	x
0.25 m/s	x	x	x	x
0.3 m/s	x	x	x	x
0.35 m/s		x	x	x
0.6 m/s	x	x	x	x
1.5 m/s	x	x	x	x

Table 3.12: Experimental Matrix for Straight Pipe Angle Variation 0° to -5°.

Apart from the straight pipe experiments, the third phase experiments also included the variation of the angle between 0° to 90° using the U-section pipe. This was done to pinpoint the transition angle between stratified flow and dispersed flow, as this transition region has major implications for the flushing efficiency. As will become clear in the results chapter, the measurements at 0.1 m/s showed to be more effective in this setup compared to 0.05 m/s. The resolution of the angle variation was increased between 5° and 20°, after this was determined to contain the previously mentioned transition region.

U_s water \ Inclination	0°	5°	7.5°	10°	12.5°	15°	17.5°	20°	30°	40°	50°	60°	70°	80°	90°
0.05 m/s	x			x				x	x	x	x	x	x	x	x
0.1 m/s	x	x	x	x	x	x	x	x	x	x	x	x	x	x	x

Table 3.13: Experimental Matrix for Angle Variation 0° to 90° Relative to the Horizontal Plane.

In addition to the experiments depicted in tables 3.12 and 3.13, some extra experiments were performed. To check the reproducibility of the experiments, the experiment in which the straight pipe is oriented to -1° has been repeated several times at a superficial water velocity of 0.15 m/s and 0.2 m/s, of which some with 8 pipevolumes instead of the usual 4 pipevolumes. Other extra experiments were performed at several flushing velocities and a pipe orientation of -5°.

3.4 Measurement Procedure

This section summarises the measurement procedures. The full in depth instructions for performing the experiments can be found in the appendix in section A.1.

Each experiment consists of three different flushing stages in sequence. The first stage starts with the pipe filled with water, which is flushed with four volumes of water at the desired velocity. The signal from the mass flow meters and the scale are recorded and used for reference.

In the second stage the water is removed from the pipe using compressed air, after which the pipe is filled with oil. The oil filled pipe is then flushed with four volumes of water, the same as in the flush in stage I.

The third stage begins with the pipe filled partly with remnants of oil that might have been left behind after the flushing in stage II, and partly water. These contents are flushed from the pipe with four pipe volumes of water at a superficial water velocity of 1.5 m/s.

After each of the three stages the fluid level in the collection vessel is noted using the tape measure inside the vessel. After these three stages have been performed, one experiment is concluded.

3.4.1 Orientation of the Pipe During Measurements

When the pipe needs to be emptied of water at the end of stage I of the experiment, the upstream part of the pipe section is lifted to make sure everything flows out of the pipe. When the pipe is filled with oil, the upstream part of the pipe is lowered such that any air bubbles can flow out of the downstream end of the pipe.

The principle of the experiments is the same for the 0° to -90° angle variation experiments. When filling and emptying the pipe the upstream part of the pipe can be lifted or lowered to aid in the process.

A strap holds the downstream U-section at a certain angle, after which the experiment is carried out. Apart from the configuration change, the experiments are carried out as usual. The main difference is that the point of interest is the top horizontal part of the pipe in between the U-sections. The upstream U-section is held at a constant vertical orientation during all the experiments, while the downstream U-section is varied in its angle relative to the horizontal plane.

Depending on the angle at which the section is held relative to the horizontal plane, a certain amount of oil will remain. After the flow stops, this oil will drift upstream to the horizontal section between the two U-sections. Since the superficial water velocity is constant between each experiment, the amount of oil left in the horizontal section after the experiments will only be influenced by the angle of orientation. The amount of oil left after each experiment can therefore give information about the holdup in the varied angle section. Using the the conventional measuring techniques, it would not have been possible to determine this holdup.

As mentioned at the beginning of this section, section A.1 elaborated the complete process in much more detail.

3.5 Data Processing

This section will cover the data acquisition, and the processing of this data. The section is divided into the two main sources of experimental data, the mass flow meters and the camera system.

3.5.1 Mass Flow Meters

The mass flow meters form the basis of the setup. As mentioned before, each experiment consists of 3 stages, where the flow during each experiment is recorded with the mass flow meters. The logical way to determine how much oil is flushed from the pipeline is to compare the values of the two mass flow meters, since the volumetric flow rate through each is the same. In this way the volumetric flow rate of oil flowing from the pipe could be calculated using the different mass flow rates, and the known difference in density between the two fluids, as in equation 3.1.

$$\dot{v} = \frac{\dot{m}_1 - \dot{m}_2}{\rho_{\text{water}} - \rho_{\text{oil}}} \tag{3.1}$$

The difference between the signals of the flow meters is small compared to the overall signal. This means that small systematic errors cause large differences in the measured oil fraction. Therefore, post processing is necessary to reduce these errors. The difference between the mass flow rate at the inlet and the outlet, is only a small fraction of the total signal. Since 4 times the pipe volume is flushed during each experiment, the fraction can be determined as in equation 3.2:

$$\frac{V_{\text{oil}}}{V_{\text{water}}} = \frac{4 \cdot V \cdot \rho_{\text{water}} - (3 \cdot V \cdot \rho_{\text{water}} + V \cdot \rho_{\text{oil}})}{4 \cdot V \cdot \rho_{\text{water}}} = \frac{\rho_{\text{water}} - \rho_{\text{oil}}}{4 \cdot \rho_{\text{water}}} \tag{3.2}$$

This number is the maximum fraction, which will only be the case when all oil flushed from the pipe during the experiments. For cases with Fuchs Renolin DTA7 oil this number will be 0.043, for cases with the Mobil Velocite No. 10 oil this fraction will be 0.038. Since this fraction is so small, the simple method of just comparing the mass flow rates between the two mass flow meters will not be suitable for analysing the experimental data.

Since this oil fraction is so small compared to the total signal post-processing has to be done. In order to correct for the systematic error in the flow meters, just before each time an actual flushing will be performed (Stage II in 3.4) a reference measurement has to be done (Stage I in 3.4). Using this measurement, a correction factor between the flow meters can be determined, which can be done in four ways.

1. The output of the mass flow meters is corrected using the output of the scale in the reference measurement (stage I). In the reference measurement the final weight, measured at the scale, is recorded. Then for each flow meter a correction factor is determined, such that the integral of the mass flow at each flow meter matches the final weight of the scale. These correction factors are then applied in the second measurement (stage II).

2. The difference in the output between the flow meters in stage I is subtracted from the difference in the output between the flow meters in stage II. Note that this method assumes that the mass of water flushed in the two experiments is equal. The scale is not used.
3. The output from flow meter 2 is corrected with a factor, such that the mass measured by flow meters 1 and 2 in stage I is equal. This factor is then applied in stage II. The scale is not used.
4. The difference in mass at the scale in stage I and stage II is corrected for the difference in mass measured in flow meter 1 in these experiments.

The oil flushed during stage III of an experiment is also determined. Since experiments with a flushing velocity of 1.5 m/s are performed where the starting point is an oil-filled pipe, these are used as a reference for the analysis of the stage III part of each experiment. After the third stage of each experiment, in principle all oil is removed from the pipeline. This is also confirmed by visual observations.

Selected Method of Correcting Raw Data

During the work done by Van Nimwegen and Pereboom [20] in Phase I and Phase II of the flushing project it was determined that method one, out of the four methods presented in the previous paragraph, is the preferred method. Of the four options, method one gave the best results looking at how close the average fraction of all oil flushed in an experiment came to 1(1.0072) in phase I and II, and the value for the standard deviation of oil flushed (0.0718).

Table 3.14 shows the average fraction of oil flushed and the standard deviation for each of the correction methods, for the Mobil Velocite No. 10 experiments. Correction method one shows sufficient accuracy in the average fraction of oil flushed, and stands out from the other three methods when looking at the standard deviation. These results confirm the analysing method choice made during the earlier phases.

	Average fraction of oil flushed	Standard deviation of oil flushed
Method 1	1.0104	0.0361
Method 2	0.9717	0.0549
Method 3	0.9411	0.0550
Method 4	0.9927	0.0496

Table 3.14: Average fraction of total oil flushed and standard deviation for the four correction methods for the Mobil Velocite No. 10 oil experiments.

3.5.2 Measurement Reproducibility

This section covers the reproducibility of the recorded data from the mass flow meters, as well as the effect of reusing the oil.

Oil Property Reproducibility

There are visually observable changes between fresh oil from the barrel, and after it is recovered from mixing with the water during the experiment. Strictly speaking this is called recycling, as reuse would suggest that the mixture produced in the experiments is not separated into its base contents. Some of the experiments that were performed according to the experiment matrix were repeated to verify any possible effects of recycling the oil after use in earlier experiments. The coming figures give a clear view of the effects of recycling the oil after mixing with water. Oil that is fresh from the barrel is labelled as "new" oil, oil that has only been recycled a few times will be labelled as "recycled a few times", oil that is recycled often is labelled as "recycled often".

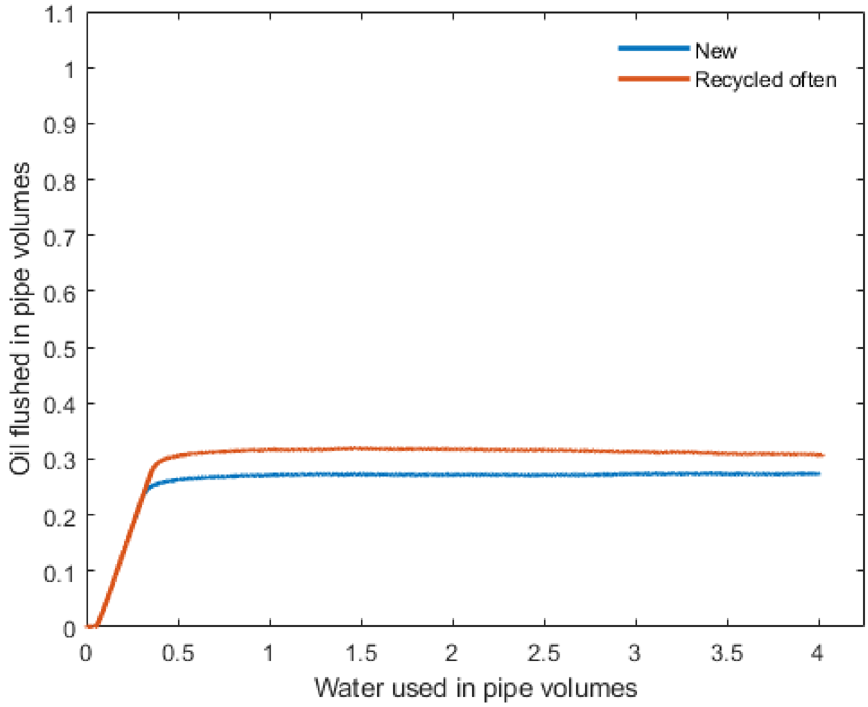

Figure 3.10: Effect of recycled oil at an angle of -5° and a superficial water velocity of 0.05 m/s.

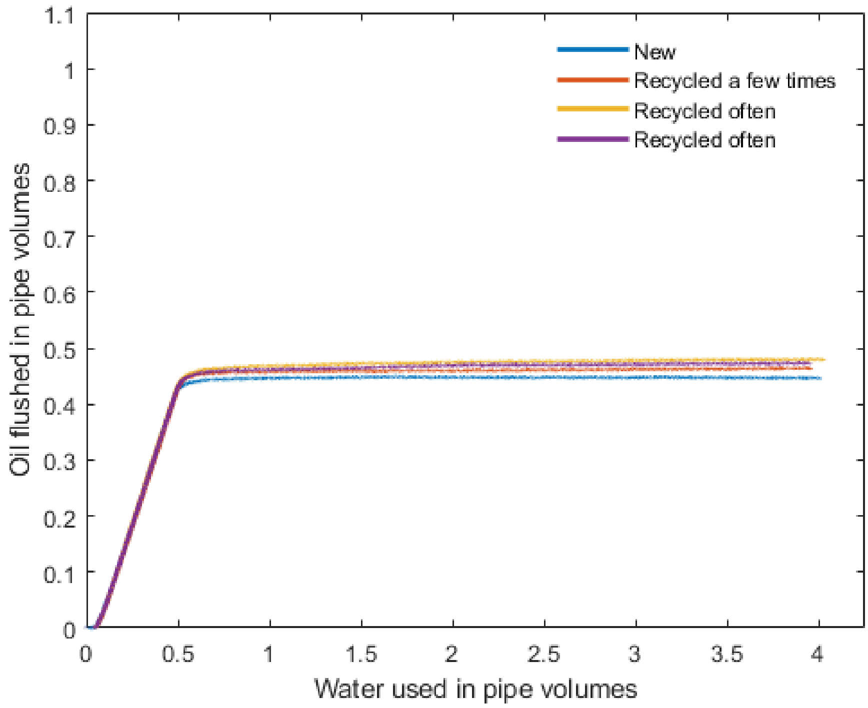

Figure 3.11: Effect of recycled oil at an angle of -5° and a superficial water velocity of 0.1 m/s.

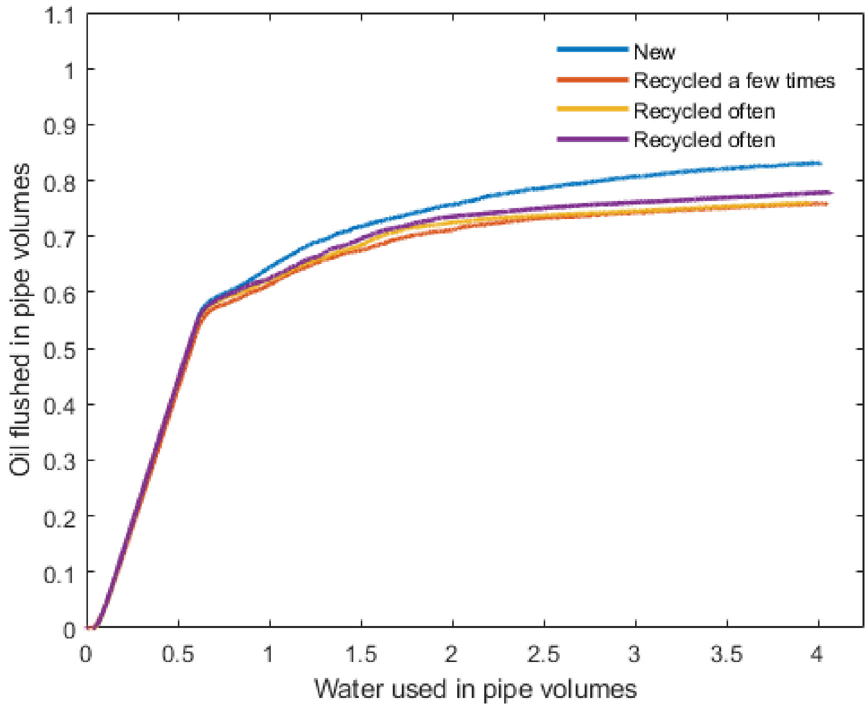

Figure 3.12: Effect of recycled oil at an angle of -5° and a superficial water velocity of 0.2 m/s.

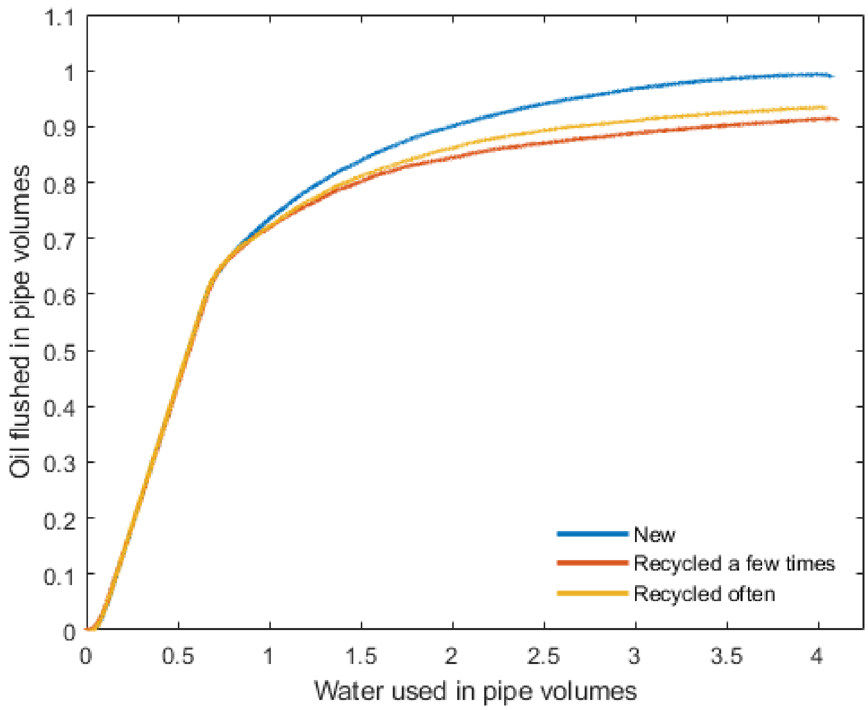

Figure 3.13: Effect of recycled oil at an angle of -5° and a superficial water velocity of 0.35 m/s.

Figures 3.10, 3.11, 3.12 and 3.13 show that there is a difference in flushing behaviour between new and once recycled oil, but that further reuse does not have significant effects on the flushing efficiency of the Mobil oil. This effect is not the same for all flushing velocities. For lower flushing velocities like a superficial water velocity of 0.05 m/s the recycled oil is flushed better from the pipe section compared to oil fresh from the barrel. However, this effect changes with the flushing water velocity. At a superficial water velocity of 0.1 m/s there is no significant difference, while at relatively higher velocities of 0.2 and 0.35 m/s the effect is turned around, and recycled oil is harder to flush from the pipe section. This effect, detected by the mass flow meters, was also visually observed.

Because of the change in magnitude and sign of this effect, it is hard to say whether this effect is significant with respect to the reproducibility. The changes in the measured density and viscosity are not of a magnitude to justify these changes. A note is made that the 0°and -5 °experiments have been conducted with fresh oil, the -1° and -2° and all following experiments were performed with recycled oil.

Flow Meter Data Reproducibility

To investigate the reproducibility of the flow meters themselves a selection of experiments have been performed repeatedly, with recycled oil as well as often recycled oil. These experiments have been done with a flushing volume of 8 pipe volumes instead of with the regular 4 pipe volumes. Figures 3.14 and 3.15 show the curves for these experiments. The curves show that the reproducibility is quite good, with the results within a ± 0.02 pipe volume range.

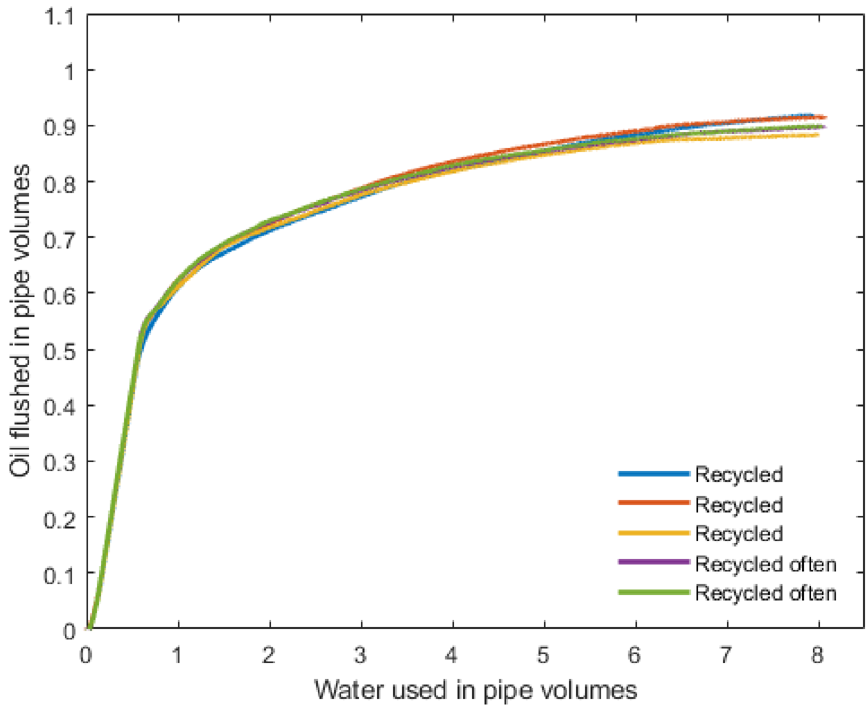

Figure 3.14: Effect of recycled oil at an angle of -1° and a superficial water velocity of 0.15 m/s.

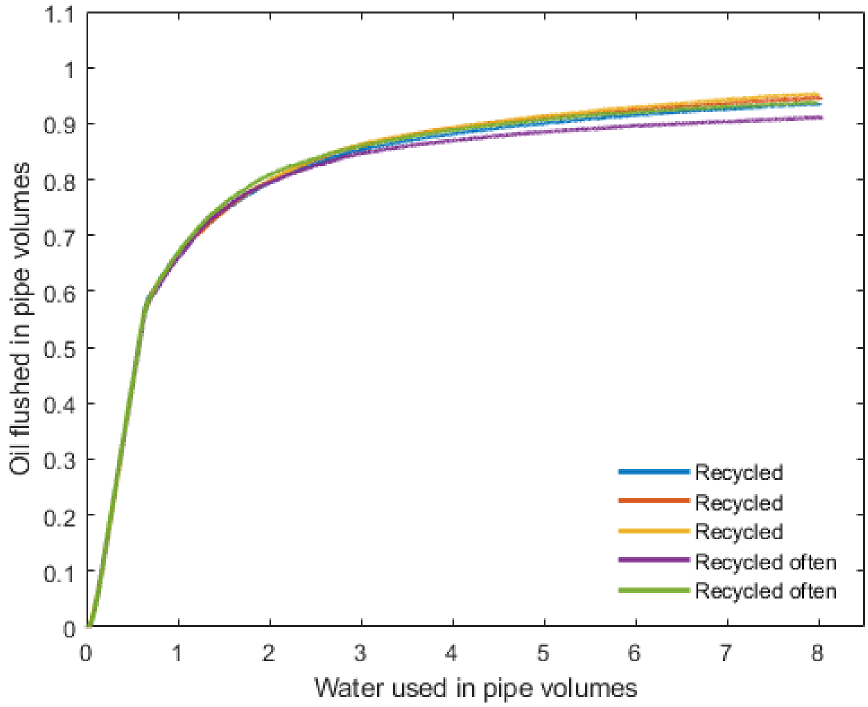

Figure 3.15: Effect of recycled oil at an angle of -1° and a superficial water velocity of 0.2 m/s.

3.5.3 Video Analysis

To be able to analyse the video data, first the position of the cameras with respect to the pipe has to be known. The position of the cameras is shown in figure 3.6. Like mentioned in section 3.1, the cameras are pointed such that they are as far apart as possible, to detect possible variations in the water holdup relative to the position in the pipe. The cameras cannot be placed close to the inlet and outlet however, because the flow is not fully developed in the beginning, and could be influenced by the constriction in the outlet on the downstream end of the pipe.

The positioning of the cameras for the 0° to -90° variation is different from the straight pipe setup. As briefly addressed in section 3.1.2, in the U angle variation setup only one camera is used to gather data on the water holdup in the pipe. The camera is pointed such that the horizontal part of the image just covers the pipe from socket to socket in between the two U-sections. In this way as much of the horizontal resolution is used to cover the pipe. The earlier posted figure 3.5 can help to illustrate this. The second camera is pointed at the vertical part of the second U-section for flow type observation purposes.

Apart from capturing the points of interest, the resolution of the images is also very important. When the camera is situated far from the pipe, it might be able to see a lot of it, but there will be a limited number of pixels along the width of the pipe. During phase II of the flushing study the cameras were placed a number of meters away from the setup to capture as much pipe as possible. During phase III the two cameras only captured sections of about 50 centimetres wide, such that the vertical resolution was increased about fourfold.

The level of ambient lighting has an impact on the video data, despite additional LED lighting placed near the setup. On bright and sunny days the brightness of the light in the experimental hall changes to some degree, when for instance a cloud rolls by. In the following section regarding the workings of the MATLAB script, this effect is described more in detail. A recommendation for future research will be to add even more artificial lighting such that even on bright sunny days the brightness level will not be influenced significantly.

There are some limitations to the video analysis. First of all, when dealing with multiple different transparent materials and media, there's always refraction between the medium an the pipe wall. This will distort the view of what is happening in the pipe. While it might be possible to somehow correct for this effect, it will be time consuming, and will still probably not be 100% accurate. This is because during some parts of the experiment the pipe will be filled with oil, while during other parts of the experiment the pipe will be filled with water, having a different refractive index to polycarbonate.

Another effect is the height of the interface during wavy flow. In experiments with low superficial water velocities(see figure 3.16), the interface height is relatively low. However when the superficial water velocity increases to only 0.15 about m/s, significant waves and bubbles occur(see figure 3.17). These are three-dimensional phenomena, while the image that is captured is only two-dimensional. This means that, the more wavy and turbulent the flow, the more the accuracy of the video analysis is limited.

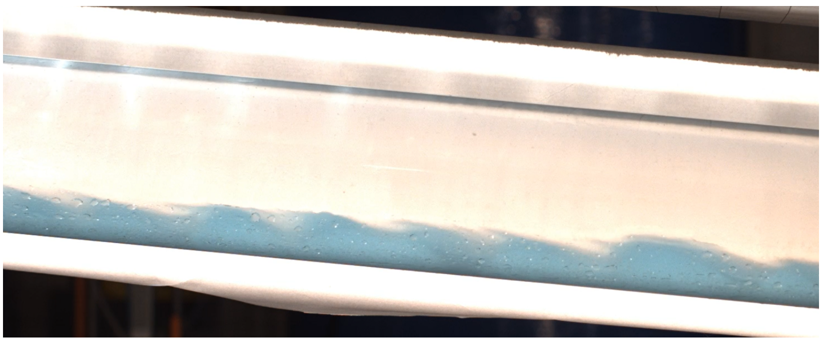

Figure 3.16: Flow under -5° and U_s 0.05 m/s.

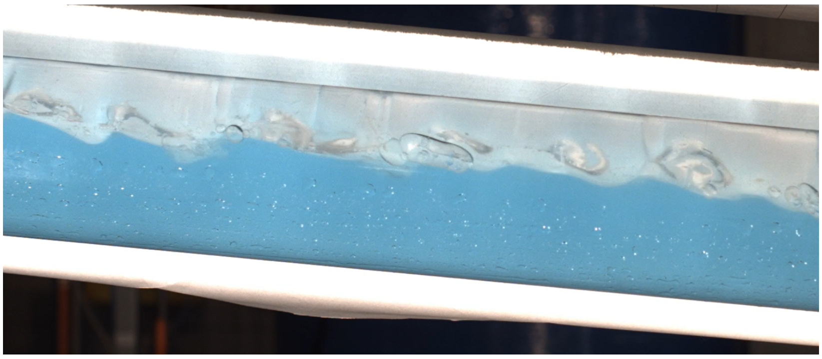

Figure 3.17: Flow under -5° and U_s 0.05 m/s.

Camera Data Reproducibility

To illustrate the reproducibility of holdup measurements using the camera, video analysis data is shown in figure 3.18 of the eight volume flushing experiments presented in section 3.5.2. It can be seen that the curves for all three 0.15 m/s experiments and two out of three 0.2 m/s velocity experiments are similar. However, one of the 0.2 m/s experiments is off for the left camera. This affects the average of the two cameras. A likely cause of this is a combination of the erratic behaviour of the interface combined with local changes of the ambient lighting like a ray of sunlight striking that part of the experimental setup. Although the 0.15 m/s experiments are very similar, one the three 0.2 m/s experiments shows that attention is necessary while processing the data.

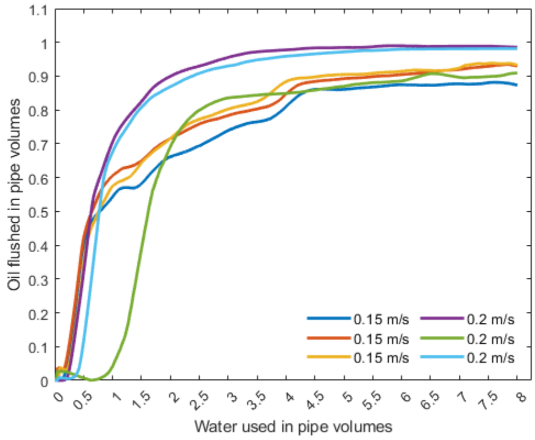

(a) Repetition video analysis for Mobil oil for the amount of oil flushed for an pipe orientation of -1° at 0.15 m/s and 0.2 m/s, left camera, 8 flushing volumes.

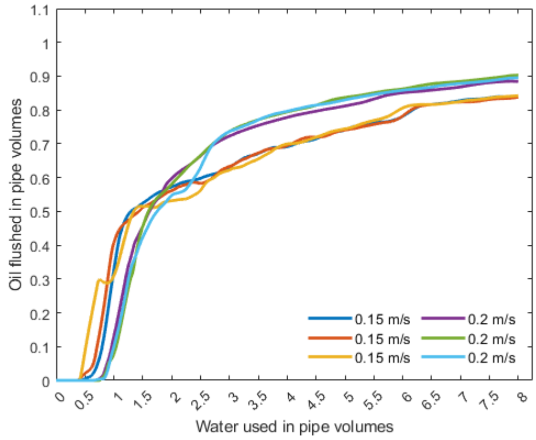

(b) Repetition video analysis for Mobil oil for the amount of oil flushed for an pipe orientation of -1° at 0.15 m/s and 0.2 m/s, right camera, 8 flushing volumes.

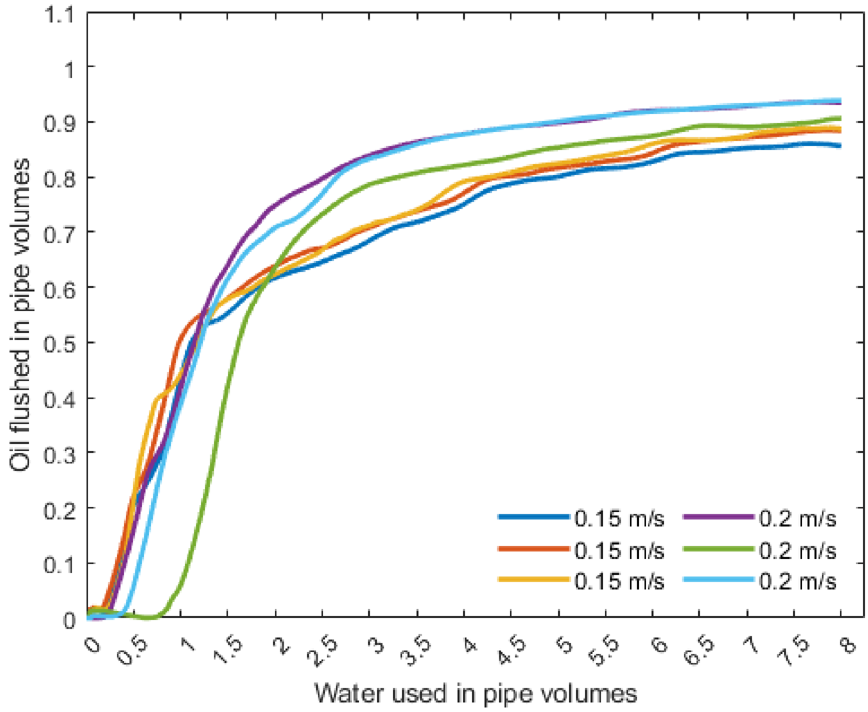

(c) Repetition video analysis for Mobil oil for the amount of oil flushed for an pipe orientation of -1° at 0.15 m/s and 0.2 m/s, average of the two cameras, 8 flushing volumes.

Figure 3.18: Camera Data Reproducibility analysis.

Operation of the Video Analysis MATLAB Script

In this section the MATLAB video analysis script will be described. Simply put, the goal of the script is to determine at any frame, at each pixel within the pipeline in the picture, whether the pixel represents oil or water. The results can be converted to the average holdup in the pipe.

Although the distance between the pipe and the cameras is not equal for all experiments, the same processing script was used throughout The images from phase II show a section of around two meters of the measurement section, compared to the around 50 centimetres in the phase III images. The cameras are positioned around four times closer to the pipe section in Phase III, which means that the vertical resolution is also about four times higher.

At the end of the last stage of an experiment(stage III), the pipe is completely filled with water (dyed blue to increase the contrast), as seen in figure 3.19. At the start of stage II of each experiment, the pipe is completely filled with oil as seen in figure 3.20.

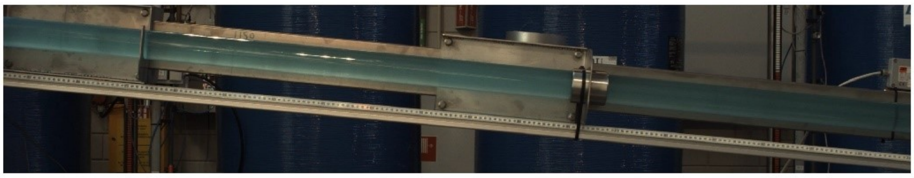

Figure 3.19: Water filled pipe at an angle of -5°.[20]

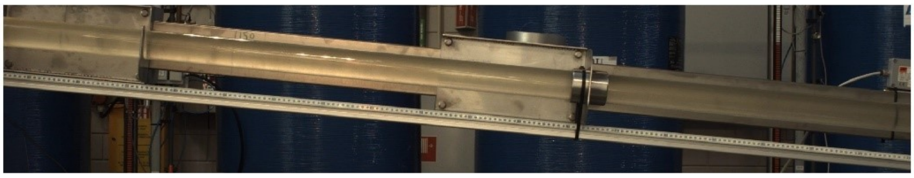

Figure 3.20: Oil filled pipe at an angle of -5°.[20]

Since the experiments are performed at different inclinations, and precisely rotating the cameras with the pipe for each experiment would be very tedious, the image is rotated to show the pipe as horizontal. The rotated versions of figures 3.19 and 3.20 can be seen in figures 3.21 and 3.22 respectively. In the first of the script the red colour channel of the two images is subtracted. The difference between the two images is the largest in the red channel as opposed to the blue channel, since the oil is whitish in colour. This means that the RGB values for each of the three colours is relatively high. The blue water filled pipe section contains very little red colour, giving the largest difference.

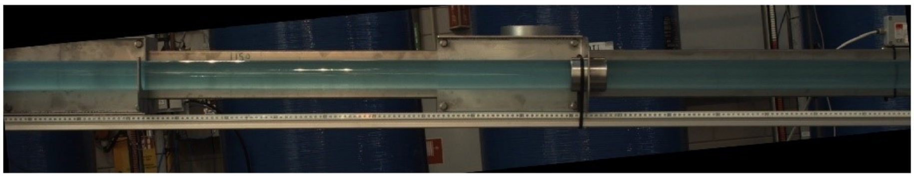

Figure 3.21: Water filled pipe rotated to be horizontal.[20]

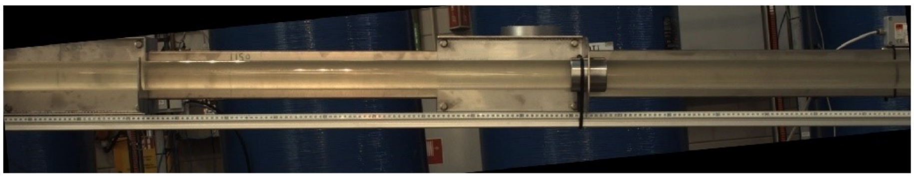

Figure 3.22: Oil filled pipe rotated to be horizontal.[20]

One of the inputs the MATLAB script needs is the approximate diameter of the pipe section, in pixels. The subtracted red channel is rotated under all angles between -5° to 5° with a step size of 0.1°. For each of the rotated images, the height of the pipe is determined using the red channel data. The image in which this value is lowest is the image which is rotated such that the pipe is oriented horizontal. In figures 3.21

and 3.22 the rotated images are shown. The rotated image showing the difference in red channel is shown in figure 3.23.

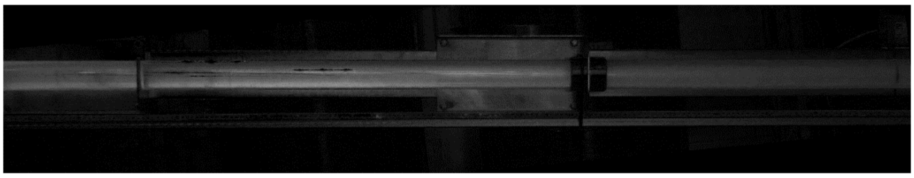

Figure 3.23: Difference in red channel between the water and oil filled pipe.[20]

After determining the difference between the two images, the edges of the pipe section need to be determined. The approximate position of the centre of the pipe section was already found during the rotation of the image. The edges are then found using an edge detection algorithm.

The maximum in the moving average of the horizontally summed difference in red value is located at the y-pixel at the centre of the pipe. From this centre pixel the largest gradients in the graph are determined, both below and above the centre. The location where the largest gradients in difference occur are the edges of the pipe section. The image of the difference with the determined edges overlayed is shown in figure 3.24.

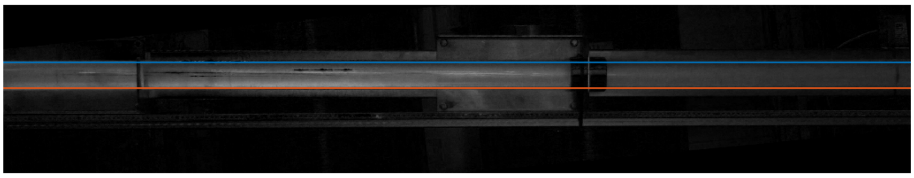

Figure 3.24: Difference in red channel between the water and oil filled pipe, with detected edges of the pipe.[20]

Sometimes not all parts of the pipe section can be used in the analysis because of a pipe socket or a reflection on the pipe. For the image of the oil filled pipe, and the water filled pipe, the difference in red channel value has been determined. When this value reaches a certain threshold, the script determines that this position in the image must be part of the pipe. For the positions showing a pipe socket, the difference in red channel value will be very small to none. Only those x positions of which at least 90% of the pixels above it exceed the threshold are taken up into the analysis. The total image which consists of pixels that are taken up into the analysis is shown in figure 3.25. Note that in this specific image an error is made, two vertical lines are taken up into the analysis by mistake. This is probably because of a reflection, or even a small shift of the entire pipe.

Figure 3.25: Part of image that is considered to be part of the pipe section.[20]

When the pipe section is rotated and the edges of the pipe located, the actual determining of the holdup of the pipe section can take place. For each selected frame, the difference between the red value of the oil filled pipe, and the pipe in the current frame is determined. When the difference is large enough, the pixel is determined to be water, otherwise the pixel is considered to be oil.

The blue hue of the water is often reflected at the top of the pipe, such that the algorithm detects water at the bottom and the top of a vertical section of pixels. To counteract this, gaps in the holdup of a vertical section of pixels are not allowed.

An example of this system in action is seen in figure , with at the top the rotated pipe section, in the second image the difference in the red channel between the images, and at the bottom the resulting calculated holdup.

The finally determined numerical holdup is sum of the total pixels that were determined to contain water. This sum is weighted since a pixel in the middle of the pipe relative to the height represent more volume compared to pixels located at the top or bottom of the pipe, because the cross section of the pipe is circular. Figure 3.26 shows an example of the detected flow of water in the pipe, seen in the bottom image in red.

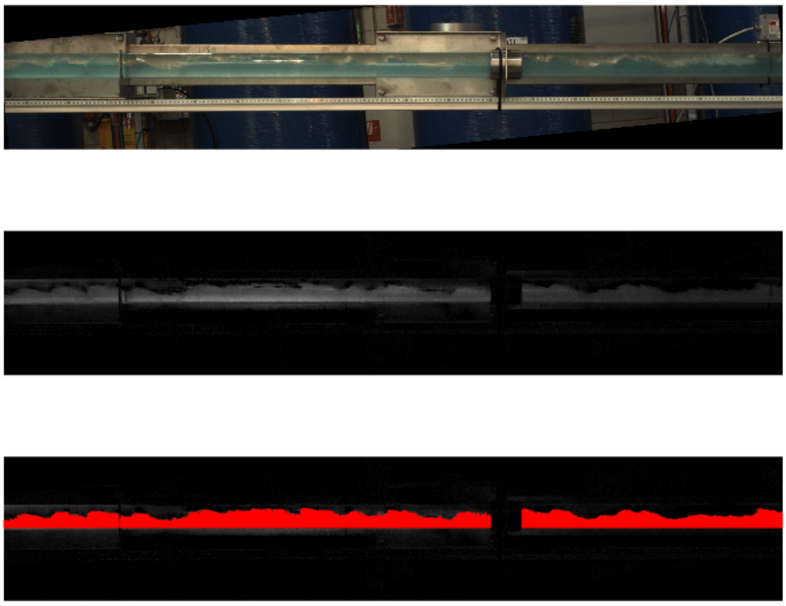

Figure 3.26: Final result of the video analysis, with in red the detected water in the pipe section.[20]

In previous sections the influence of rapidly changing weather conditions where deemed as detrimental to the analysis. Reflections, or changes in ambient light cause a shift in red channel values. In certain occasions light is reflected in a different way depending on the holdup in the pipe section. The threshold value that was set originally, might not be correct anymore for such a case. For certain experiments the threshold value had to be set specific for that experiment, to make sure the holdup data was correctly determined. This is very time consuming, which again supports the action to bring in even more artificial lighting to provide stable lighting conditions.

3.5.4 Photo Method

To capture additional information on the water holdup, during Phase III photos were taken after the second stage of each experiment, to determine the amount of oil that was flushed during the first oil flush. To achieve this, after each experiment the upstream end of the measurement section was lifted to maximise the downward inclination of the pipe. After letting the contents of the pipe settle, a photo was taken. Using the tape measure, running along the measurement section, the position of the interface between the water and the oil could be determined, and the concentration of oil and water in the pipe could be calculated. Subsequently, the pipe was oriented back to its original test position, such that stage III, the second oil flush, could commence as usual.

The holdup values determined using this photo method are shown in chapter 6 to verify and compare the results obtained using the mass flow meter system, the video capturing system and the OLGA modelling.

4 Experimental Results

During the experimental phases a lot of data has been produced, both from the physical experiments as well as from the software tool OLGA. In section 4.1, the data from the mass flow meters in the experimental setup is analysed. This is done separately for the experiments performed with Fuchs Renolin DTA7 oil, and the experiments performed with Mobil Velocite No. 10 oil. The development of the average water holdup in the pipe is shown, using curves for the amount of displaced oil as a function of the amount of water used. This is later referred to as the flushing curve. Subsequently a summary is shown for the straight pipe experiments, which shows all end values for the amount of oil flushed after using four pipe volumes of water. After this, a comparison is made between the amount of oil flushed when the pipe is filled with Fuchs oil and when the pipe is filled with Mobil oil.

Section 4.4 displays the processed video data for the straight pipe experiments performed with Mobil Velocite No. 10 oil. Only the Phase III data is displayed here, as the vertical resolution in these experiments was significantly higher than in phase II. The data is presented in a similar fashion as the flow meter data, displaying the course of the experiments, with the amount of oil flushed per amount of water used to flush the setup. Since two cameras are used, for each orientation of the pipe section first the two are displayed separately followed by the average of the two cameras. This average does not necessarily equal the average of the total holdup in the pipe section, since the cameras only see about a meter of pipe in total, less than 20% of the total length. This important note should be kept in mind when comparing the two data sources.

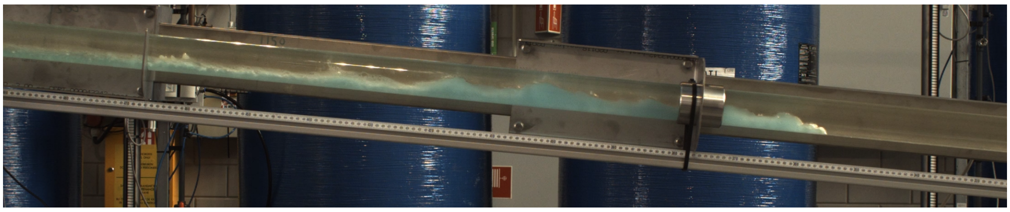

Figure 4.1: Flow in the experimental pipe section, in this case Fuchs oil with 0.05 m/s water and an orientation of -5°.

4.1 Mass Flow Meter Data Analysis - Fuchs Renolin DTA7 Oil

Like explained in the previous chapter, the experimental section is filled with oil before starting each experiment. Subsequently, water is fed through the setup in order to flush the oil from the pipe section, something that would look something like figure 4.1. The mass flow meter data coming from these experiments is analysed and the results are displayed in the figures presented in the coming sections. The exact list of experiments that were performed can be found in section 3.3.

4.1.1 Straight Pipe Section Experiments

The following four figures(4.2, 4.3, 4.4 and 4.5) represent Fuchs Renolin DTA7 oil being flushed from the system at an angle of 0°, -1°, -2° and -5° respectively.

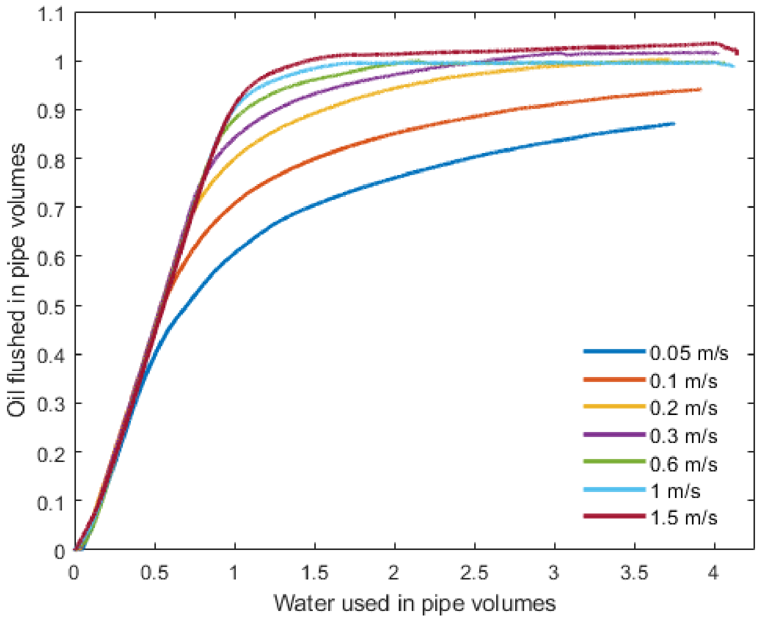

Figure 4.2: Fuchs oil flushed from the pipeline at an orientation of 0° at several velocities.

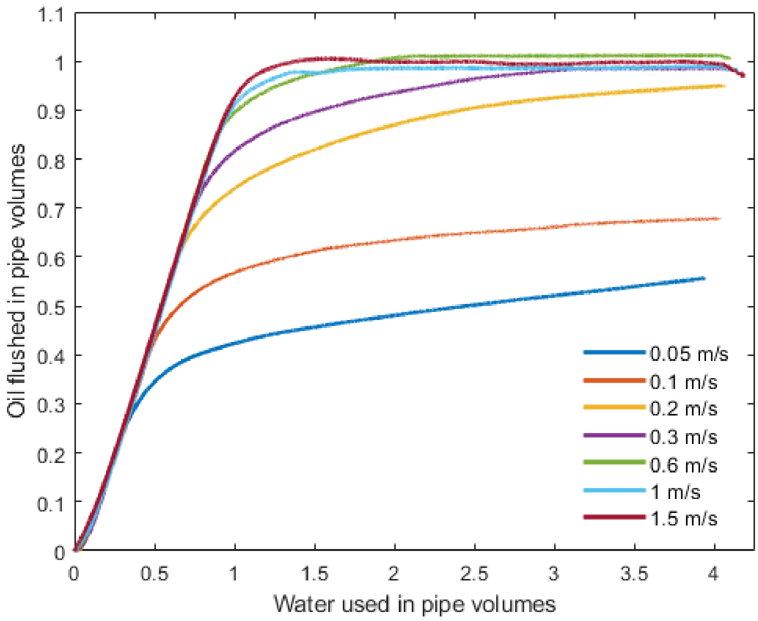

Figure 4.3: Fuchs oil flushed from the pipeline at an orientation of -1° at several velocities.

For a pipe orientation of 0° a relatively large part of the oil is flushed from the pipe section, even at the lower superficial water velocities. At a -1° inclination at low flushing velocities ($\leq$ 0.15 m/s), significantly less oil is flushed from the pipe relative to the horizontal case.

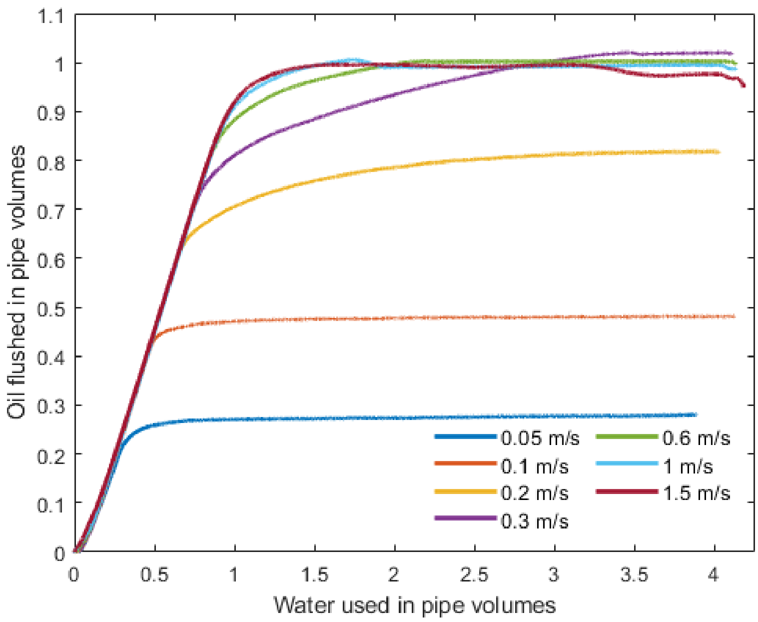

Figure 4.4: Fuchs oil flushed from the pipeline at an orientation of -2° at several velocities.

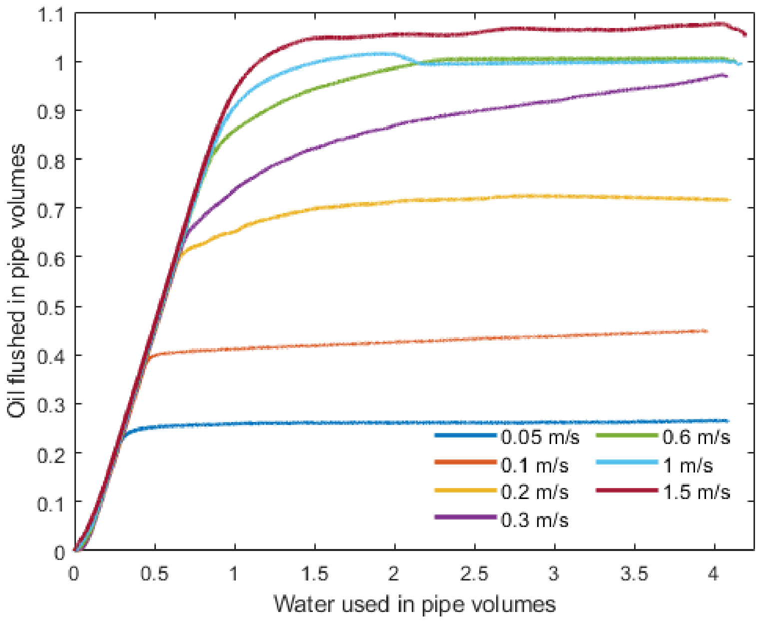

Figure 4.5: Fuchs oil flushed from the pipeline at an orientation of 0° at several velocities.

The larger the negative inclination angle, the less oil is flushed from the pipeline. What can be seen in figure 4.4 and 4.5 is that for the lower flushing velocities a plateau is reached wherein no more oil is flushed, although water is still flowing. What was observed visually is that the water is "flowing underneath" the oil, in such a way that no more oil is taken with the water flow. A conclusion that can be drawn from these experiments is that for the case of Fuchs Renolin DTA7 oil and an inclination of 0° to -5°, a velocity of at least 0.3 m/s is always sufficient to flush all oil from the pipe section.

Experiments were also performed for positive inclinations of +2°, and +5°. The results of the data analysis can be seen in figure 4.6.

The density difference helps the flushing process in this case, where the water displaces the oil, almost in a piston like motion. The conclusion that can be drawn from these results is that all oil is flushed from a pipe with a positive inclination for any positive superficial water velocity.

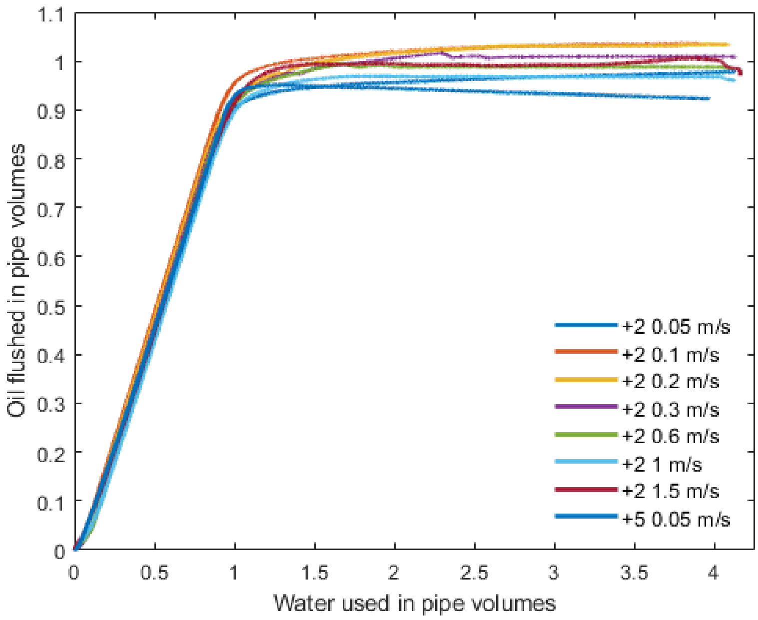

Figure 4.6: Fuchs oil flushed from the pipeline at an orientation of $+2°$ at several velocities, and for $+5°$ for a superficial flushing velocity of 0.05 m/s.

To summarise, the flushing of the pipeline consist of three parts. In the first part, the volume of oil being flushed is exactly the same as the volume of water entering the upstream pipe section. Once the front of this water reaches the outlet section of the measurement section, a transition region is reached, in which the volume of oil that is flushed is lower than the amount of water coming in, but still higher than zero. Eventually, a plateau is reached, where the volume of water coming in is equal to the volume of water exiting the pipe. This plateau can be reached with, or without oil still present in the pipe.

Straight Pipe Section Experiments - Final Flushing Values

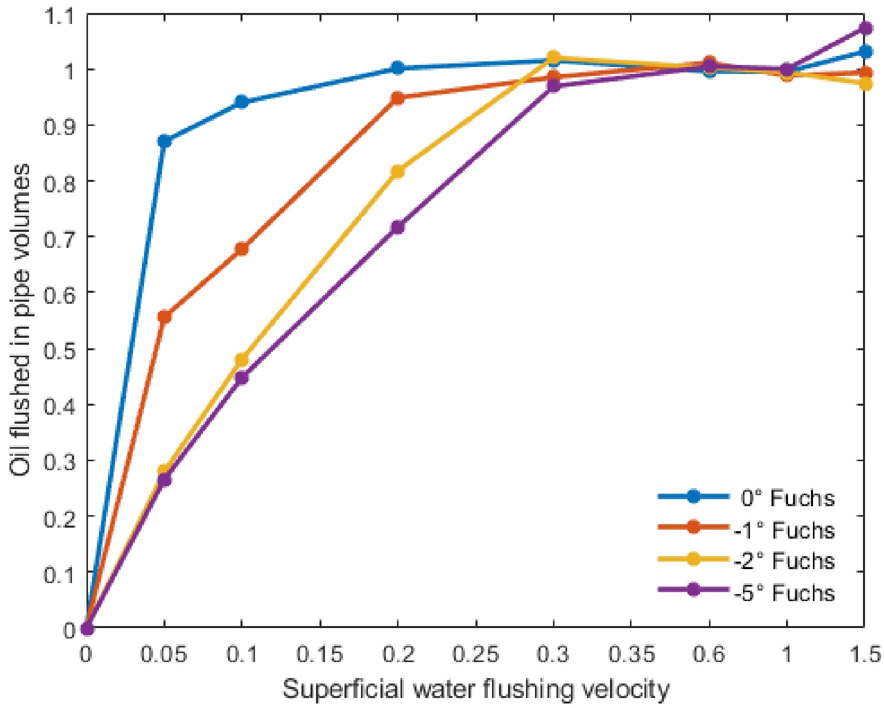

Figure 4.7: End values for Fuchs oil flushed from the pipeline after 4 flushing volumes, at several orientations and velocities.

Figure 4.7 shows the final flushing results for all previous 28 experiments performed with Fuchs Renolin DTA7 oil, for inclinations between 0° and -5°, and superficial flow velocities between 0.05 and 1.5 m/s. The points in the graph represent the fraction of oil that was flushed from the pipe after flushing with four pipe volumes of water.

What can again be seen is that a higher superficial water velocity always increases the flushing efficiency. Additionally, increasing the negative inclination has an adverse effect on the flushing efficiency.

4.1.2 U- and V-Section Experiments

Using the Fuchs Renolin DTA7 oil, experiments were also performed using two U and V sections. The overall orientation of the experimental pipe section was held horizontal. Figures 4.8 and 4.9 respectively show the results of those experiments.

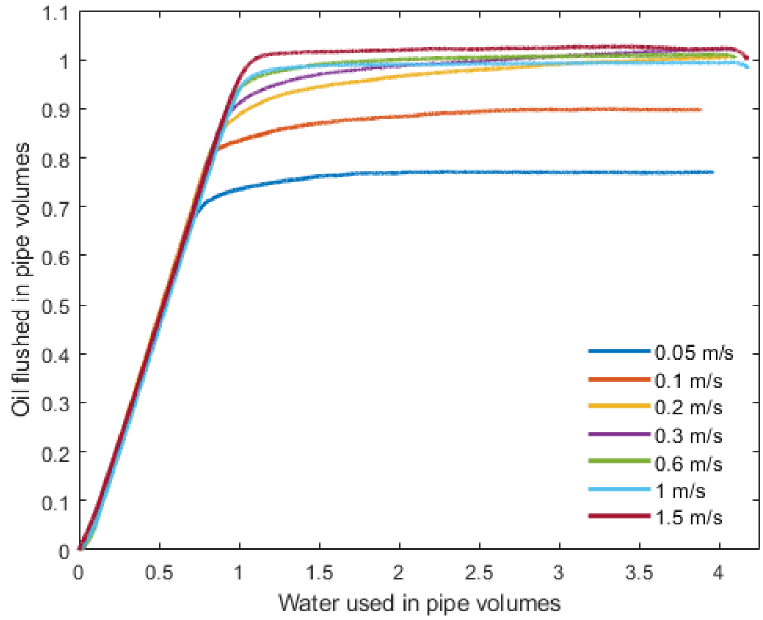

Figure 4.8: Fuchs oil flushed from the pipeline containing two U-sections, at several velocities.

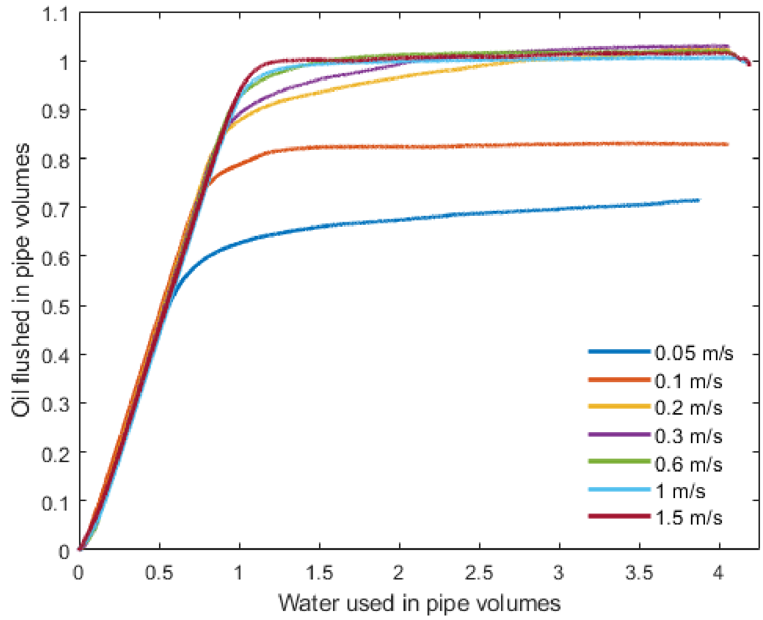

Figure 4.9: Fuchs oil flushed from the pipeline containing two V-sections, at several velocities.

In general, the oil seems to be flushed almost as good compared to the completely horizontal straight pipe section experiments, even though there are some significant negative inclined sections in the U and V setups. The more inclined sections showed more mixing between the two phases, which seemed to increase the flushing. A further study into where the transition point lies between stratified flow and mixing was performed, the results are shown in section 4.4.3.

The bends in the pipe sections had an adverse effect on the flushing. An example can be seen in figure 4.10, which shows a part of one of the V sections, for a flow of 0.1 m/s. The oil upstream of a downward bend is not fully flushed by the water.

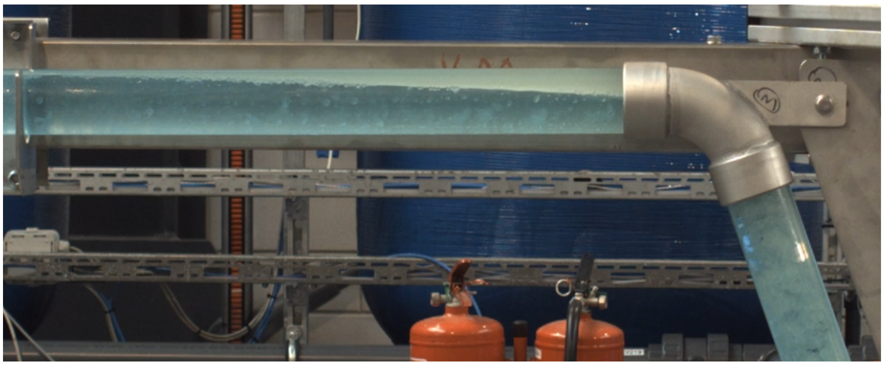

Figure 4.10: Oil residue stuck upstream of a sudden bend in the setup.

A comparison between the horizontal straight pipe, a -2° inclined straight pipe, a double V-section and a double U-section can be seen in figure 4.11. The superficial water velocity used in these four experiments was 0.1 m/s.

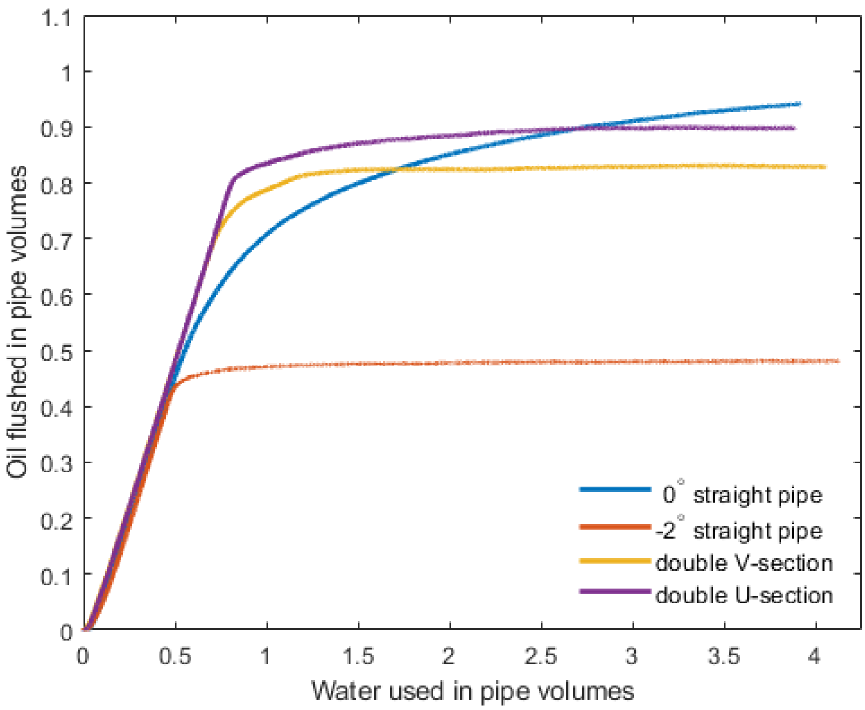

Figure 4.11: Comparison between the a straight pipe with an orientation of 0° and -2° and U and V-sections for Fuchs oil at a superficial water velocity of 0.1 m/s.

Where in the -2° inclination experiment, no further oil is flushed at a certain point, the oil in the U- and V-section experiments is flushed considerably better, despite the presence of the downward inclined sections in these experiments. The V-section pipe seems to be flushed the best, likely because this geometry induces the most mixing between the two phases compared to the other three geometries.

4.2 Mass Flow Meter Data Analysis - Mobil Velocite No. 10 Oil

As a follow up on the Fuchs oil experiments, the same straight pipe experiments were repeated with Mobil Velocite No. 10 oil. The results from the data analyses is shown in this section. To study the effects of larger inclinations, experiments with an angle variation from 0° to 90° were also added. The results of these experiments are shown in section 4.3.2.

4.2.1 Straight Pipe Section Experiments

Figures 4.12, 4.13, 4.14 and 4.15 show the results of the experiments in a straight pipe for the Mobil oil.

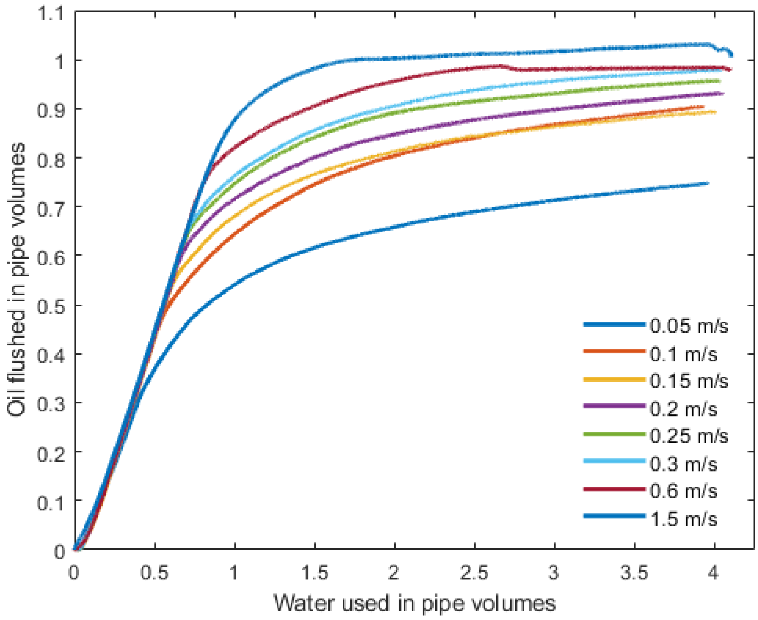

Figure 4.12: Fuchs oil flushed from the pipeline at an orientation of 0° at several velocities.

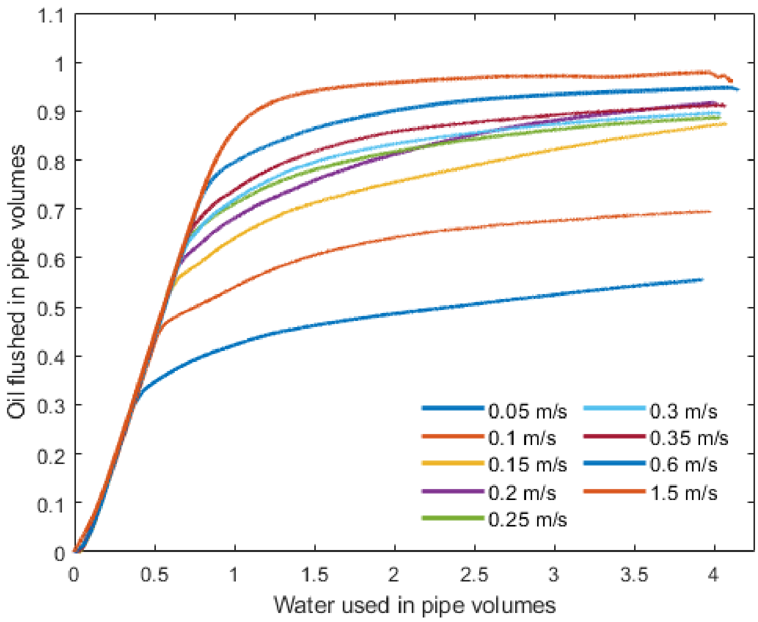

Figure 4.13: Fuchs oil flushed from the pipeline at an orientation of -1° at several velocities.

What can be observed from figures 4.12 and 4.13 is that a higher flushing velocity is beneficial for the flushing process. At these inclinations of 0° and -1° the flushing process has not yet reached a plateau when the four flushing volumes have been reached, suggesting that by flushing with more water, more oil might be flushed from the pipe.

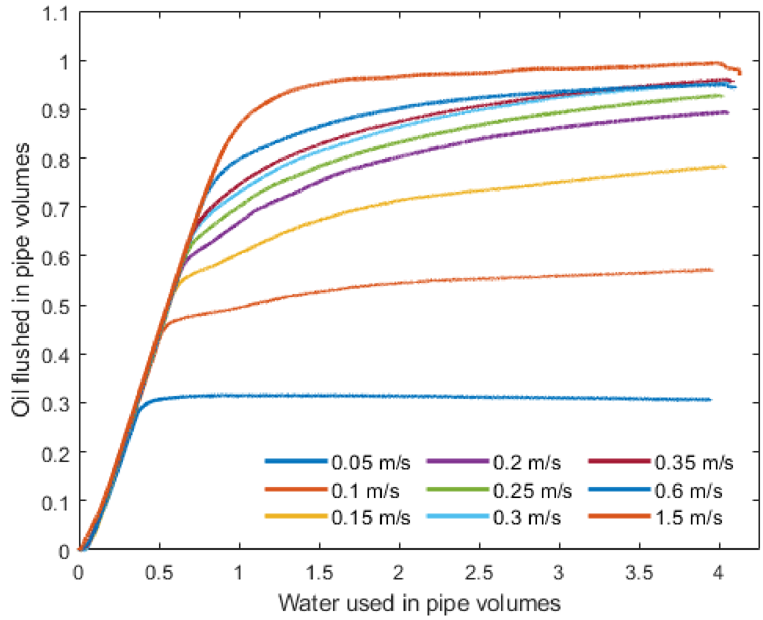

Figure 4.14: Fuchs oil flushed from the pipeline at an orientation of -2° at several velocities.

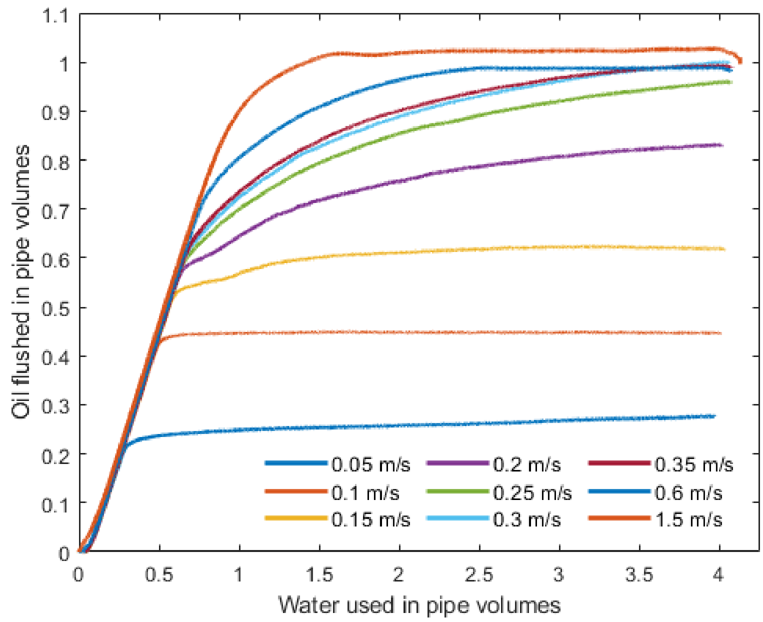

Figure 4.15: Fuchs oil flushed from the pipeline at an orientation of -5° at several velocities.

In figures 4.14 and 4.15 the experiments for a pipe inclination of -2° and -5° are shown. For the lower flushing velocities in these experiments, the flushing process reached an equilibrium relatively quickly. When the incoming stream of water has pushed some of the oil out of its way, not much more oil is flushed, and the water phase flows underneath the oil phase. The same phenomenon seems to be taking place for superficial water velocities of 0.15 m/s and 0.2 m/s in figure 4.15, where an equilibrium is reached and no further oil is flushed.

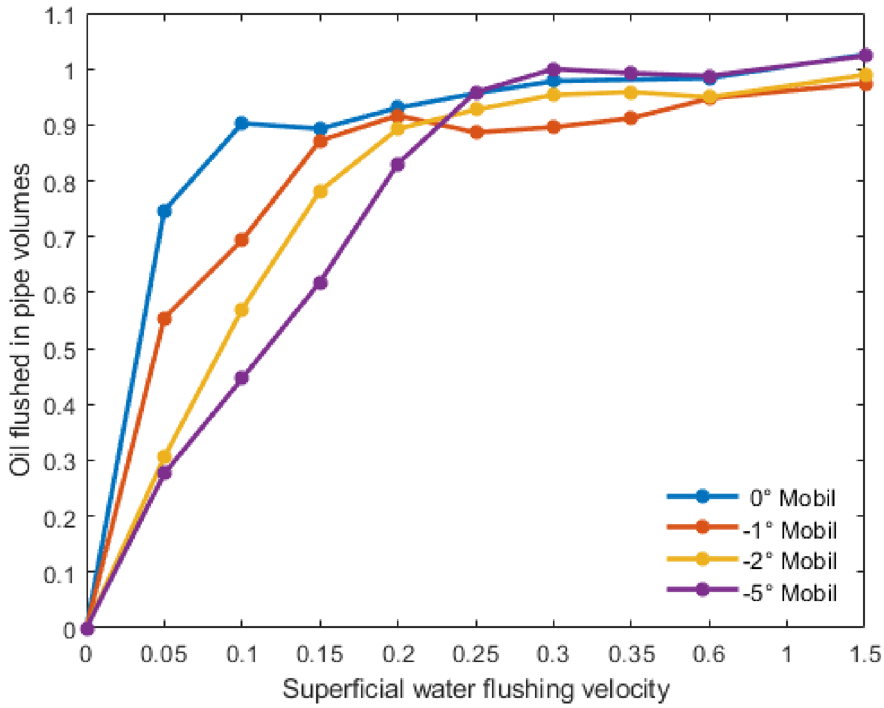

Figure 4.16: Mobil oil flushed from the pipeline after 4 flushing volumes, at several orientations and velocities.

An overview of all straight pipe experiments with Mobil oil is found in figure 4.16. Note again that in this figure only the end values after 4 pipe volumes are displayed. The trend is, just like with the Fuchs Renolin DTA7 oil, that a higher flushing velocity leads to a more thorough oil abandonment of the pipe section. Similarly, a flushing velocity ≥ 0.3 m/s seems to be sufficient to flush the bulk of the oil from the pipeline.

4.3 Mass Flow Meter Data Analysis - Fuchs Renolin DTA7 and Mobil Velocite No. 10 Oils - End Value Comparison

Figure 4.17 summarises the end values for the over 60 experiments in the straight pipe section. for both Fuchs and Mobil oil. Later in this section the flushing curves are compared between the two types of oil.

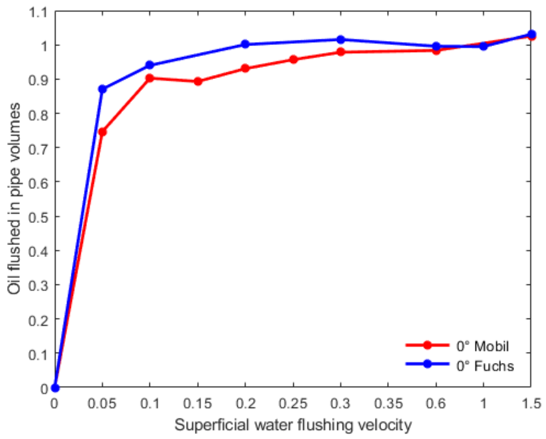

(a) Pipe orientation of 0°.

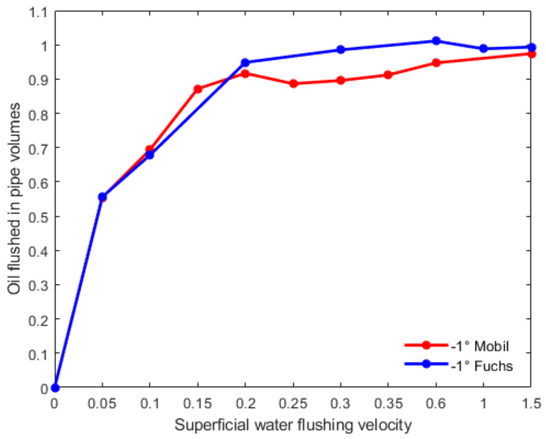

(b) Pipe orientation of -1°.

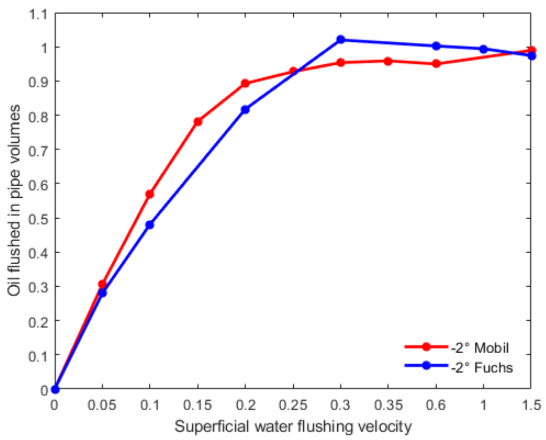

(c) Pipe orientation of -2°.

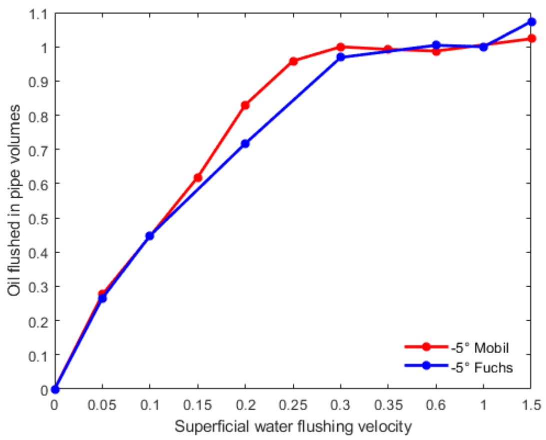

(d) Pipe orientation of -5°.

Figure 4.17: End value comparisons between the selected Fuchs and Mobil oils, all after four flushing volumes of water. The pipe orientation for each figure is found in its caption, the superficial water velocity on its x-axis, and the flushing fraction on the y-axis, where a value of 1 means full flushing.

At an inclination angle of 0°, it is clear that the more dense and viscous Mobil oil is flushed less efficiently from the pipe section than the less dense, less viscous Fuchs oil. Both oils, however, were fully flushed from the pipe section at a flushing velocity of 0.3 m/s. This trend does not continue for negative inclinations. For an inclination of -1° both oils flush equally well, but for the inclinations of -2° and -5° the denser and more viscous Mobil oil is flushed marginally better from the pipeline.

4.3.1 Mass Flow Meter Data Analysis - Fuchs Renolin DTA7 and Mobil Velocite No. 10 Oils - Flushing Curve Comparison

In figures 4.18, 4.19, 4.20 and 4.21 the curve of flushing is shown for a selection of the experiments shown in figure 4.17. The results for experiments done with a superficial water velocity of 0.05, 0.1, 0.3 and 0.6 m/s are displayed, other velocities are left out in this figure for clarity. The experiments done with Mobil oil are displayed with a continuous line, whereas those performed with Fuchs oil are represented with a dashed line.

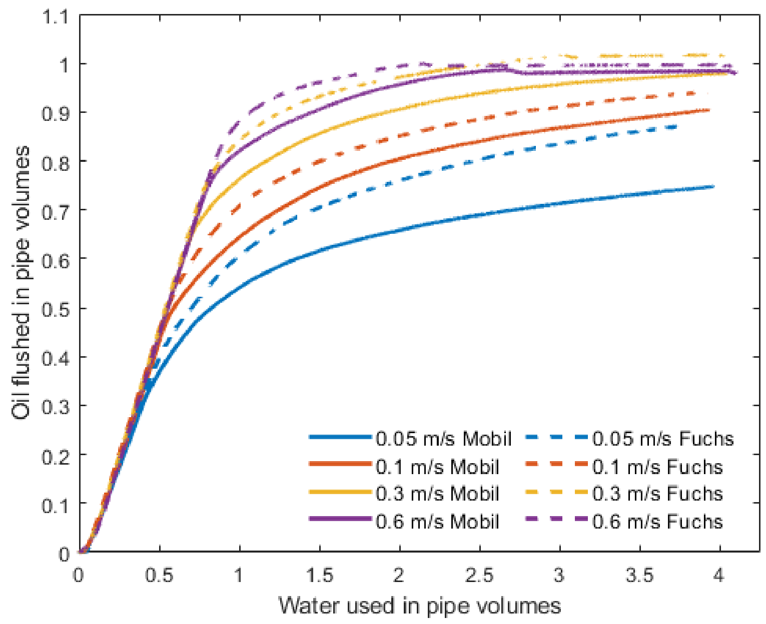

Figure 4.18: Flushing curve comparison between Fuchs and Mobil oil for the amount of oil flushed for a pipe orientation of 0° at several velocities.

Like in the comparison in figure 4.17, it is seen clearly in figure 4.18 that for a horizontal pipe Fuchs oil is flushed from the pipe much better than the selected Mobil oil. Although the amount of flushing is not the same, the shape of the flushing curve is very similar for both oils.

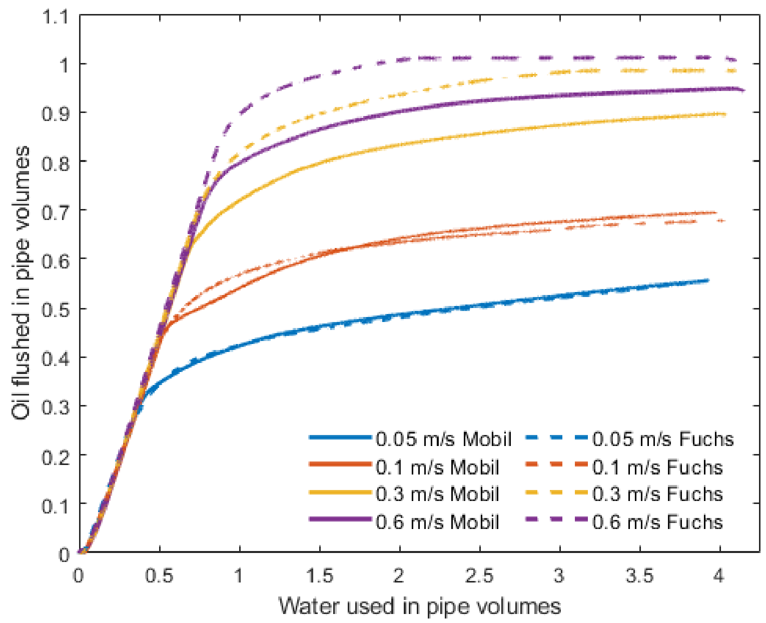

Figure 4.19: Flushing curve comparison between Fuchs and Mobil oil for the amount of oil flushed for a pipe orientation of -1° at several velocities.

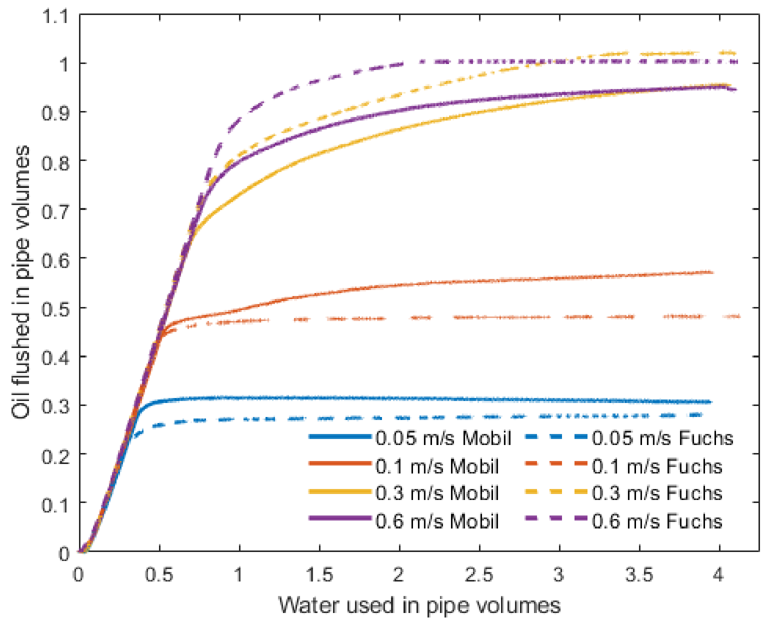

Figure 4.20: Flushing curve comparison between Fuchs and Mobil oil for the amount of oil flushed for a pipe orientation of -2° at several velocities.

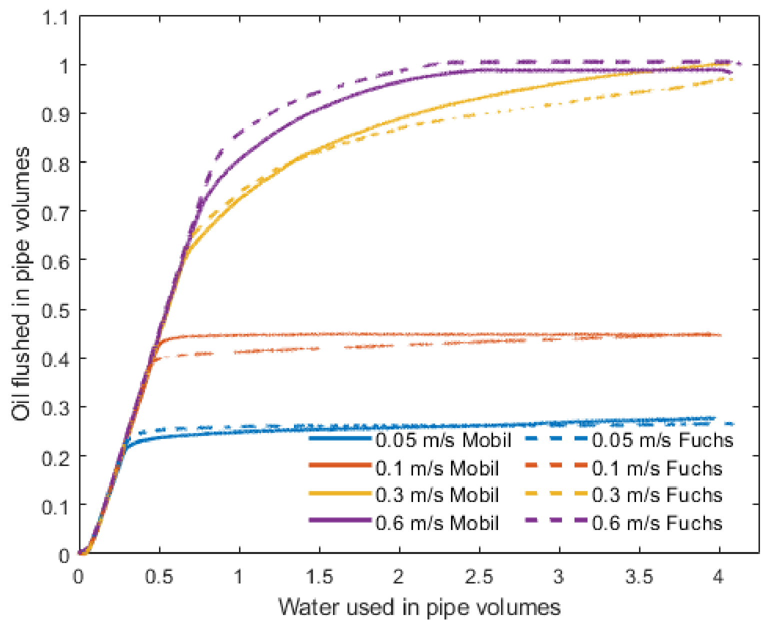

Figure 4.21: Flushing curve comparison between Fuchs and Mobil oil for the amount of oil flushed for a pipe orientation of -5° at several velocities.

Figures 4.19, 4.20 and 4.21 show again that while the final amount of flushed oil is not the same, the shape of the curve of flushing is very similar for both types of oil, for the same flushing velocity and inclination.

4.3.2 U-section 0° to 90° Angle Variation Experiments

In the results for the U- and V-section pipe geometries during phase II of the flushing project performed with Fuchs Renolin DTA7 oil, improved flushing was observed compared to the slightly negatively inclined straight pipe setup. This is because when inclinations are small, little mixing occurs between the phases, and the flushing efficiency is low. In the experiments involving large inclinations, a lot of mixing was observed, which is beneficial to the flushing efficiency. The question that arises is where the transition is between these two flow regimes.

Section 4.4.3 shows the results regarding the 0° to 90° angle variation experiments for the video data analysis, which are much more clear than the flow meter data analysis.

To study the effect that a more steep inclination has on the flow, additional experiments were performed using the U-sections. The upstream U-section was held stable in a vertical position. The downstream U-section was rotated in the axial direction, between a horizontal position and a vertical one. More information and a picture of the setup can be found in section 3.1. Using the U-section meant that only a small section of the total length of the pipe would rotate to the desired orientation. The rest of the setup would remain stable between the different experiments. This means that the difference in the fraction of oil that is flushed from the pipe is relatively limited, making it harder for the mass flow meters to detect the difference. Therefore, the video analysis system is used to determine the water holdup.

Figure 4.22 shows the flow meter data analysis results for the 0° to 90° angle variation experiments with a superficial water velocity of 0.05 m/s. Figure 4.23 shows the results for a superficial water velocity of 0.1 m/s. In subfigures 4.22a and 4.23a the full experiments can be seen, in subfigures 4.22b and 4.23b a zoomed-in version of those same experiments is shown, such that the final flushing values are more clear. The horizontal orientation shows better flushing than the inclined orientations, but other than that, no clear trend can be made out between the different orientations.

A difference to some degree is expected between the curves, since the geometry of the pipe is not the same between each curve. The curves show an uncertainty however that is larger than to be expected. Section 6.1.2 treats the reproducibility of the mass flow meters in more detail.

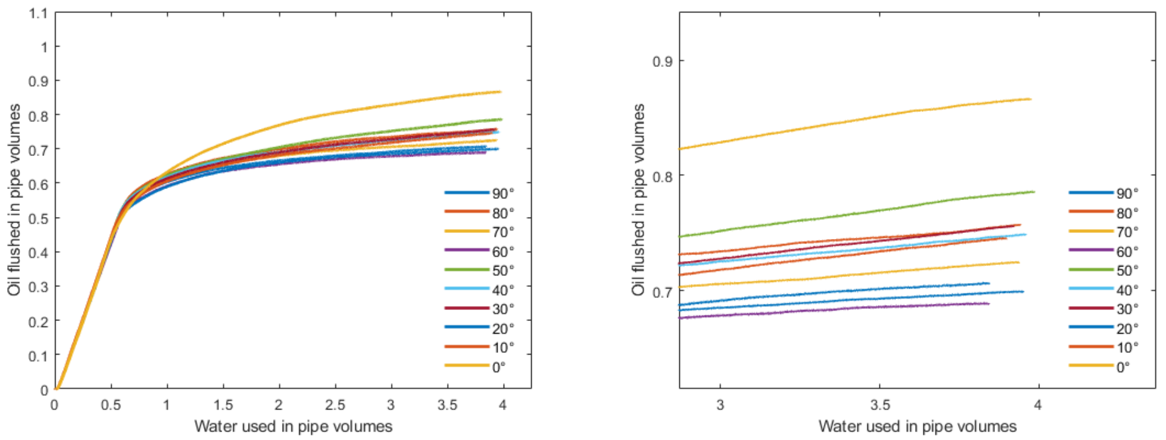

(a) (b)

Figure 4.22: Flow meter data for the amount of Mobil oil flushed for angle variation between 0° and 90° relative to the horizontal plane for 0.05 m/s superficial water velocity.

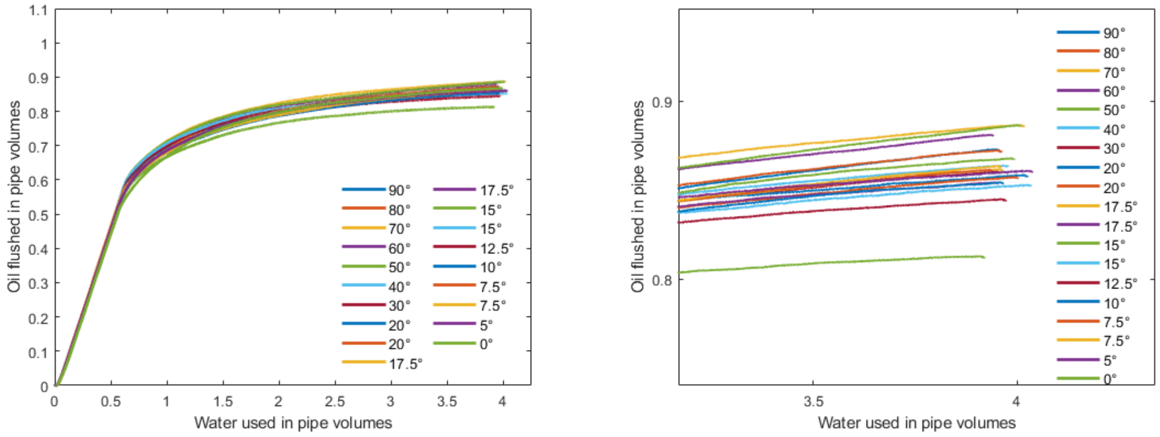

(a) (b)

Figure 4.23: Flow meter data for the amount of Mobil oil flushed for angle variation between 0° and 90° relative to the horizontal plane for 0.1 m/s superficial water velocity.

4.4 Video Data Analysis

Apart from collecting data with the mass flow meter system, every experiment was also recorded using the video data acquisition system. This footage was used for visual observations, but more importantly, used to determine the holdup in the experimental pipe section using a script developed in the software tool MATLAB. A detailed coverage of the video data acquisition system can be found in section 3.5.3. The results of video data analysis are shown in this section.

Like mentioned in section 3.5.3, the 3D contours of the two phase interface are only partly captured on the 2D camera image. To present the data more clearly, a moving average has been applied to the curves in the video data analysis results below. A moving average of ± 6 seconds has been applied as this gave the best results with respect to the water holdup in the pipe, without losing too much detail. The interfacial wave height increases as the superficial water velocity increases. This affects the video data analysis, which is why the video data analysis is only applied up until a superficial water velocity of 0.3 m/s. A steeper inclination also increases the height of the interfacial waves, which decreases accuracy of the holdup curves. This effect is seen in the latter video data analysis section 4.4.1.

In each of the sets of video data results, two smaller figures are displayed which represent the upstream and downstream camera respectively. In the larger figure the average of the two is displayed. Note that this does not necessarily equal the average water holdup in the full pipe, as the cameras only see about 1/12th each of the total pipe length. Another observation might be that the curves in the second small figure never originate at zero. This is because it takes some time for the water to reach this part of the pipe section after flushing is commenced.

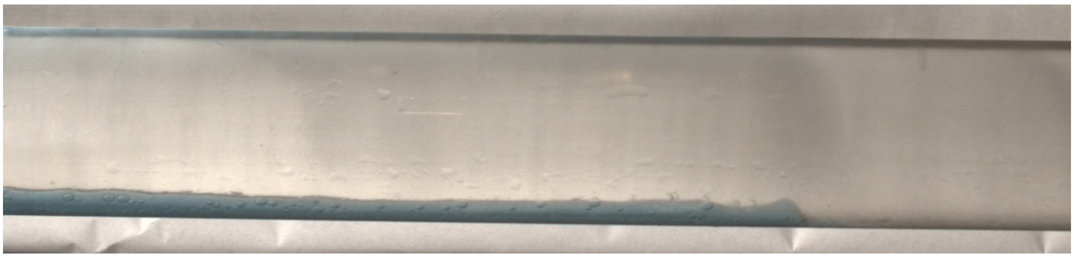

(a) Low velocity flow water front.

(b) High velocity flow water front.

Figure 4.24: Difference in water front shape between low and high superficial water velocity flow.

For the lower superficial water velocity, the flushing curve initially rises to a higher value than the curves for a higher superficial water velocity. This is seen best in the downstream camera. Due to the lower water front (see figure 4.24a), the first water reaches the camera after a smaller flushed water volume. The highest superficial water velocities move the oil in an almost piston like motion, pushing a larger fraction of oil ahead of the water front(see figure 4.24b). Although a higher velocity flushes a lot of oil quickly in terms of time, in terms of water used, this is "slower". The camera data can give a detailed picture of this varying holdup throughout the pipe, something the mass flow meters cannot detect. A schematic overview of the camera setup including dimensions was provided in section 3.6.

Another observation is that the flushing curve observed by the downstream camera is not the time-delayed curve observed by the upstream camera. Drawing an imaginary control volume(CV) around the section of pipe that is seen by the camera can explain this phenomenon. Since the upstream camera is closer to the inlet of the pipe, this control volume is mostly fed with water from the upstream side, while a mixture of water and oil leaves the CV on the downstream part. This causes the number for the water holdup to increase to unity quickly.

When again imagining a similar control volume for the downstream camera, this CV is fed with a mixture of oil and water from the upstream side of the pipe, while a slightly richer oil-water mixture leaves this CV on the downstream side. This lower difference in entering and leaving oil causes the water holdup to rise slower.

4.4.1 Straight Pipe Section Experiments

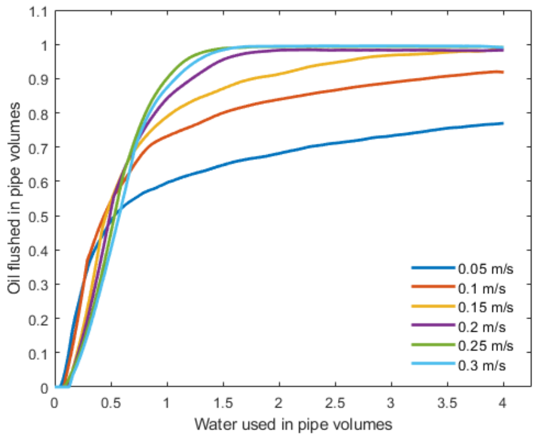

(a) Video analysis for Mobil oil, left camera.

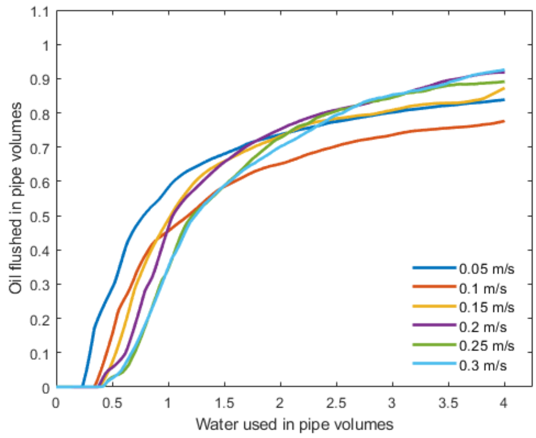

(b) Video analysis for Mobil oil, right camera.

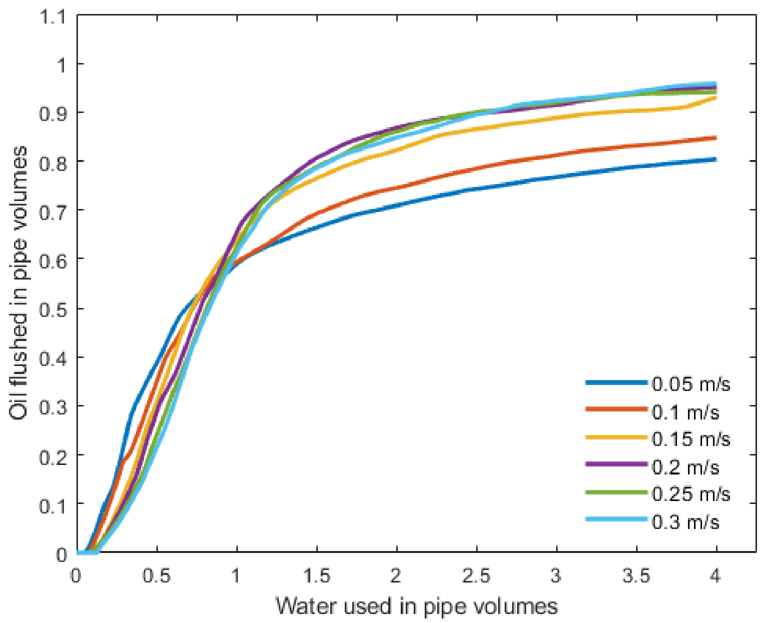

(c) Video analysis for Mobil oil for the amount of oil flushed for an pipe orientation of 0° at several velocities, average of the two cameras.

Figure 4.25

Figure 4.25 shows the video data analysis for Mobil Velocite No. 10 oil, with a horizontal pipe orientation. The difference in holdup between the up- and downstream parts of the pipe as described in the previous paragraph is seen clearly. The upstream part of the pipe flushes relatively quickly, while the downstream section takes more time. The average of the two curves can be seen in part 4.25c. Although the average water holdup for the two camera sections does not necessarily equal the average holdup throughout the whole pipe, the flushing curve produced by the camera data system is very similar in shape to the curve produced with the mass flow meter data analysis, seen earlier in this chapter.

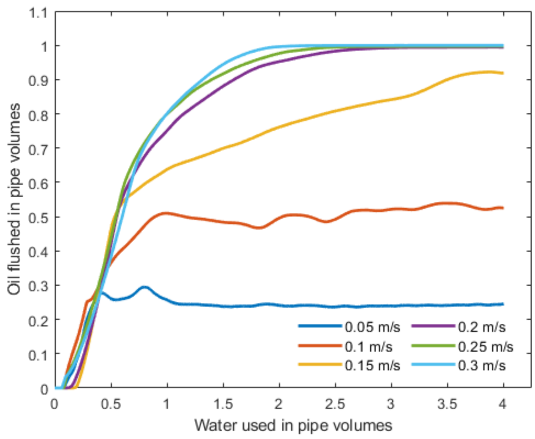

(a) Video analysis for Mobil oil for the amount of oil flushed for a pipe orientation of -1° at several velocities, left camera.

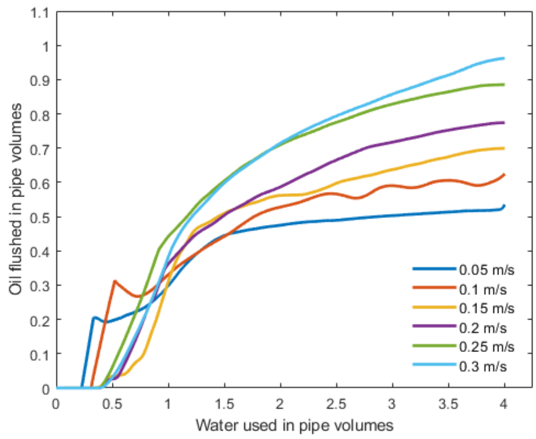

(b) Video analysis for Mobil oil for the amount of oil flushed for a pipe orientation of -1° at several velocities, right camera.

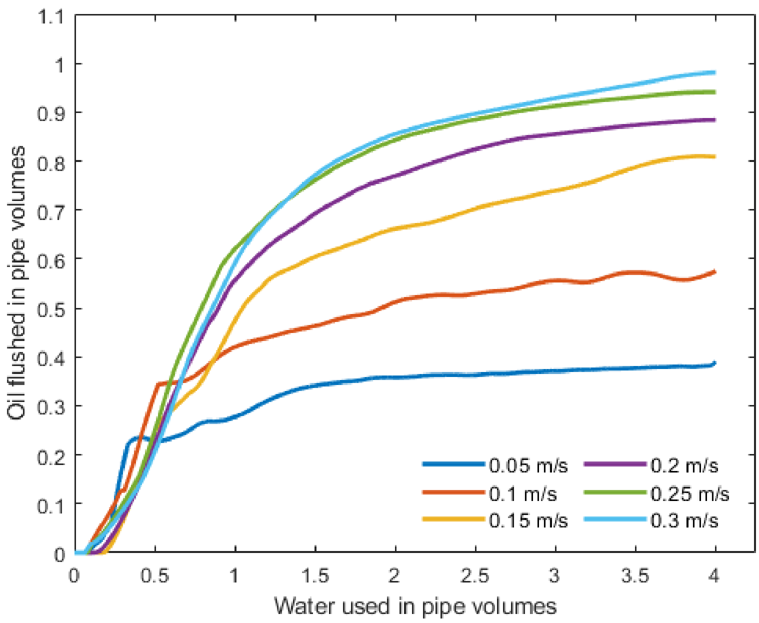

(c) Video analysis for Mobil oil for the amount of oil flushed for a pipe orientation of -1° at several velocities, average of the two cameras.

Figure 4.26

Figure 4.26 shows the the video data analysis for Mobil oil, where the pipe orientation is downward inclined with an angle of -1°. In part 4.26b it can be seen that the shape of the initial water front causes some extra variation in the curve, but the rest of the curves show a clear representation of the water holdup in the selected sections of the pipe. Figure 4.29 treats the shape of this front and its effect on the video analysis further.

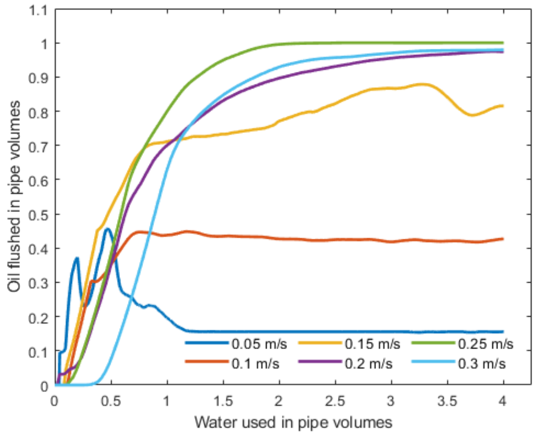

(a) Video analysis for Mobil oil for the amount of oil flushed for a pipe orientation of -2° at several velocities, left camera.

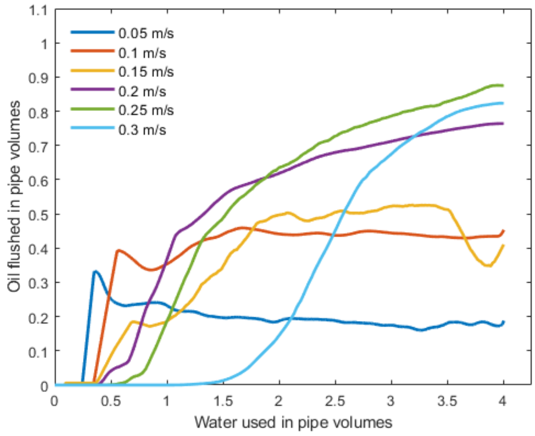

(b) Video analysis for Mobil oil for the amount of oil flushed for a pipe orientation of -2° at several velocities, right camera.

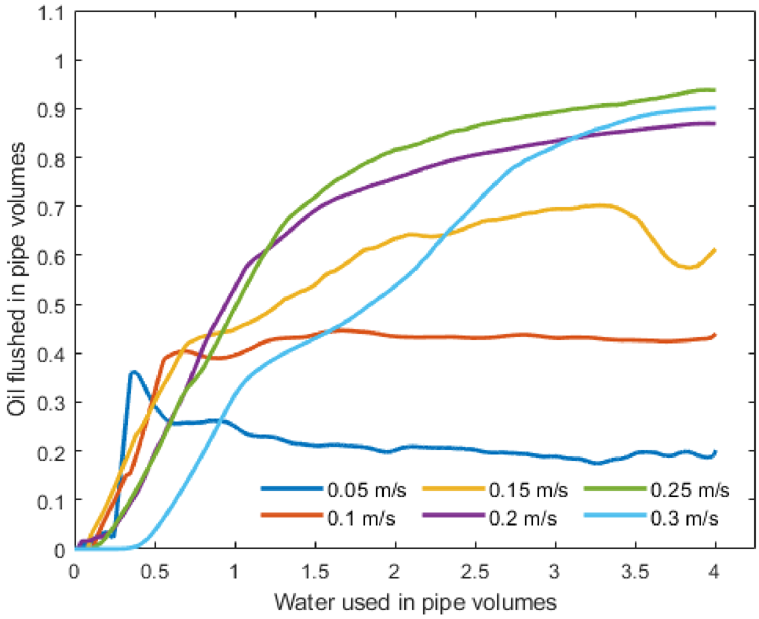

(c) Video analysis for Mobil oil for the amount of oil flushed for a pipe orientation of -2° at several velocities, average of the two cameras.

Figure 4.27

In figure 4.27 the effects of increased interfacial wave heights on the video data analysis become apparent, as the holdup curves become more erratic. The measurement for the downstream camera(4.27b) and 0.3 m/s is off, through influences of ambient lighting like a ray of sunlight striking the pipe section. Unfortunately, factors like the difference in ambient lighting levels and the increased height of interfacial waves make the holdup curves less representative of the actual holdup.

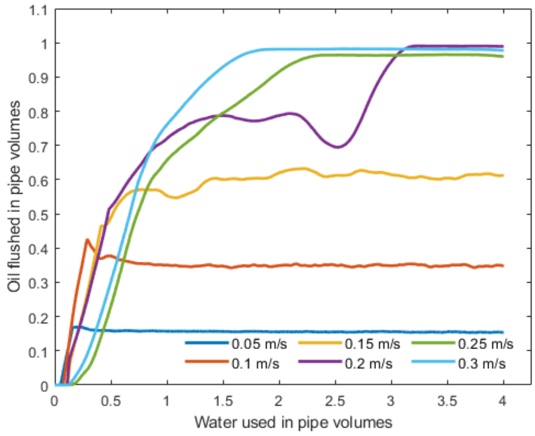

(a) Video analysis for Mobil oil for the amount of oil flushed for a pipe orientation of -5°, left camera.

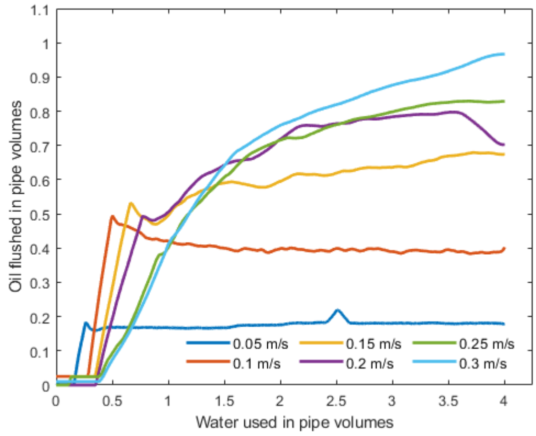

(b) Video analysis for Mobil oil for the amount of oil flushed for a pipe orientation of -5°, right camera.

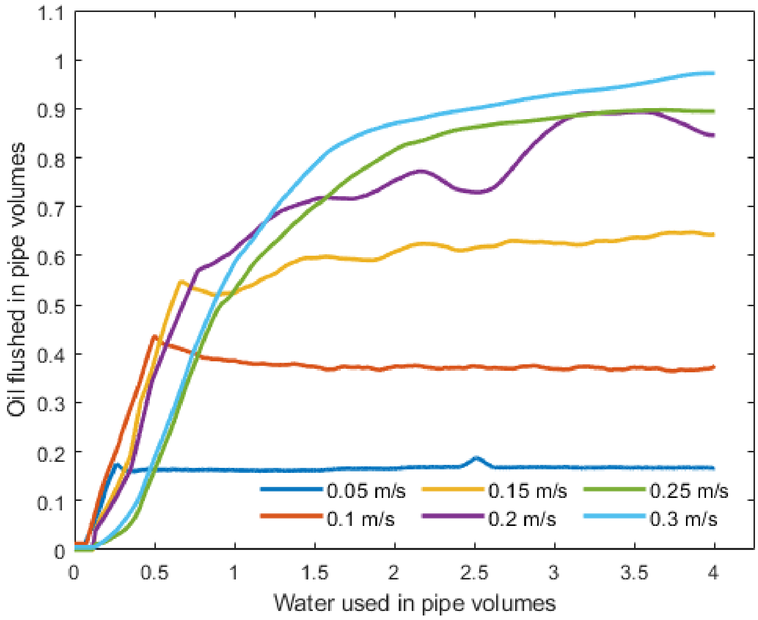

(c) Video analysis for Mobil oil for the amount of oil flushed for a pipe orientation of -5° at several velocities, average of the two cameras.

Figure 4.28

The initial water front develops even more strongly in the steeper inclined orientations. The downstream holdup(figure 4.28b) shows an initial peak for velocities of 0.05 to 0.2 m/s, which is the cause of this initial water front. The image in subfigure 4.29a shows this initial water front for an inclination of -5° and a superficial flow velocity of 0.05 m/s. Subfigure 4.29b displays the same experiment, only 4 seconds later. After the initial water front has passed, the local water holdup decreases significantly. To visualise a similar looking effect, one might think of a dry riverbed flash flood, where the front of the flood is slowed by debris. while the water following this front catches up quickly, increasing the volume and height of the front. The applied moving average lessens the effect in the curves in figure 4.28b, but the initial peak caused by the water front can still be observed.

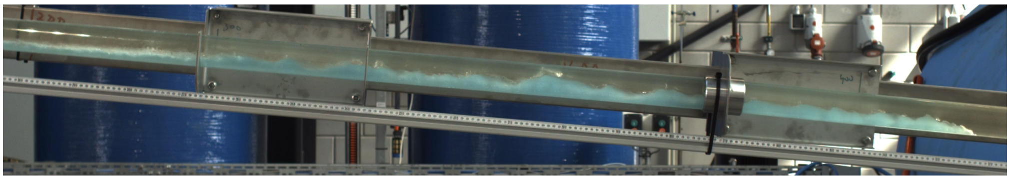

(a) Initial water front, -5°, 0.05 m/s.

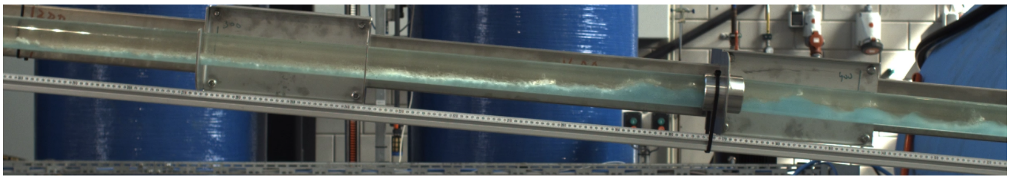

(b) Same initial water front, 4 seconds later.

Figure 4.29: A water front develops along the pipe, with a higher water holdup leads, where-after a lower water holdup follows. To visualise a similar looking effect, a dry riverbed flash flood can be thought of.

4.4.2 Comparison Between Mass Flow Meter and Video Data - End Values

To summarise the experiments performed with the straight pipe section, figure 4.30 shows an end value comparison for the two data analysis methods. The blue bars display the final flushing values determined using the flow meter data, the red bars display the final flushing values determined using the video analysis data. Although the two methods agree very well on the average flushing value, with only a 0.13 percentage point difference, the variance between the two methods is quite significant. This variance is the largest for the lowest superficial water velocities. These measurements last the longest, allowing more time for ambient lighting conditions to change, affecting the measurements of the video system.

Both methods agree very well on the trends that an increased flushing velocity and a more horizontal orientation are beneficial to the flushing process. Caution should be taken however when taking the precise final flushing values, because of the significant spread between the two methods. A detailed comparison between the end values for both methods is found in the discussion chapter 6.

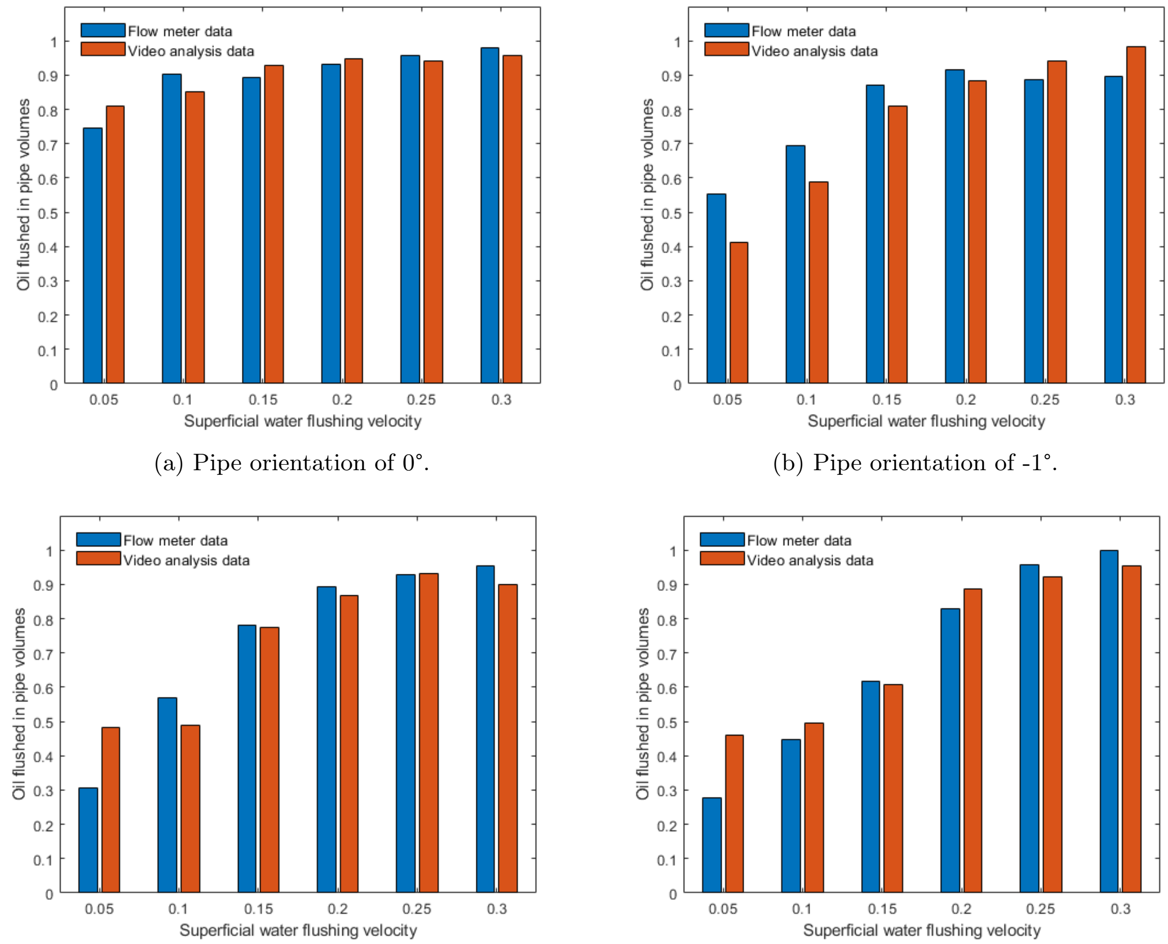

(a) Pipe orientation of 0°.

(b) Pipe orientation of -1°.

(c) Pipe orientation of -2°.

(d) Pipe orientation of -5°.

Figure 4.30: Comparison between the flow meter data and the video analysis data for the amount of oil flushed after 4 pipe volumes flushed.

4.4.3 Video Data Analysis - U-section 0° to 90° Angle Variation Experiments

To study the effect that a more steep inclination has on the flow, additional experiments were performed using the U-sections. While the upstream U-section was held constant, the downstream U-section was rotated in the axial direction, creating a section of pipe in which 0° to 90° experiments could be performed. For the vertical arrangement of the U, an equilibrium is reached early in the experiment, as can be seen in figure 4.8 in section 4.1.2. Apart from this section staying constant between all 0° to 90° experiments, this ensures that oil coming from the upstream U-section does not interfere with the angle variation experiments. More detail on the operations of these experiments is found in section 3.4.

These experiments were performed with a superficial water velocity of 0.05 m/s. This velocity turned out to be insufficient, because the oil holdup in the horizontal part of the pipe would reach one for certain experiments using this geometry, without all oil being settled. Thus, the experiments were repeated with a superficial water velocity of 0.1 m/s.

Figure 4.31 shows the results of the data analysis. The x-axis displays the inclination angle of the selected pipe section, the y-axis displays the holdup in the horizontal pipe section. Note that the value for the holdup does not mean the same as in the other figures in this report. The total amount of oil in this horizontal pipe section between the U-sections, consists of oil not fully flushed because of the downward bend entering the U-section, and oil that drifts back up from the tilted pipe section of interest.

The goal of this part of the study was to find the transition point where the flushing efficiency would be lowest and highest, not necessarily to attach a specific number to the holdup in the tilted section. Instead of providing a possibly inaccurate number for the holdup in the vertical section, the effect of the angle variation can be shown directly by looking at the holdup settled in the horizontal section. The resolution of angle variation was increased in the angle range for which the flushing efficiency was lowest.

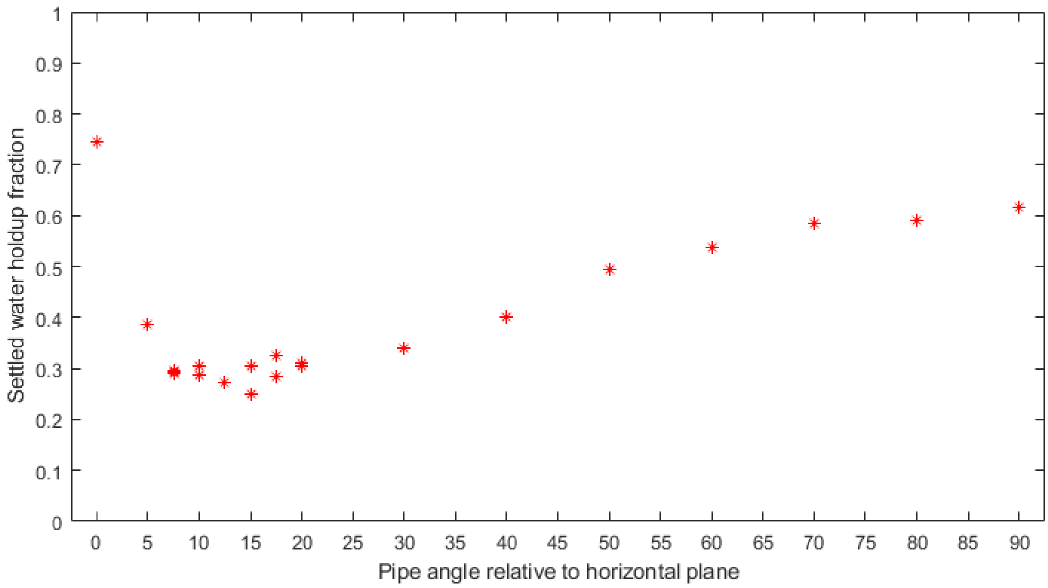

Figure 4.31: Amount of oil that is flushed represented by a non-dimensional flushing factor on the y-axis, drawn against the angle of the pipe in each experiment

The flushing efficiency was highest for the case where the pipe section was oriented horizontally, like expected from the straight pipe experiments. Decreasing the angle of inclination relative to the horizontal, the flushing efficiency deteriorates quickly. The transition point seems to be around the 7.5° to 20° range for Mobil Velocite No. 10 oil and a superficial water velocity of 0.1 m/s. At this point, interfacial waves are forming, but their amplitude is not sufficient enough to induce enough mixing for the water to flush the oil. The four figures in figure 4.32 show this transition in flow regime, after roughly one pipe volume of flushing. Note that the camera is oriented to the same angle as the pipe, the caption mentions the angle relative to the horizontal plane.

When the pipe section is turned downwards even more, the interfacial waves break up and the two phases start to mix. This causes the flushing efficiency to rise again, with a local maximum at 90° relative to the horizontal plane, as more and more mixing occurs. Note again that the value for the water holdup is determined in the horizontal part between the two U-sections, and does not directly equates to the holdup in the tilted pipe section.

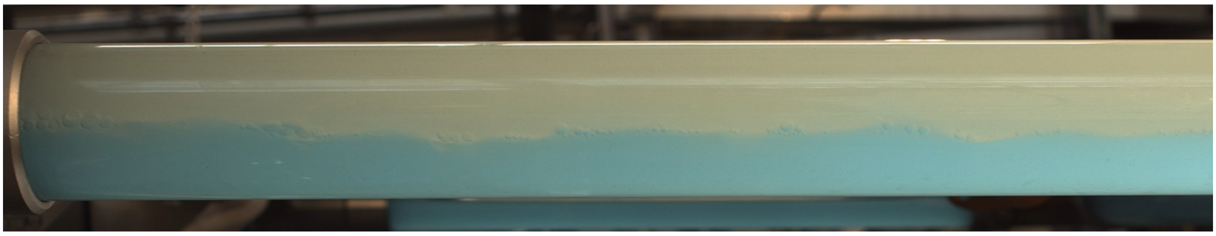

(a) Pipe orientation of -5°.

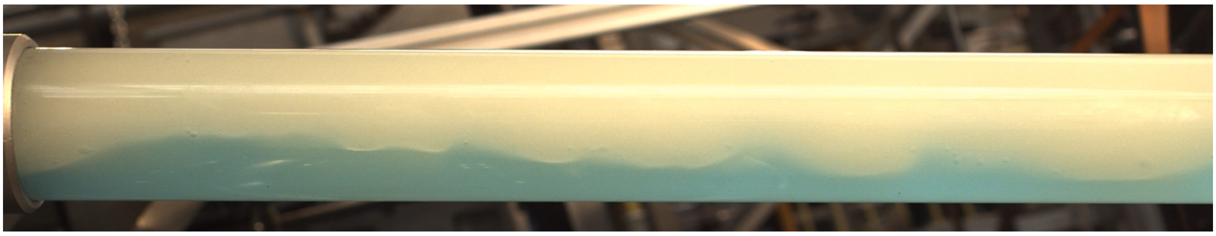

(b) Pipe orientation of -15°.

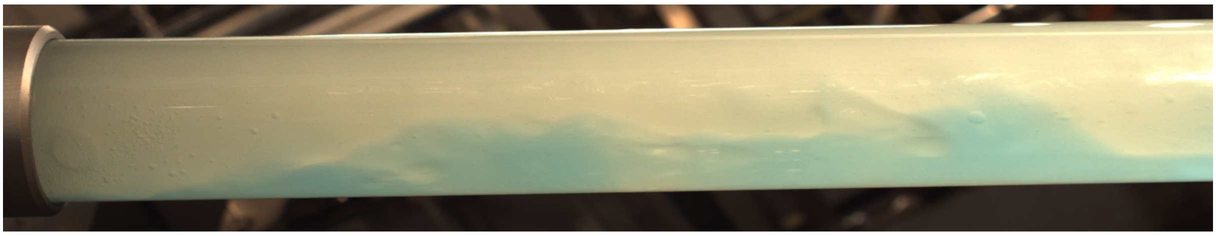

(c) Pipe orientation of -30°.

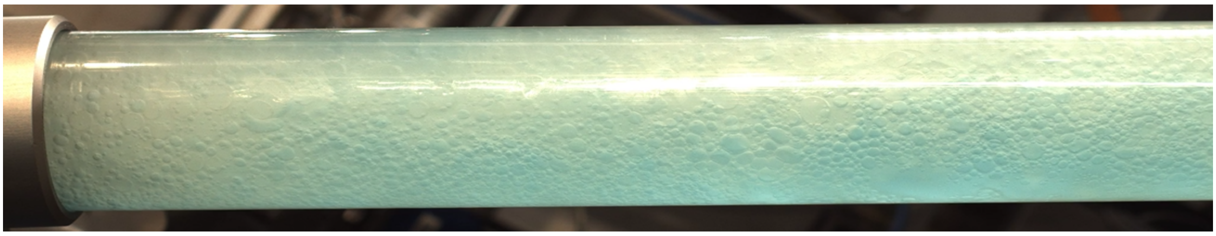

(d) Pipe orientation of -60°.

Figure 4.32: Flow transitioning from stratified to wavy to mixed for various pipe inclinations relative to the horizontal plane.

5 | Modelling Results

As an addition to the experimental work, the straight inclined pipe section experiments have been simulated using the dynamic multiphase flow simulation software tool OLGA. This chapter first provides an introduction to the model used, and its inputs. Sensitivity studies performed on the model are shown, which substantiate some of the model inputs.

In the second part of the chapter the results of the simulations are shown. Since the software tool allows varying individual parameters, two additional, virtual oils are introduced, and the results of those simulations are shown in this section as well. Interpretations are provided too, more in depth interpretation and the treatment of some peculiarities will be done in the Discussion, chapter 6.

The chapter concludes with a comparison between the different types of oil, and their effect on the final results of the amount of oil flushed after each experiment. This is done to provide an answer to the question to what extent the density and viscosity influence the flushing dynamics.

5.1 OLGA - Model Inputs, Design and Sensitivity Analysis

5.1.1 Dynamic Multi-phase Flow Simulation Software Tool OLGA

OLGA is a dynamic multiphase flow simulation software tool. It is used to provide a more detailed understanding of flow behaviour without having to perform physical experiments. OLGA models time-dependent behaviours, or transient flow, which provides an added dimension to steady-state analyses by predicting system dynamics such as time-varying changes in flow rates, fluid compositions, temperature, solids deposition and operational changes. OLGA is used a lot in the Oil and Gas discipline, hence its name.

In this study, OLGA is used to model the straight pipe experimental setup used in the experiments. The results coming out of these simulations are compared with the flow meter and video data results in chapter 6. The setup is modelled as simple as possible, as can be seen in figure 5.1. The left hand, upstream side is closed off, a source is put in place to impose a mass flow. The flow coming from the source flows through a 5.65 meter long pipe with a diameter of 56 mm, towards the outlet.

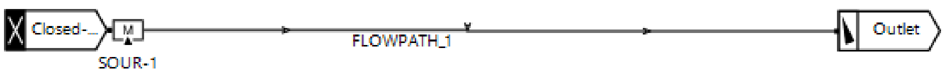

Figure 5.1: OLGA model of the straight pipe setup.

To model the setup, the following initial and boundary conditions were implemented. The content of the pipe prior to starting of the experiment is solely oil, just like in the experiments. The flushing water originates from the source, located at the start of the pipe section. For the simulation to converge, a possibility for inflow from the outlet of the pipe section had to be put in place. In the simulation this inflow is set to water, but in all of the tests a positive flow was observed, regardless of other conditions. In other words, no inflow from the outlet takes place. To simplify the model, all fluids were set to a temperature of 20 °C, without any transport of heat through the pipe walls. The minimum time step was set to 0.001 seconds. The number of elements used in this simulation was set to be the total length divided by pipe diameter, 100 elements were used. Further settings and numbers can be found in table 5.1.

Length	5.65 meter
Diameter	0.056 meter
Wall roughness	5E-5 meter
Temperature	20 °C
Heat transport	NO

(a)

Inlet gas fraction	0
Inlet water fraction	1
Inlet pressure	1 bar
Outlet gas fraction	0
Outlet water fraction	1
Outlet pressure	1 bar

(b)

Min DT	0.0001 sec
Max DT	1 sec
DT start	0.001 sec
Flow Model	OLGAHD
MassEqScheme	2^{nd} order
DT plot	0.5 sec

(c)

Table 5.1: Selection of simulation settings and inputs.

5.1.2 Wall Roughness

The absolute wall roughness of the pipe section is an important factor when looking at flow through a pipe section. It has effects on the pressure loss over the pipe section, and might therefore also have an effect of the flushing efficacy. Figure 5.2 shows 5 simulations performed with Mobil Velocity N10 oil, under an inclination of -5°, with a superficial water velocity of 0.1 m/s. The sole variation between the simulations is the absolute wall roughness. This value is varied between 5E-04 meter and 5E-06 meter.

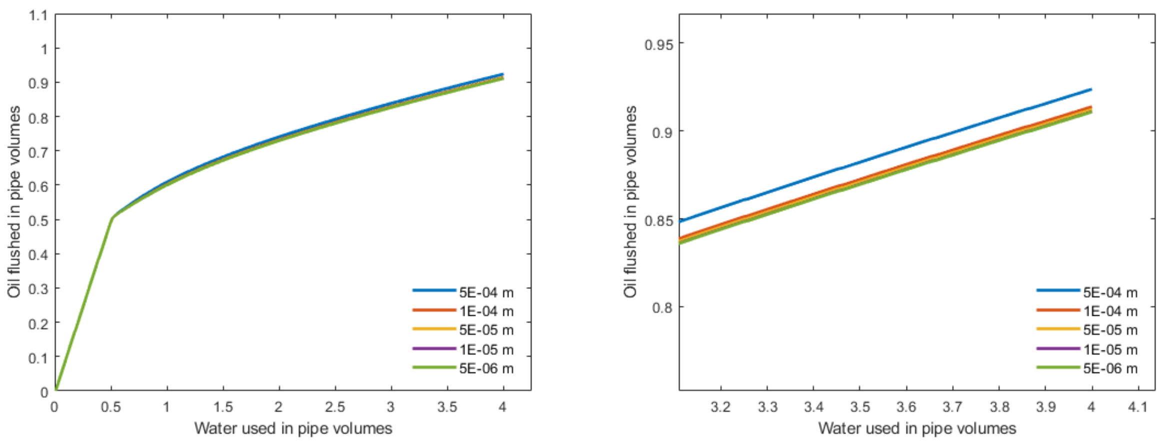

(a) (b)

Figure 5.2: Effect of the wall roughness on flushing efficacy.

From figure 5.2a the conclusion can be drawn that the wall roughness does not have a large impact on the flushing efficacy. A zoomed-in version of the same graph is shown in figure 5.2b. It can be seen that, especially for very smooth walls, a difference in wall roughness needs to be very large for the flushing to be affected. Only when roughness is increased to 5E-04 meter, an increase in flushing efficacy can be observed. A possible cause is that imperfections on the pipe wall cause miniature disturbances in the flow, increasing mixing, which in turn increase the amount of oil that is flushed from the pipe. In the further simulations, an absolute wall roughness of 5E-05 meter is used to represent the polycarbonate pipe wall. This is on the higher end of the range for typical wall roughness for polycarbonate piping[21], to anticipate any roughing during handling and cleaning of the pipes.

5.1.3 Superficial Water Velocity Ramp-up Style

Unlike what is possible in computer simulations, in real world experiments the source at the inlet of the pipe section cannot impose the flow of water with a step function. In the real world experiments, the velocity builds up starting from a zero flow velocity. For the lowest superficial water flow velocity, 0.05 m/s, an overshoot in flow velocity was observed of up to 1.4 times the set flow velocity. For a superficial water flow velocity of 0.1 m/s this overshoot in flow velocity is reduced to only about 10 to 20% of the final set velocity. For higher superficial flow velocities this effect diminishes quickly. The flow velocity buildup phase takes roughly 1.5-2 seconds, regardless of the set superficial flow velocity. After the peak is reached, the superficial water velocity settles to the set value in about 0.5-1 seconds. Figure 5.3a shows the water velocity ramp up for an experiment with an intended water velocity of 0.1 m/s, and a pipe inclination of -5°.

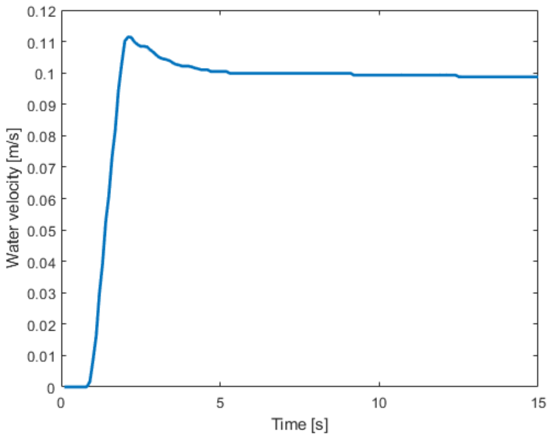

(a) Water velocity buildup for an intended water velocity of 0.1 m/s, and a pipe inclination of -5°.

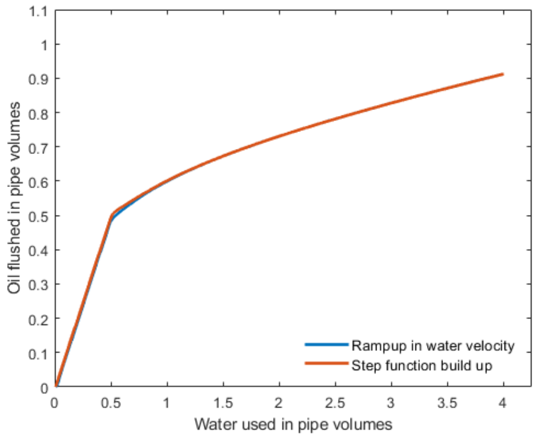

(b) Difference in flushing efficacy between a gradual buildup in water velocity as opposed to a step function type buildup.

Figure 5.3

Figure 5.3b shows two simulations performed with Mobil Velocity N10 oil, under an inclination of -5°, with a superficial water velocity of 0.1 m/s. The variation between the two flows is the type of velocity buildup. In the blue simulation the velocity builds up to 0.125 m/s in 2 seconds, after which the flow settles to the set 0.1 m/s in the following second. The red curve represents a simulation in which the flow is stepped to 0.1 m/s from the start.

At first sight the step function type buildup simulation seems to flush a bit more oil from the pipe. The ramp up type buildup catches up however, after the full four pipe volume flush. The final flushing amounts are 91.238% and 91.232% respectively, showing the insignificant influence of the type of water velocity ramp-up. In the following simulations, the step function type build up is used for all superficial water velocities.

5.1.4 Effects Gooseneck and other Tail Sections

Pieces like the gooseneck or other pipe infrastructure following the experimental pipe section, might have an effect upstream. This section aims to see if this is the case, and if yes, to what extent. Two simulations were performed, one with just the straight pipe setup as described before, and one where an outlet section is added. This tail piece consists of a constriction representing the three way flow valve, a U section representing the flow meter, and an inverted U section representing the gooseneck in the system. In this model, the constriction is modelled with a section of pipe, two pipe diameters long(0.112 meter), with a diameter half of the pipe diameter(0.026 meter). The flow meter is modelled as a U shape, starting with a downward vertical section of 0.3 centimetres high. This U section was modelled to be 0.112 meters wide. The gooseneck was modelled to have the same dimensions as the flow meter, but in this case as an inverted U. The distance between the two is 0.3 meters. This modelled outlet section resembles the outlet of the experimental setup.

Note that the effect of the gooseneck has also been tested in the physical experiments, the results can be found in section 6.1.3.

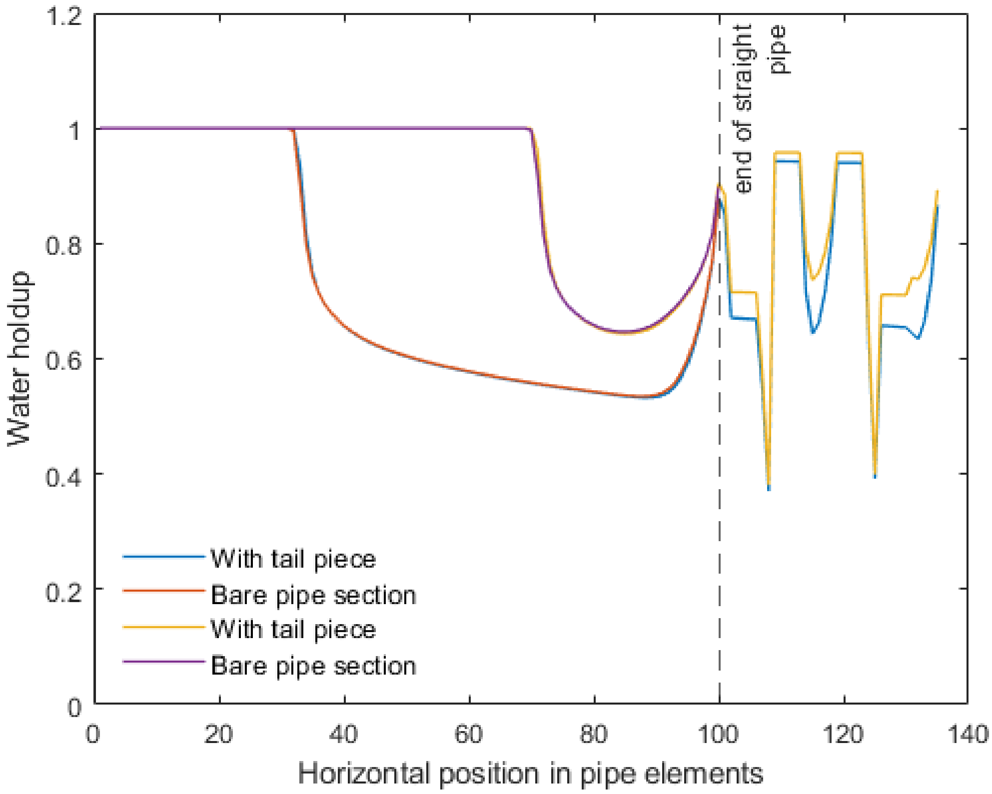

Figure 5.4: Difference in flushing efficacy between the bare experimental pipe section, and the experimental pipe section followed by a tail piece. The blue and red curve represent the local water holdup after 2 pipe volumes of flushing, the yellow and purple curve the local water holdup after 4 pipe volumes of flushing.

Figure 5.4 shows the results for these two simulations. Rather than the previously used representations, this graph displays the flushing curve relative to the position in the pipe section. The blue and red curve represent the local water holdup after 2 pipe volumes of flushing, the yellow and purple curve the local water holdup after 4 pipe volumes of flushing. The experimental pipe section ends after 100 pipe elements, whereafter the section representing the valve, flow meter and gooseneck follows. The exact flushing course of this latter section is not of interest here, as the question is whether there are effects upstream. The curves in figure 5.4 represent the flushing course after 2 pipe volumes and 4 pipe volumes of flushing respectively. What can be seen from these curves is that up until the end of the experimental pipe section the flushing course is practically the same. After 2 pipe volumes of flushing, the difference in average holdup in the pipe is 0.06 percentage points, after the full 4 pipe volumes of flushing this difference is reduced to only 0.027 percentage points. From this result, it is concluded that the simulation can by simplified by leaving out a representation of the downstream infrastructure, without any effect on the simulation of the straight pipe experimental section.

5.1.5 Spatial Solving Scheme, 1st or 2nd Order

Another important factor in the settings of the OLGA simulation is whether to use a first or second order solving scheme. Generally speaking, a first order scheme is more robust and is the preferred choice in most situations. In the case of oil-water flushing, apart from the local water holdup, the shape of the initial water front is also of interest. A second order scheme has less numerical diffusion and is therefore better able to represent holdup fronts. To study the differences between the first and second order schemes, 4 simulations were carried out. Note that the superficial flow velocity is 0.05 m/s in figures 5.5a and 5.5b, and 0.1 m/s for figures 5.6a and 5.6b, as these values gave the best view of the water fronts.

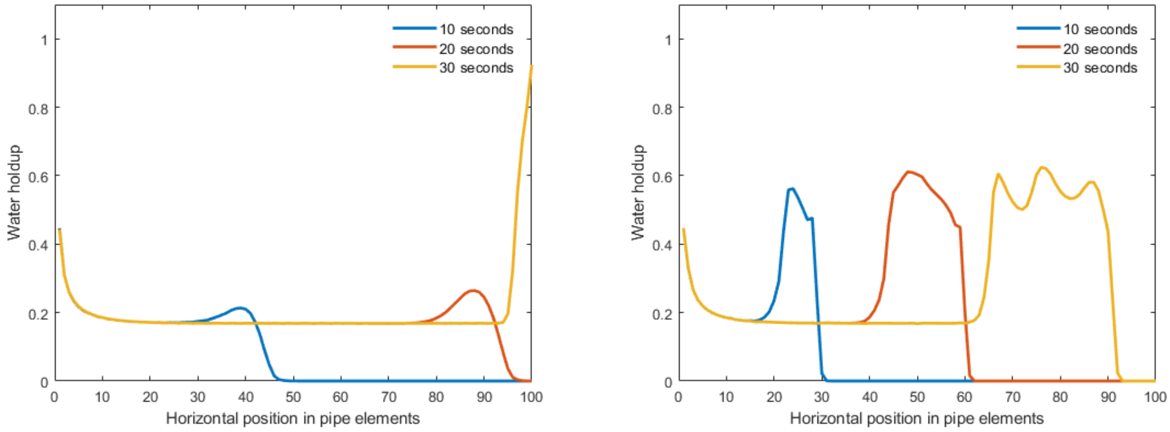

(a) First order scheme

(b) Second order scheme.

Figure 5.5: Differences in water front shape and flushing course between the first and second order solving scheme, using Fuchs Renolin DTA7 oil at an inclination of -5° and a superficial water velocity of 0.05 m/s.

The first set of simulations is performed with the measured properties of Fuchs Renolin DTA7 oil, at an inclination of -5° and a superficial water velocity of 0.05 m/s, see figure 5.5. Three curves are shown, which represent the water holdup in the pipe after 10, 20 and 30 seconds of flushing respectively(0.09, 0.18 and 0.27 pipe volumes of flushing respectively).

Like expected, the water front is much more apparent in figure 5.5b, as opposed to the curve in figure 5.5a. As the flow progresses, the length of this water front, seen as the jump in water holdup, increases. This corresponds closely to what is observed in the physical experiments.

The second set of simulations was done using Mobil Velocite No. 10 oil, as seen in figure 5.6. The inclination and superficial flow velocity are the same as in 5.5. In this figure, four curves are shown, representing the flushing course in the pipe after 10, 20, 30 and 40 seconds of flushing respectively(0.18, 0.35, 0.53 and 0.71 pipe volumes of flushing respectively).

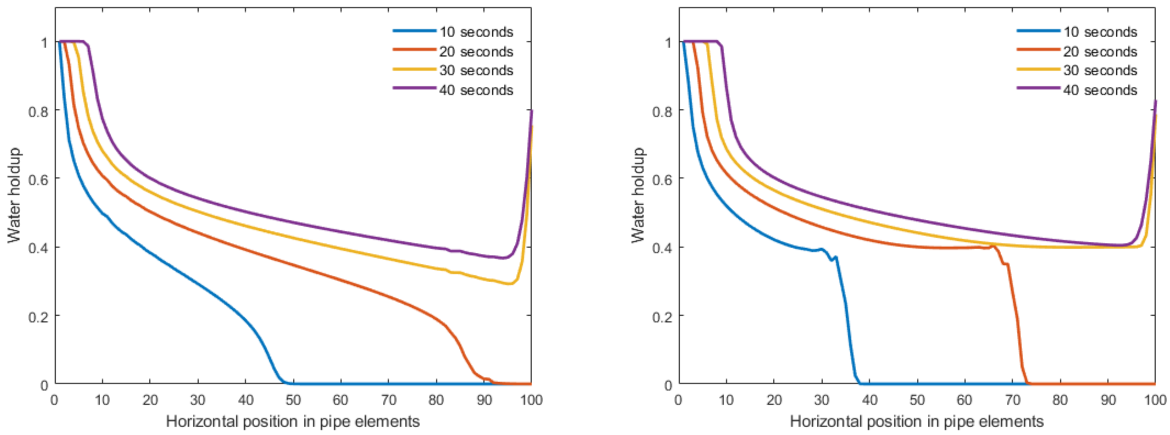

(a) First order scheme

(b) Second order scheme.

Figure 5.6: Differences in water front shape and flushing course between the first and second order solving scheme, using Mobil Velocite No. 10 oil at an inclination of -5° and a superficial water velocity of 0.1 m/s.

The main difference between the first order and the second order scheme as seen in figure 5.6a and figure 5.6b respectively is the shape of the water front. Where the front can be clearly seen in the second order scheme in figure 5.6b, in the first order scheme this front is virtually non-existent. Here too, the representation produced using the second order solving scheme is much more alike the physical experiments than the first order scheme is.

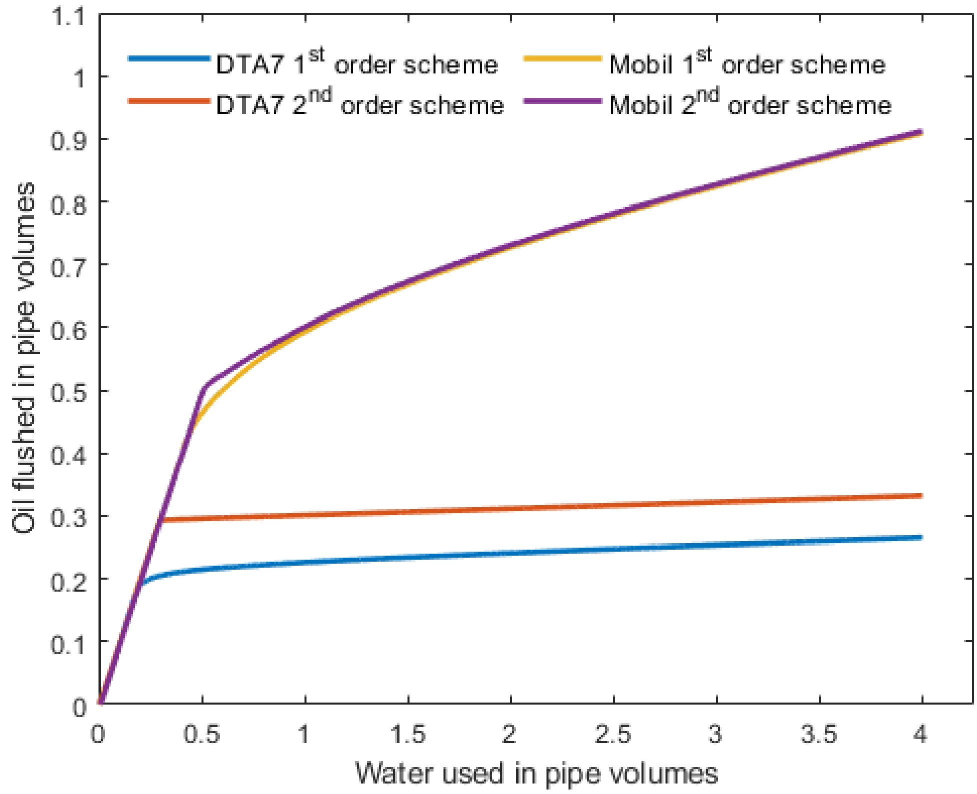

Figure 5.7: Amount of oil flushed per pipe volumes of water used, same simulations as displayed in figures 5.5 and 5.6.

Figure 5.7 shows the same experiments as shown in figures 5.5 and 5.6, the x-axis displays the amount of water used in pipe volumes, the y-axis the fraction of oil flushed from the pipe in pipe volumes. Although the curves in figure 5.6 for the local water holdup for the first and second order schemes are quite dissimilar, the oil flushed per volume of water used is remarkably similar. The final values, for the amount of Mobil oil flushed from the pipe section, are 0.9092 and 0.9123 for the first and second order scheme respectively. I.e. the front is captured only by the 2^{nd} order scheme, but the steady state is captured by both.

The final flushing values for both the 1^{st} and the 2^{nd} order schemes overestimate the amount of oil flushed. Where the amount of oil flushed in the experiments amounted to a fraction of 0.244, the 1^{st} and the 2^{nd} order schemes calculated fractions of 0.2655 and 0.3325 respectively.

The final choice for the solving scheme is the 2^{nd} order solving scheme, for its superior ability to display the water front correctly at lower superficial water velocities.

5.1.6 Longer Flushing

Using the parameters determined in the previous sections, a simulation is made to see how OLGA would model an experiment that is performed for much longer than the usual four pipe volumes of water. For physical experiments using Mobil Velocite No. 10 oil, an inclination of -5° and a superficial water velocity of 0.05 m/s, the amount of flushed oil reaches a plateau quite rapidly and no further oil is flushed. This is confirmed visually as well as with the camera footage, see figure 4.28. In figure 5.8, the OLGA simulation for the same parameters is shown. According to this simulation, when the experiment would be run long enough, all oil would be flushed from the pipe.

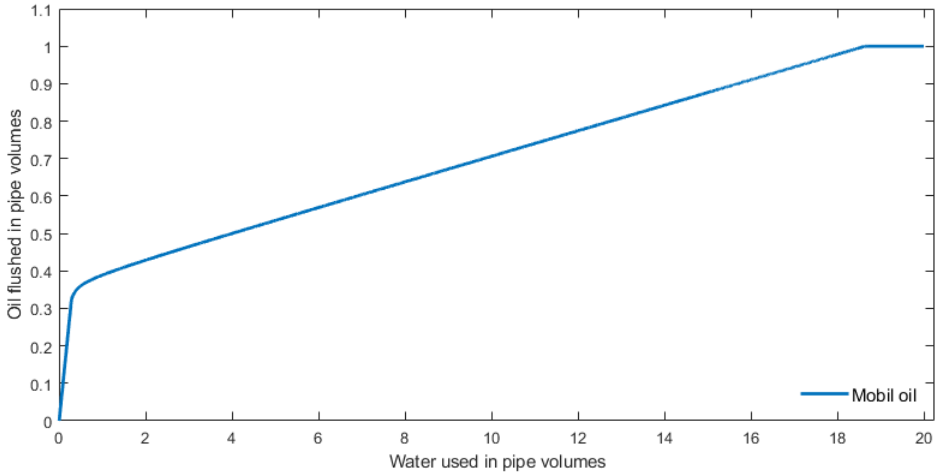

Figure 5.8: Amount of oil flushed per pipe volumes of water used, 20 pipe volumes of flushing.

5.2 OLGA Simulation Modelling Results

Using the settings and parameters determined in the previous sections, the modelling results of all OLGA simulations are presented in this section. The section starts with the results for Fuchs Renolin DTA7 oil, followed by the results for the same type of experiments, performed with Mobil Velocite No. 10 oil.

The results will be displayed like in the experimental results chapter, where the results are divided between the different oils, and subdivided according to each angle of inclination. Each graph displays the flushing curves for superficial water velocities of 0.05, 0.1, 0.15, 0.2, 0.25, 0.3, 0.35 and 0.6 m/s.

After displaying the results for the Fuchs Renolin DTA7 oil and Mobil Velocite No. 10 oil, an important advantage of modelling software is used: in order to determine the effects of density and viscosity independently from each other, additional simulations are performed with two virtual types of oil. One of these oils is set to have the density of the Fuchs Renolin DTA7 oil, and the viscosity of Mobil Velocite No. 10 oil. In the other virtual oil, these parameters are exactly the opposite. The properties of all four oils are shown in table 5.2

In the last section of this chapter the final flushing values for each simulation are displayed side by side, to clearly see the differences between the inclinations, superficial water velocities and the different types of oil.

	Density [kg/m^3]	Viscosity [mm^2/s]
Fuchs Renolin DTA7	828.0	12.16
Mobil Velocite No. 10	845.5	44.79
Density Fuchs - Viscosity Mobil	828.0	44.79
Density Mobil - Viscosity Fuchs	845.5	12.16

Table 5.2: Properties of the four types of oil modelled.

5.2.1 Fuchs Renolin DTA7 Oil

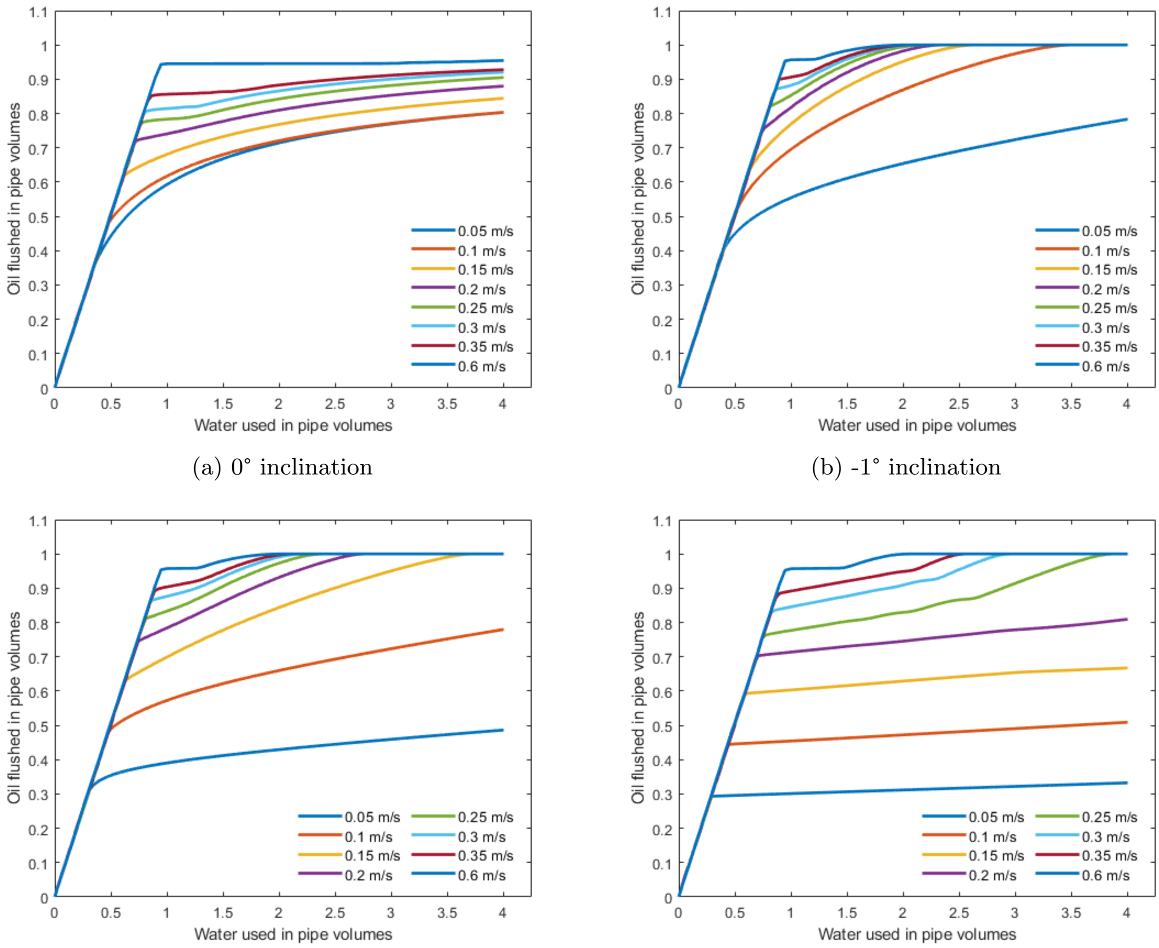

(a) 0° inclination

(b) -1° inclination

(c) -2° inclination

(d) -5° inclination

Figure 5.9: OLGA simulation at various superficial water velocities for Fuchs Renolin DTA7 oil, for the amount of oil flushed per pipe volume of water used, at an inclination of 0°, -1°. -2° and -5° respectively.

Figure 5.9 shows the results of the simulations for Fuchs Renolin DTA7 oil. In the experiments, a 0° inclination leads to a much better flushing than the -1° inclination. This is not the case in this figure. In the discussion in chapter 6 a further look will be taken into the behaviour of the model for minute inclination differences around 0°.

Apart from this deviation around an inclination of 0°, the simulation behaves in line with the experiments, where an increase in flushing velocity leads to an increase in the amount of oil flushed. Ranging from -1° to -5°, the larger the decline, the lower the efficacy of flushing.

OLGA seems to overestimate the amount of oil flushed from the pipe. Not only does OLGA expect oil the flushing to continue when the flow of water continues (section 5.1.6), also the value for the amount of oil that is flushed is overestimated. Where the experimental results gathered from the flow meters as well as from the video analysis showed that, for an inclination of -5° and a superficial water velocity of 0.05 and 0.1 m/s, a plateau would be reached in less than 1 pipe volume of flushing, this is not the case for the OLGA simulation. Although the flushing curve looks straight, it has a slight incline upwards, meaning that as flushing progresses, oil keeps flowing from the pipe section, never reaching a steady state in the concentration of oil and water in the pipe.

Another phenomenon that can be observed from the figures in 5.9 is that for the higher superficial water velocities, the flushing curve is sometimes kinked and not smooth like what was seen in the physical experiments. It is not entirely clear as to what might cause these ripples in the simulated flushing curves.

5.2.2 Mobil Velocite No. 10 Oil

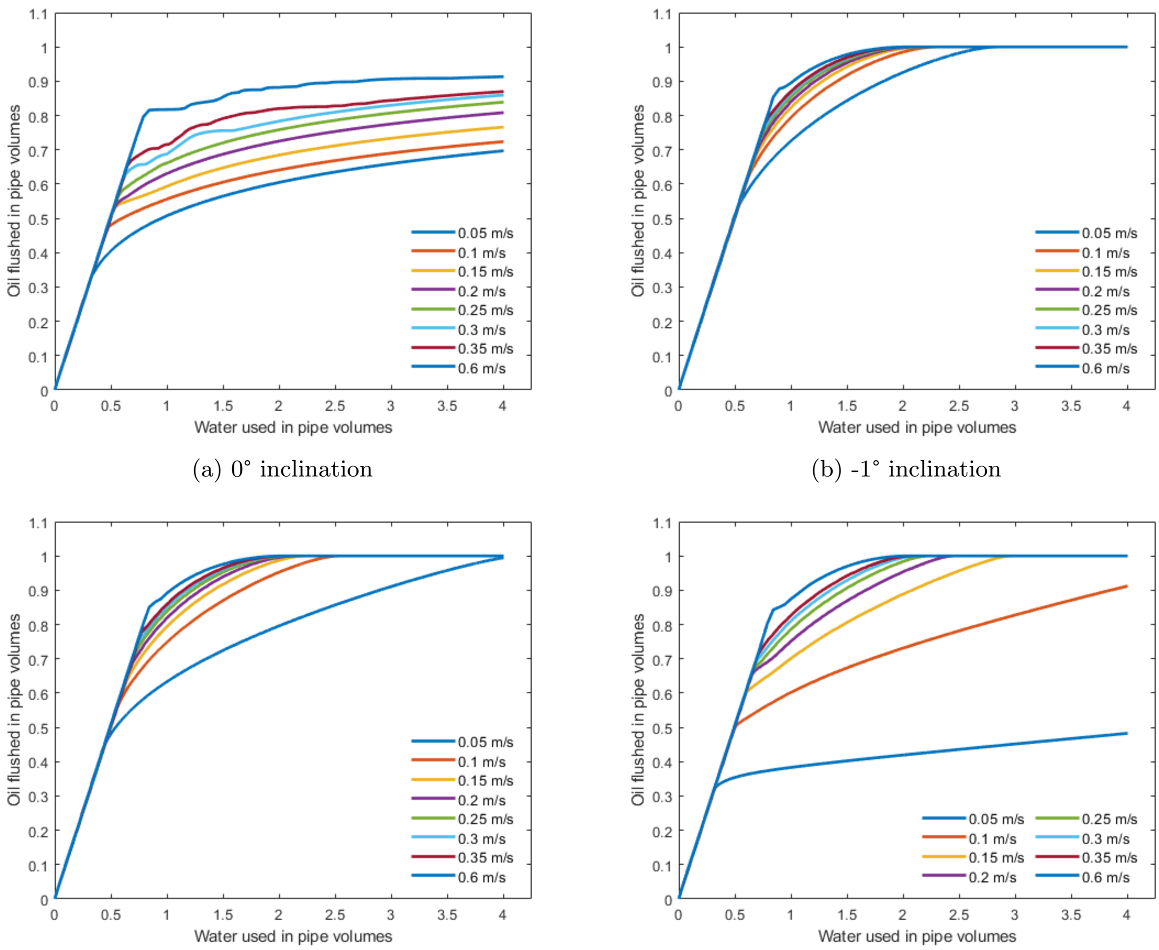

(a) 0° inclination

(b) -1° inclination

(c) -2° inclination

(d) -5° inclination

Figure 5.10: OLGA simulation at various superficial water velocities for Mobil Velocite No. 10 oil, for the amount of oil flushed per pipe volume of water used, at an inclination of 0°, -1°. -2° and -5° respectively.

Figure 5.10 shows the results for the simulations using Mobil Velocite No. 10 oil, which is more dense as well as more viscous than the Fuchs Renolin DTA7 oil. Some of the observations that were made from the figures in 5.9 are seen in figure 5.10. The simulations for an 0° inclination show poor flushing compared to for instance the -1° and -2° simulations, where even the lowest superficial water velocity, 0.05 m/s, is sufficient to flush all oil from the pipe. A repeated finding is that when a higher superficial water velocity is used, less water is needed for better flushing.

The differences in properties of the oil become very apparent when looking at both figure 5.9 and figure 5.10. It is clear from these figures that the Mobil Velocite No. 10 oil is flushed with far more ease than the Fuchs Renolin DTA7 oil. From these figures only, no decisive conclusion can be made to what extent this is caused by the difference in density, in viscosity, or in a combination of both.

Ripples are seen in the flushing curves at the higher superficial velocities, and generally in the more horizontal orientations. A possible explanation could be that this is due to the more viscous properties of the Mobil oil.

5.2.3 Virtual Types of Oil:
- Density of Fuchs Renolin DTA7 - Viscosity of Mobil Velocite No. 10
- Density of Mobil Velocite No. 10 - Viscosity of Fuchs Renolin DTA7

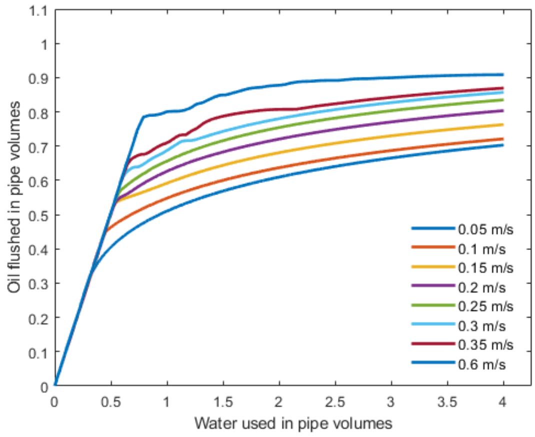

(a) 0° inclination

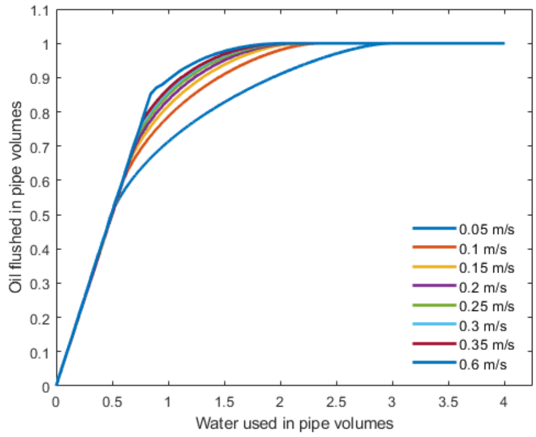

(b) -1° inclination

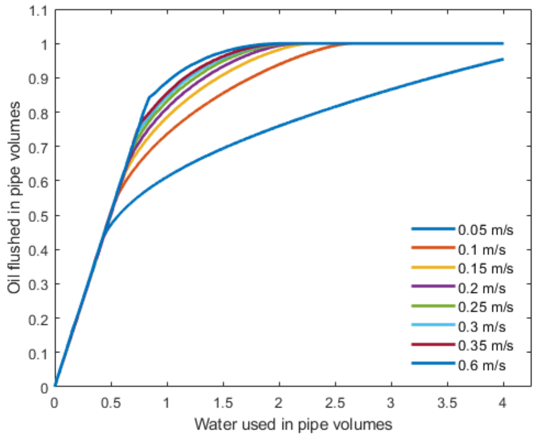

(c) -2° inclination

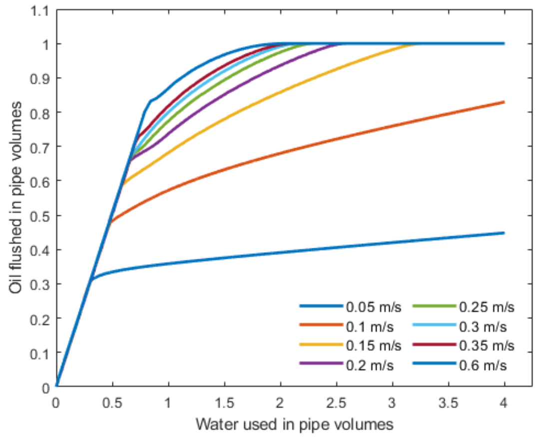

(d) -5° inclination

Figure 5.11: OLGA simulation at various superficial water velocities for virtual oil with the density of Fuchs Renolin DTA7 oil with the viscosity of Mobil Velocite No. 10 oil, for the amount of oil flushed per pipe volume of water used, at an inclination of 0°, -1°, -2° and -5° respectively.

Utilising the possibilities of software modelling, simulations were made with two virtual oils, to isolate the effects of the density and viscosity. These results can be seen in figures 5.11 and 5.12. The way in which figures 5.9 & 5.12, and figures 5.10 & 5.11 are alike is remarkable. The flushing curves look similar between the four figures, but the amount of flushing seems to be mainly determined by the viscosity of the flushed medium. Section 5.3 will directly compare the amount of flushed oil after four pipe volumes of flushing side by side.

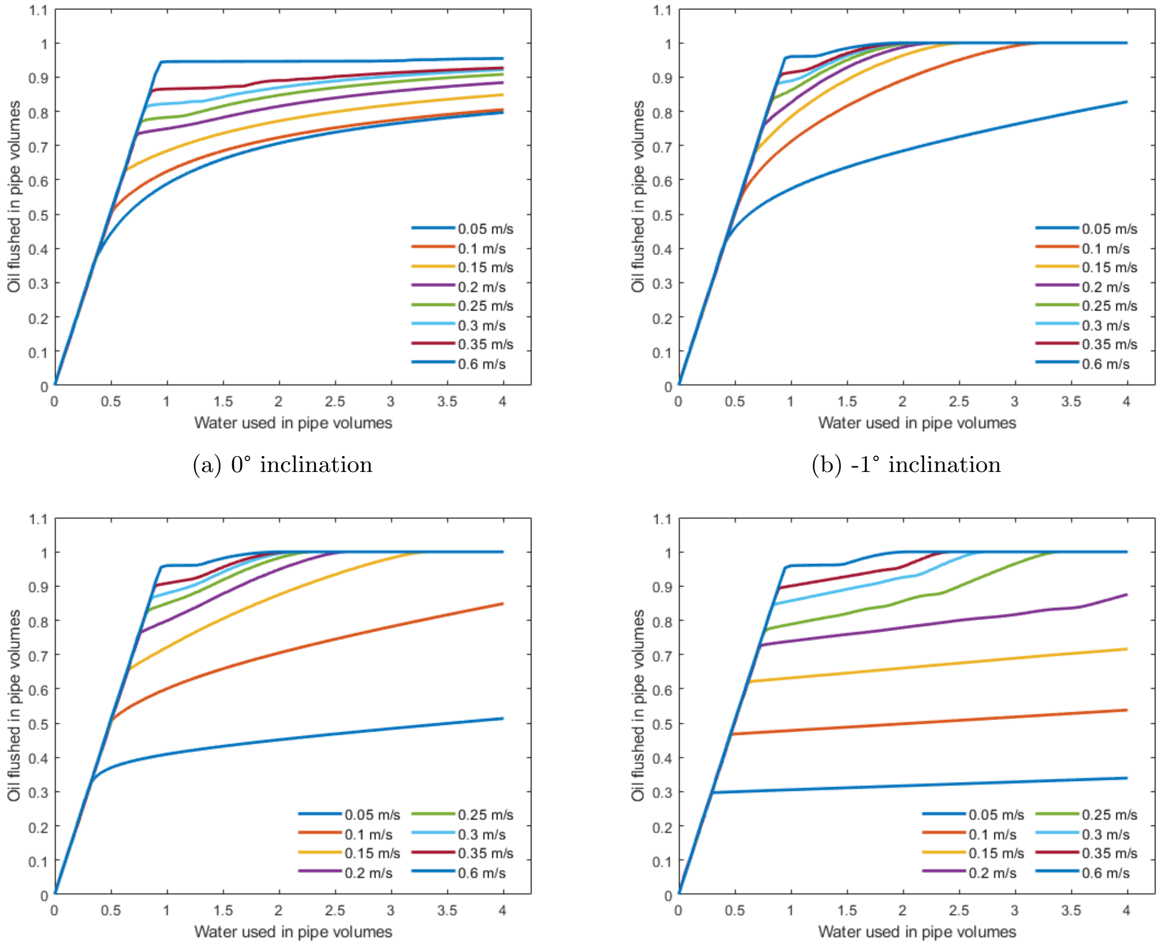

(a) 0° inclination

(b) -1° inclination

(c) -2° inclination

(d) -5° inclination

Figure 5.12: OLGA simulation at various superficial water velocities for virtual oil with the density of Mobil Velocite No. 10 oil with the viscosity of Fuchs Renolin DTA7 oil, for the amount of oil flushed per pipe volume of water used, at an inclination of 0°, -1°, -2° and -5° respectively.

5.3 Side by Side Comparison Final flushing Value, 4 Types of Oil

This section serves to illustrate the differences in flushing efficacy between the four types of oil, according to the OLGA modelling. Where previous sections primarily focused on the flushing course, figures 5.13, 5.14, 5.15 and 5.16 only show the end value for each simulation after four pipe volumes of flushing. For the case of an inclination of 0°, all used superficial flushing velocities between 0.05 and 0.6 m/s will be shown. The results for an inclination of -1°, -2° and -5°, the velocities of 0.35 and 0.6 m/s have been omitted in these figures, as in the higher superficial water velocity experiments the flushing fraction was one, for all types of oil.

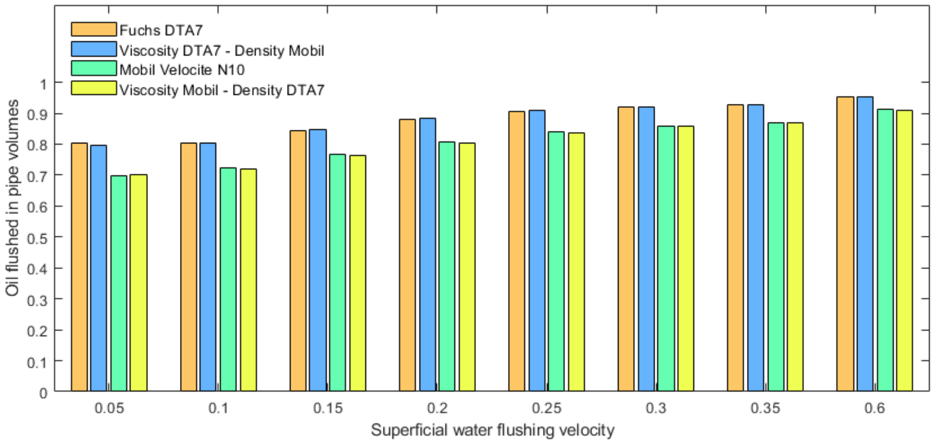

Figure 5.13: Amount of oil flushed after four pipe volumes of water used, for all four types of oil, at an inclination of 0°.

Figure 5.13 shows the end results for flushing a pipe section with a horizontal orientation. A clear trend can be seen in the amount of oil flushed between the different fluids. As observed in the flushing curves, the viscosity of the fluid seems to have a major impact on the flushing efficacy: a higher viscosity flushes out poor compared to a lower viscosity. The effect of the density cannot be made out from this figure.

Figure 5.14 with an inclination of - 1°, shows a limited amount of results, since for a flushing velocity of 0.1 m/s and higher, all oil is flushed from the pipe after flushing with four pipe volumes of water.

An influence of the density difference emerges, namely that a higher density oil flushes out better than a lower density: the virtual oil with the viscosity the same as Fuchs Renolin DTA7, but the density of Mobil Velocite No. 10 oil, flushes slightly better than the pure Fuchs Renolin DTA7. From the theory on Taylor and Benjamin bubbles, this is to be expected, since the density of Mobil oil is closer to that of the flushing fluid, water.

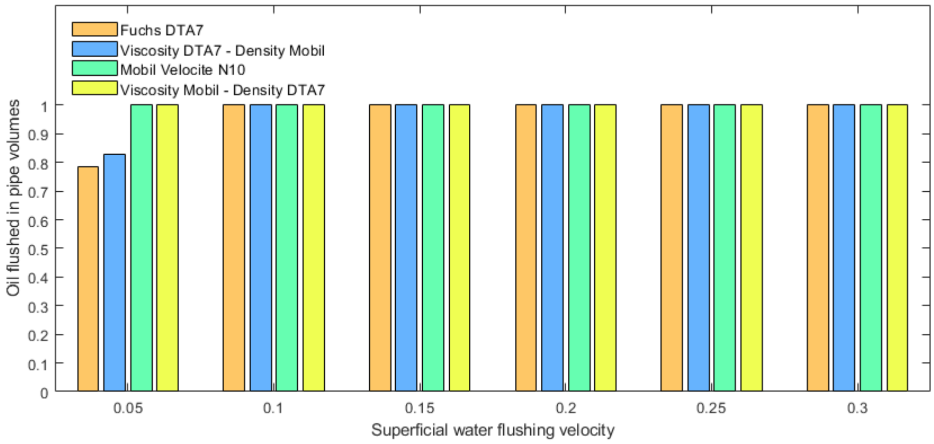

Figure 5.14: Amount of oil flushed after four pipe volumes of water used, for all four types of oil, at an inclination of -1°.

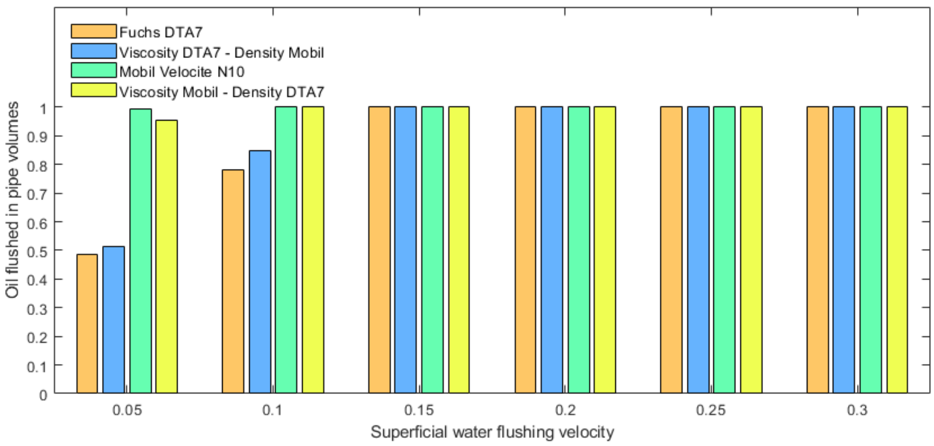

Figure 5.15: Amount of oil flushed after four pipe volumes of water used, for all four types of oil, at an inclination of -2°.

As seen in figures 5.15 and 5.16, with an inclination of -2° and -5° respectively, the oil viscosity has a larger effect on the flushing efficacy, compared to the oil density. The effect of density is not completely negligible however, as expected from the effective bubble velocity (equation 2.18).

From figure 5.16, it might be concluded that the influence of the oil viscosity on the flushing process, is in itself dependent on the flushing velocity. For the 0.1 m/s flushing velocity, the difference between the green & yellow bars and the orange & blue bars is more pronounced than for 0.05 m/s. The effect at higher velocities is unclear, since the amount of flushed oil is equal to one for those simulations. This statement is very premature because of the limited data, but it might be interesting to include in further modelling research.

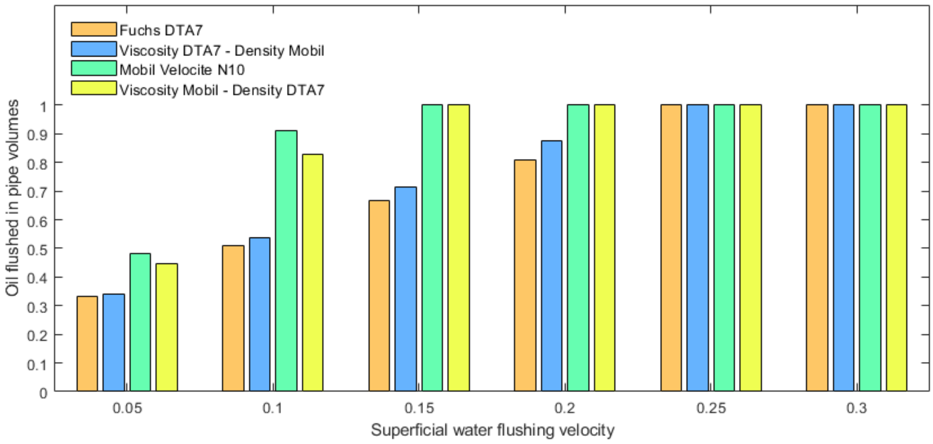

Figure 5.16: Amount of oil flushed after four pipe volumes of water used, for all four types of oil, at an inclination of -5°.

6 | Discussion

This chapter provides a discussion on the collected data and the interpretation of the results. The chapter starts by comparing the final flushing values for the flow meter data, video system data and OLGA data collection systems, with the final holdup in the experimental pipe section determined by photographing the contents of the pipe once these have settled after each experiment. The chapter continues with sections discussing various subjects on the experimental setup, the used oils and the video capturing system. Subsequently, the multi-phase flow simulator OLGA and its applicability to oil-water flushing is discussed. The chapter concludes with an discussion on the influence of the density and viscosity of the oil.

6.1 Experiments

6.1.1 Data Sources Comparison

During this project, a lot of data has been gathered by means of the mass flow meter system, the video data analysis system and the OLGA simulations. As an extra validation, during Phase III, the amount of oil left in the pipe after each first flush was also determined by tilting the pipe section to its maximum inclination angle, and letting the contents of the pipe settle. Once the contents were settled, a picture was taken, from which the average water holdup was determined. In the coming sections this method of determining the true water holdup after each experiment will be referred to as the "photo method".

This section aims to compare the final outcomes of each of the measuring methods. Figure 6.1 shows the final flushing values after 4 pipe volumes of flushing for the experiments done during Phase III, using the Mobil Velocite No. 10 oil, determined using the photo method mentioned in the previous paragraph. The x-axis shows the superficial water velocity for each respective experiment, the y-axis shows the inclination of the pipe section during each experiment. The cells are more orange when the water holdup is low, indicating that a lot of oil was still left in the pipe section after the first flush of the experiment. As the water holdup increases, the cells become more blue, up to a maximum water holdup of one, indicating that all oil has been flushed from the pipe section.

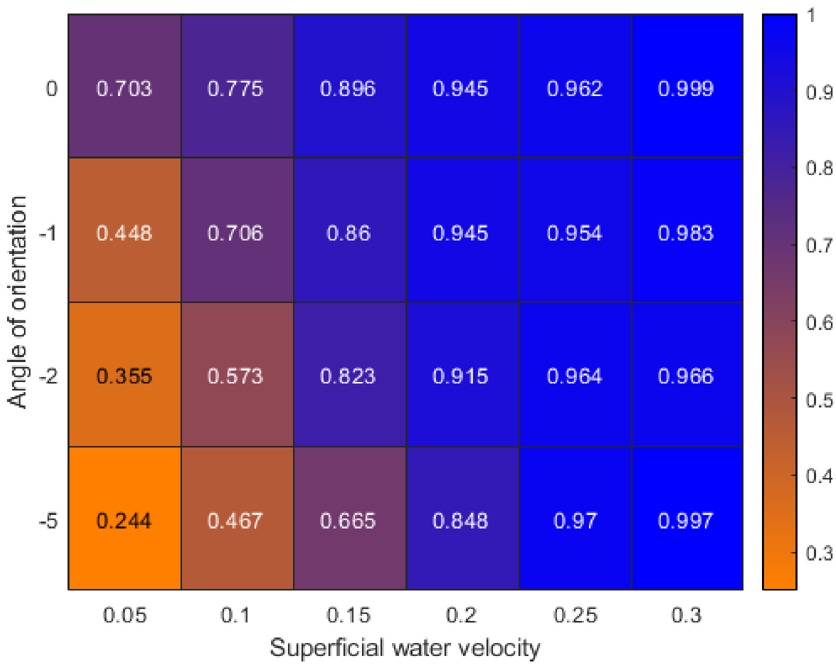

Figure 6.1: Heat map showing the final flushing value for the experiments performed with Mobil Velocite No. 10 oil, using the photo method. The x-values represent the superficial water velocity, the y-values the angle of orientation of the experimental pipe section. For increasing water holdup, cells turn from orange to blue.

The three sub-figures in figure 6.2 display a comparison of the holdup measured and expected by the flow meter data, the video analysis data & the OLGA simulations to the "true holdup", manually determined with the photo method. In these three figures, a more orange cell indicates that for that specific experiment and data acquisition method, less oil was measured or expected to be flushed compared to what was physically determined. When the cell is blue, the method measured or expects more oil to be flushed from the pipe than the amount that was determined by the photo method after each experiment. The value in each of the cells is simply determined by subtracting the true photo method holdup value from the values determined by the flow meters, video analysis and OLGA simulation for each sub-figure respectively.

As an example, the value for the experiment performed at a superficial water velocity of 0.05 m/s and a 0° inclination, seen in figure 6.2a, is 0.044. This means that for this specific experiment, the flow meters determined that 4.4 percentage points more oil was flushed from the pipe section than was determined using the photo method.

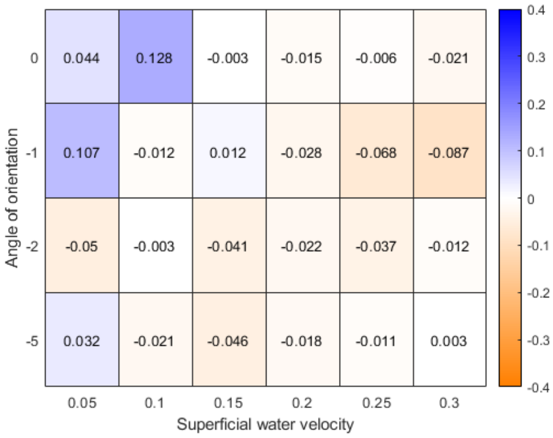

(a) True water holdup compared with flow meter data.

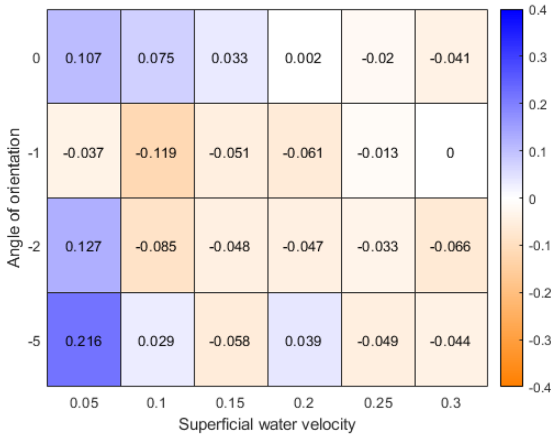

(b) True water holdup compared with video analysis data.

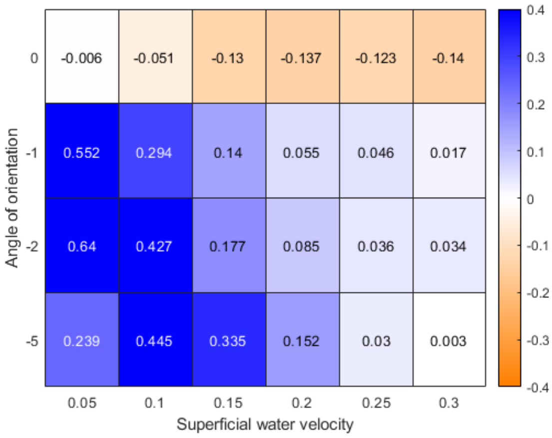

(c) True water holdup compared with OLGA simulation data.

Figure 6.2: Heat map showing the difference in final flushing values between the flow meter data, video analysis data & the OLGA simulation data, and the data determined with the photo method. A positive value (more blue cell) indicates that the data acquisition method showed an increased water holdup, equivalent to more oil flushed from the pipe compared to what was manually determined.

Deriving from figure 6.2, it can clearly be seen that the flow meter data is closest to the values determined by the photos after the first flush, compared to the other two methods. The amount of oil flushed from the pipe section is generally underestimated, by an average of 0.72 percentage points, with a standard deviation of 4.78 percentage points.

The values for the amount of oil flushed determined by the video analysis are a bit more scattered compared to those determined by the flow meter data. The amount of oil was again underestimated, this time by a mean value of 0.60 percentage points. The standard deviation however was significantly higher, with a value of 7.56 percentage points.

The values for the amount of oil flushed determined by the OLGA simulations are way off compared to the two earlier methods. For the 0° inclination the amount of oil flushed is underestimated, whereas the values for the experiments with a negative inclination were grossly overestimated. The average of overestimation for all simulations in part 6.2c was 13.0 percentage points, with a standard deviation of 21.95 percentage points. The possible reason for the difference between the horizontal simulation and those for a negative inclination is discussed in section 6.5.

As an extra comparison, figure 6.3 shows the difference in final flushing values between the video analysis and the flow meter data. Orange cells indicate that the video analysis determined the water holdup to be lower than the flow meter data determined it to be, blue cells vice versa. On average, the flow meters and the video analysis agreed well, with an average difference of 0.13 percentage points. The standard deviation however was significant, with a value of 7.84 percentage points.

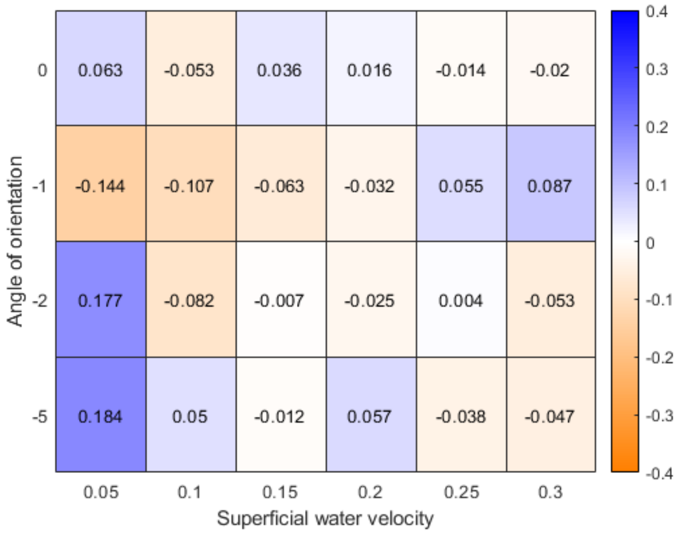

Figure 6.3: Heat map showing the difference in final flushing values between the flow meter data and the video analysis data. A positive value (more blue cell) indicates that the video analysis showed an increased water holdup, equivalent to more oil flushed from the pipe.

A similar study was done on the difference between the flow meter data and the OLGA simulations. For both types of oil, the flow meter data and OLGA simulation data was gathered in the same way, so both oils can be included in this comparison. The heat maps displaying these comparisons can be seen in figures 6.4a and 6.4b respectively.

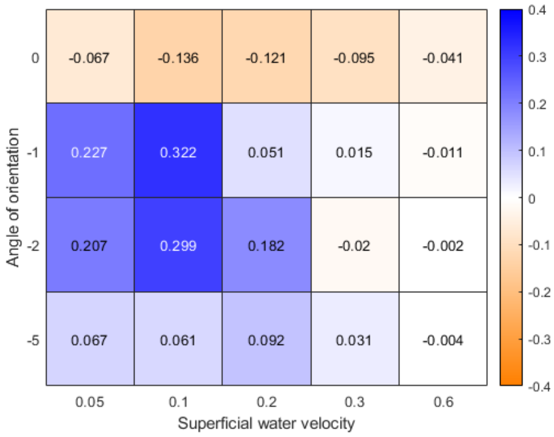

(a) Fuchs Renolin DTA7 oil.

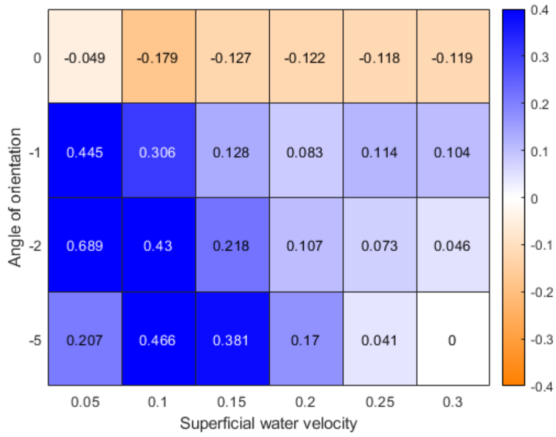

(b) Mobil Velocite No. 10 oil.

Figure 6.4: Heat map showing the difference in final flushing values between the flow meter data and the OLGA simulation data. A positive value (more blue cell) indicates that the OLGA simulation showed an increased water holdup, equivalent to more oil flushed from the pipe.

The phenomenon that was observed in figure 6.2c can again be clearly seen in figure 6.4. The OLGA simulations underestimate the amount of oil that is flushed from the pipe section in a horizontal orientation, and grossly overestimates the amount of oil flushed for negative inclinations, compared to the flow meter data. The mean overestimation for the Fuchs Renolin DTA7 experiments between OLGA and the flow meter data was 5.28 percentage points with a standard deviation of 13.26 points. The mean overestimation for the Mobil Velocite No. 10 experiments between OLGA and the flow meter data was 13.73 percentage points with a standard deviation of 22.28 points.

Section 6.5.1 will elaborate more on the influence of minor variations in the inclination angle around 0° on the OLGA simulations. Section 6.6 will discuss what different sources say on the influence of the oil density and viscosity on the flushing process.

6.1.2 Reproducibility: Amount of Water Used in Oil Flush - Applied Superficial water Velocity - Sum of Oil Flushed During the Two Flushes

In this section the reproducibility of the flow meters and the flushing system itself are examined. For the experiments to be comparable, the amount of water that is used in the experiments has to be the same. The flow fed into the experimental section is controlled using the rpm of the circulation pump in the circulation loop, in combination with the flow control valve. Especially in the control valve, hysteresis occurs, so when a certain valve opening is set, it matters if the valve is opened or closed to reach this position. Therefore, water was flowed through the system before each experiment to check the water velocity, instead of just setting a previously used valve setting for the same velocity.

The three sub-figures in figure 6.5 display the total amount of water used in the oil flush for each straight pipe experiment. These figures only show the basic experiments, additional experiments for e.g. reproducibility purposes are left out here for clarity sake. Part 6.5a represents the straight pipe section experiment using the Fuchs Renolin DTA7 oil, part 6.5b displays straight pipe experiments using the Mobil Velocite No. 10 oil. All these mentioned experiments intended to use four pipe volumes of water to flush the system. A trend can be seen that more water is used when flushing with a higher superficial water velocity. This effect can be partly explained by the property of the flushing control timer, which is only capable of accepting integer values of flushing times. All required flushing times were therefore rounded up to at least reach 4 pipe volumes of flushing. This extra partial second has a larger effect when the flushing flow rate is higher.

Part 6.5c shows the amount of water used in the straight pipe experiments using Mobil Velocite No. 10 oil, for 8 pipe volumes of flushing.

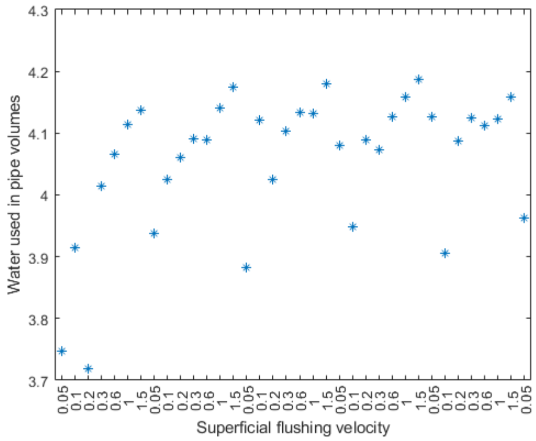

(a) Four pipe volumes of flushing - Fuchs Renolin DTA7 oil straight pipe experiments.

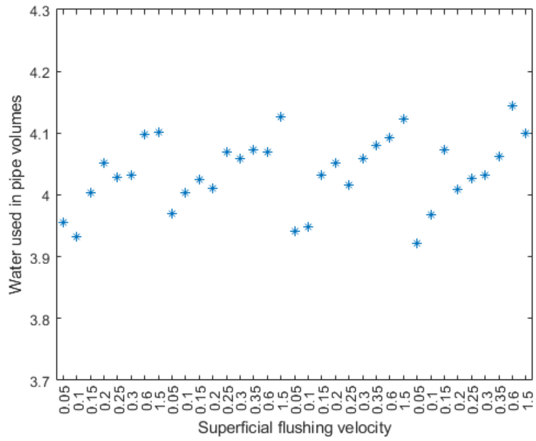

(b) Four pipe volumes of flushing - Mobil Velocite No. 10 straight pipe experiments.

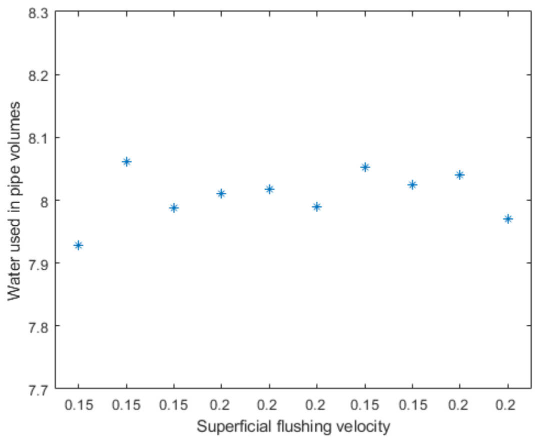

(c) Eight pipe volumes of flushing - Mobil Velocite No. 10 straight pipe experiments.

Figure 6.5: Total amount of water used during the first oil flush.

Table 6.1 shows the average amount of water used in the experiments also shown in figure 6.5. A trend downwards can be seen in the standard deviation between the measurements, while the mean trends closer to the desired value. The setup has not been changed between the experiments, so this positive trend is probably best explained by more skilled operation of the setup as time progressed.

	# of experiments	Average amount of water used	Standard deviation
Fuchs Renolin DTA7	36	4.0582	0.1075
Mobil Velocite No. 10	35	4.0371	0.0572
Mobil Velocite No. 10 (8 volumes)	10	8.0081	0.0404

Table 6.1: Water used in oil flush, average and standard deviation

The figures in 6.6 show the ratio between the realised superficial flow velocity and the intended value for the superficial flow velocity, as measured by the upstream mass flow meter. This means that when the value is lower than 1, the realised superficial flow velocity was lower than intended. On the x-axis the intended superficial flow velocities are displayed. The spread between the measurements in Phase II and Phase III is again reduced, probably because of more experienced handling. Where figure 6.5 showed that the higher superficial flow velocities generally used more water, figure 6.6a shows that for the higher intended flow velocities, this velocity is not reached. In figure 6.6b this effect is only seen for the higher superficial flow velocities of 0.6 and 1.5 m/s. The average values for the experiments in Phase II and Phase III approached the value of 1 closely, although generally the realised flow was just shy of the intended superficial flow velocity. The average values are negatively affected by the 1.5 m/s flushes, as mentioned before. The exact values are posted in table 6.2.

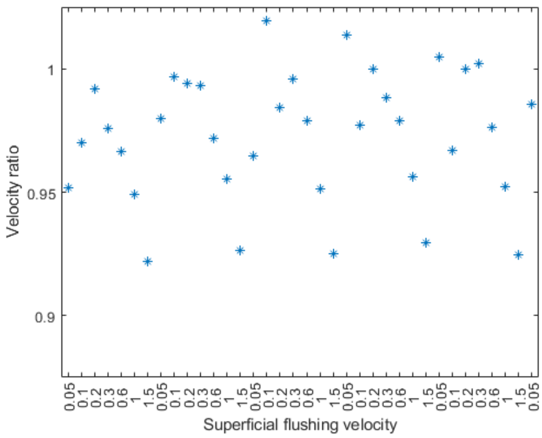

(a) Phase II straight pipe experiments.

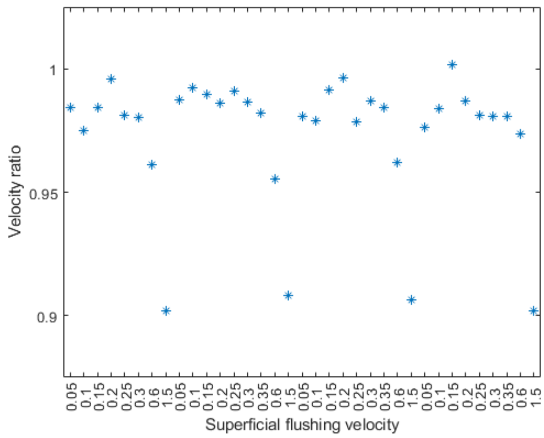

(b) Phase III straight pipe experiments.

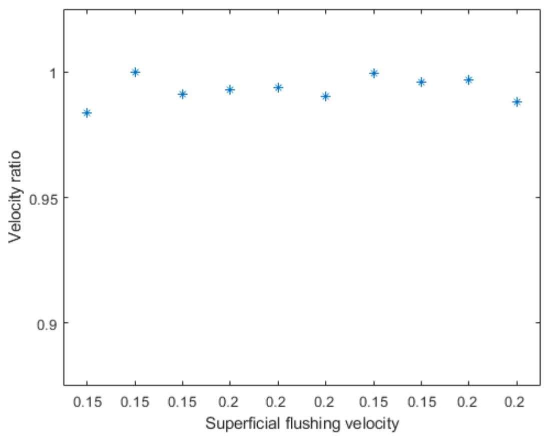

(c) Phase III - Eight pipe volumes of flushing.

Figure 6.6: Ratio between realised and intended superficial water flushing velocity.

	# of experiments	Average Velocity Ratio	Standard deviation
Fuchs Renolin DTA7	36	0.9728	0.0262
Mobil Velocite No. 10	35	0.9735	0.0268
Mobil Velocite No. 10 (8 volumes)	10	0.9931	0.0051

Table 6.2: Velocity ratio, average and standard deviation

Another very useful way of determining the level of reproducibility, is checking if the amount of oil flushed in the first and second flush combined, adds up to one. This can be done since it has been established that the superficial water velocity of 1.5 m/s is more than adequate to flush all possible remaining oil from the pipe during the second flush. Therefore the sum of the two flushes should amount to exactly one pipe volume of oil. The figures in 6.7 show the sum of the two flushes for all straight pipe experiments combined. Table 6.3 displays the average values and standard deviation, for the same experiments as in figure 6.5 and table 6.1, and figure 6.6 and table 6.2. Note again that in this table only the "basic" straight pipe experiments are included, omitting any additional experiments.

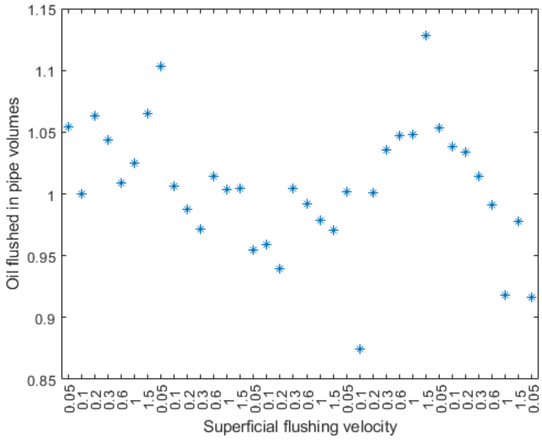

(a) Phase II straight pipe experiments.

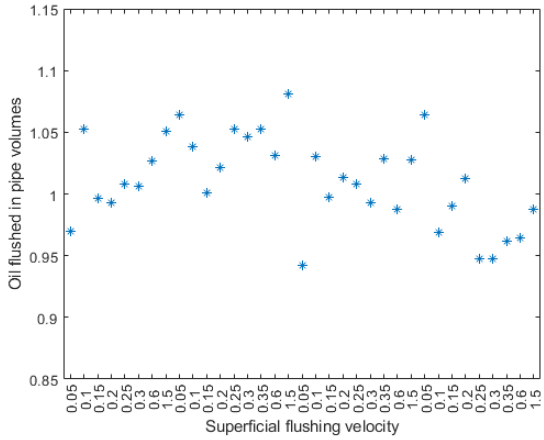

(b) Phase III straight pipe experiments.

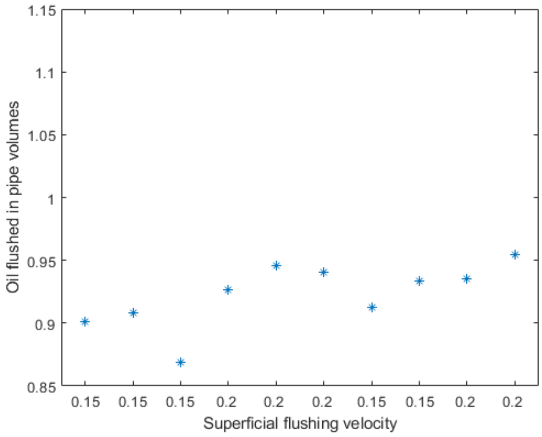

(c) Phase III - Eight pipe volumes of flushing.

Figure 6.7: Total amount of oil flushed in pipe volumes after the first and second flush.

	# of experiments	Sum of oil flushed	Standard deviation
Fuchs Renolin DTA7	36	1.0058	0.0499
Mobil Velocite No. 10	35	1.0104	0.0361
Mobil Velocite No. 10 (8 volumes)	10	0.9228	0.0255

Table 6.3: Sum of oil flushed in both flushes.

Table 6.3 displays that the average value for the total amount of oil determined by the flow meters for the Phase III experiments is very close to 1, just like in Phase II. The standard deviation decreased for the experiments performed in Phase III compared to Phase II, a sign of increased reproducibility through better handling.

The values for the eight volume flushes show an abnormality. According to the flow meter analysis, some oil remained in the pipe section after the two flushes, something that opposes what was visually observed, as shown in table 6.3. Tables 6.4 and 6.5 show a complete breakdown of the four volume flushes, compared to their four volume counterparts.

The first two rows show the values for the first and second flush as determined by the flow meters. The third and fourth row show the the values for the amount of oil flushed according to the photo method, the amount that was visually observed once the contents of the pipe had settled after an experiment. The first column shows the average value for the eight volume flushes, the second column the value for the same experiment with regards to the velocity and the inclination, but for four volumes of water flushing.

Tables 6.4 and 6.5 show that the flow meters determine that a lower amount of oil is flushed from the pipe when flushing with eight volumes of water comparing to the four volumes of flushing. This is illogical, since the eight volume flush is in essence a normal four volume flush, but extended.

The photo data shows that more oil is flushed during the eight volume flushes compared to the four volume flushes. The precise reason for the misreading of the flushing value by the mass flow meters in the extended flush is unclear. This is especially the case, since the mass flow meters establish a value too low in the first flush, but establish a value too high in the second flush, when in fact most oil is already flushed from the pipe in the first flush.

	Oil flushed (8 volume average)	Oil flushed (4 volume)
First flush - Flow meter data - 0.15 m/s	0.8255	0.8718
Second flush - Flow meter data - 0.15 m/s	0.0793	0.1183
First flush - Photo - 0.15 m/s	0.9556	0.8602
Second flush - Photo - 0.15 m/s	0.0444	0.1398

Table 6.4: Amount of oil flushed in pipe volumes during the eight volume, Mobil Velocite No. 10 oil experiments, compared to the four volume experiment, superficial flushing velocity 0.15 m/s.

	Oil flushed (8 volume average)	Oil flushed (4 volume)
First flush - Flow meter data - 0.2 m/s	0.8846	0.9169
Second flush - Flow meter data - 0.2 m/s	0.0561	0.0959
First flush - Photo - 0.2 m/s	0.9824	0.9449
Second flush - Photo - 0.2 m/s	0.0176	0.0551

Table 6.5: Amount of oil flushed in pipe volumes during the eight volume, Mobil Velocite No. 10 oil experiments. compared to the four volume experiment, superficial flushing velocity 0.2 m/s.

6.1.3 Experimental Setup - Gooseneck

To study the effects of the height of the gooseneck at the end of the experimental pipe section, two experiments were performed with different gooseneck heights as a variable. Figure 3.3a in section 3.1.1 shows the different gooseneck pipes. The experiments were performed with a pipe inclination of -5°, and a superficial flushing velocity of 0.1 m/s. Figure 6.8 shows the flushing curves for both of the experiments. The final difference in the amount of oil flushed is 0.0144 percentage points, 0.4483 for the regular (medium) gooseneck compared to 0.4338 for the taller one. This value falls well within the standard deviation of 0.0499 percentage points for the set of experiments performed in the second phase, which confirms the visual observation that the height of the gooseneck is not of influence to these experiments.

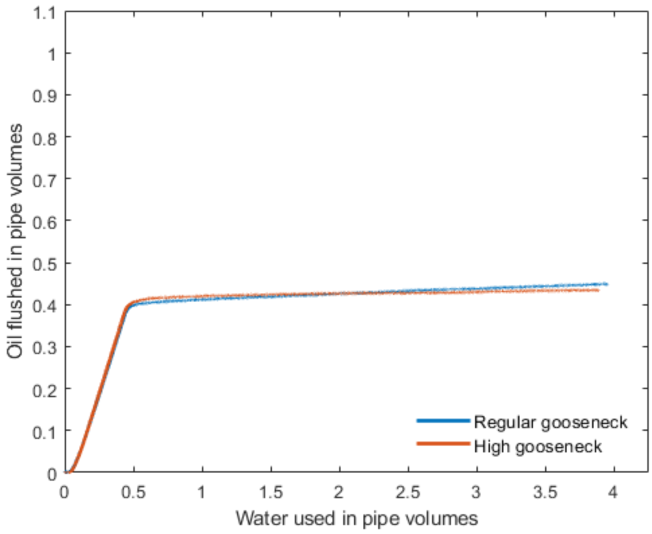

Figure 6.8: Amount of oil flushed against the amount of water used in the flushing process. The blue line represents an experiment performed with the regular medium sized gooseneck, the red line represents a similar experiment performed with a taller gooseneck.

6.2 Relating the Benjamin and Taylor Bubbles to the Experiments

Section 2.2.3 introduced the theory that the effective bubble velocity between two phases in a pipe can be approximated by combining the equations for the Taylor bubble and the Benjamin bubble, together with the inclination angle of the pipe. Further information regarding the effective bubble velocity can be found in section 2.2.3, the equation itself is repeated in equation 6.1.

$$U_{\mathrm{E}} = U_{\mathrm{T}} \cdot sin(\phi) + U_{\mathrm{B}} \cdot cos(\phi) \tag{6.1}$$

Table 6.6 shows the results for the effective bubble velocity for the two different oils used in the experiments. The values in the table represent the velocity the bubble of the oil is expected to reach, in a pipe filled with water, oriented to the angle shown in the table, for the two oils used. The values for the Fuchs Renolin DTA7 oil are slightly higher than those for the Mobil Velocite No. 10 oil, since the former is less dense than the latter. When the superficial water velocity is higher than the oil bubble velocity, flushing occurs.

	0°	-1°	-2°	-5°
Fuchs Renolin DTA 7	0.1662	0.1681	0.1698	0.1749
Mobil Velocite No. 10	0.1575	0.1592	0.1609	0.1657

Table 6.6: Effective bubble velocities [m/s] for Fuchs Renolin DTA7 oil and Mobil Velocite No. 10 oil, for several angles of pipe orientation.

Table 6.7 shows a study into the bubble velocity observed in the experimental results for Fuchs Renolin DTA7 oil. Part 6.7a shows the observed velocity with which the last bit of oil was flushing out of the pipe. This was determined by analysing the video data, an example of this last "wake" of oil is shown in figure 6.9. Part 6.7b shows the difference between the superficial flow velocity in the experiments, and the observed velocity at which the bubble of oil was moving downstream. With this subtraction, the observed real bubble velocity is obtained.

What can be seen when comparing table 6.6 and 6.7b is that for the lowest superficial water velocity where the oil wake is seen, the observed bubble velocity matches the calculated bubble velocity remarkably well. When the superficial water velocity increases, the observed oil bubble velocity also increases. This could be related to the fact that the equation for the effective bubble velocity assumes no mixing between the phases. Turbulence and waves compromise this assumption, and cause the observed bubble velocity to be higher than the calculated bubble velocity.

U_s	0°	-1°	-2°	-5°
0.2 m/s	0.044	0.044	≤ 0	≤ 0
0.3 m/s	0.102	0.099	0.093	0.078
0.6 m/s	0.283	0.292	0.288	0.218
1.0 m/s	0.566	0.574	0.563	0.460

(a) Observed bubble velocity.

U_s	0°	-1°	-2°	-5°
0.2 m/s	0.156	0.156	$0.2 \leq$	$0.2 \leq$
0.3 m/s	0.198	0.201	0.207	0.222
0.6 m/s	0.317	0.308	0.312	0.3825
1.0 m/s	0.434	0.426	0.437	0.540

(b) Sf. water velocity, minus observed bubble velocity.

Table 6.7: Comparison between observed and calculated effective bubble velocity.

Determining the exact holdup in a pipe section after a certain amount of flushing with water, at a certain superficial water velocity is problematic. The location of the last oil wake can be approached using the effective bubble velocity, but since the shape of the wake of the oil bubble is not constant, the holdup in the downstream section of the bubble cannot accurately be determined.

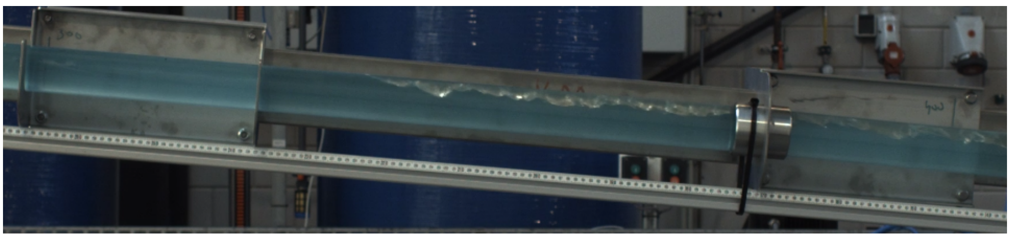

Figure 6.9: Last volume of oil, flushed from the pipe.

6.3 Oil Properties

During Phase II of the flushing experiments using the Fuchs Renolin DTA7 oil, it was observed that the appearance of the oil was not constant, as mentioned in section 3.2.1. As seen in chapter 3, sections 3.2.1 and 3.2.1, measurements showed that nor the viscosity, nor the density of the oil was significantly affected. Still, the repeated mixing of oil and water did have visible effects, as described in section 3.2.1. The oil turned from clear to cloudy, and seemed to stick more to the pipe walls, especially at the lower superficial flushing velocities. In the large 5000 liter separation tank, a layer was building on top of the oil, which, judging by the smell, was a layer of micro-organisms feeding on the oil. This theory of micro-organisms affecting the oil seems to be the most plausible cause of degradation of the oil, since the setup is mostly closed off to the environment, leaving little room for large amounts of dust or other contaminants to enter the system.

Although the viscosity and density did not change significantly, the sticking of the oil to the pipe walls affected the results to a small extent, as a fraction of the oil was left behind on the pipe walls. This effect was again seen using the Mobil Velocite No. 10 oil despite the precautionary measures described in the next paragraph. The amount of oil sticking to the wall is estimated to be around roughly 0.5 to 1% of the total amount of oil in the pipe. This was determined when cleaning the pipes between sets of experiments, by pushing a rag through the pipe. Although any amount of sticking oil is undesirable, this amount falls within the standard deviation of flushed oil, and is therefore not taken into account in the data analysis.

During Phase III of the flushing experiments, using the Mobil Velocite No. 10 oil, a precautionary measure was taken in order to try to prevent the oil from degrading. A 1000 liter intermediate bulk container, or IBC, was taken, and wrapped in UV resistant foil. All the fluids produced from each experiment were first pumped into this IBC. Once the water and oil settled and separated, the water would be pumped from this IBC to the larger 5000 liter tank, originally used as the separator. The oil would be partly pumped back into the barrels it was delivered in, and partly left in the IBC. The idea behind this was that the surface area between the water and the oil in the IBC would be around four times smaller than it would be in the larger tank.

The bacteria layer was not observed in the IBC, but did again develop in the larger separator. This might be caused by small amounts of oil still finding their way to the larger tank, in combination with traces of the bacteria from Phase II. Note that the tank was professionally cleaned, but not disinfected, between the phases.

Density measurements performed on the new and used Mobil oil showed little change, similar to the measurements performed on the new and used Fuchs Renolin DTA7. The visual changes, however, still persisted. The reused oil also seemed to stick more to the pipe wall than the new oil. A small amount of oil even remained after the 1.5 m/s superficial water velocity flush, normally sufficient to flush all oil from the pipeline. This remaining film was very thin, with the total amount of oil left in the pipeline regarded to be insignificant to influence the measurements.

Another observation was that, after the contents of the pipe settled for some time, e.g. for a weekend, a white residue built up in the top parts of the pipe, as seen in figure 6.10. This residue is guessed to mainly consist of oil, although not having the exact same consistency when flushing. A 1.5 m/s superficial water velocity flush would be sufficient to flush the residue from the pipe again.

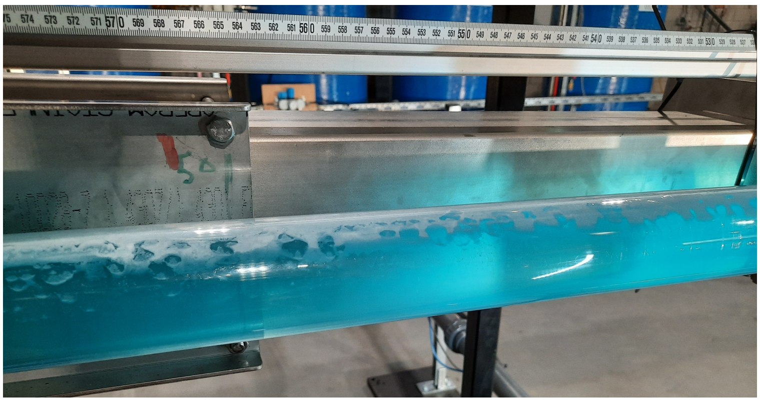

Figure 6.10: White residue settling after a weekend, even after flushing the pipeline with a superficial water velocity of 1.5 m/s on Friday end of the day.

Further methods for the prevention of degradation of the oil have only been briefly investigated. A UV-light treatment was considered, but this would need to be very high powered, with continual circulation in the tank. This would still not completely solve the problem, as bacterial buildup on the tank wall could still be possible, as the UV rays would not reach every spot within the container. As mentioned earlier, it is not probable that contaminants like dust or dirt from the lab environment got into the system to such a degree that it would influence the oil degradation. Adding significant amounts of salt, or antibacterial substances would certainly slow or stop the growth of micro-organisms, but would also affect the flushing experiments or the oil.

6.4 Video Data Analysis Setup

The usefulness of the video data for the holdup determination has progressed a lot in Phase III as compared to Phase II, by decreasing the distance between the cameras and the experimental pipe section. This increased the vertical resolution significantly, improving the quality of the captured holdup data. The accuracy was still not up to the level of that of the mass flow meters, as partly can be seen in figure 6.2. Providing a stable environment from a lighting aspect again proved to be hard in practise. Although extra lights were added, and dimming sheets were strategically placed to remove unwanted reflections, simple effects as a cloud moving in front of the sun could still affect the data collection. The long duration of the three flushes total for each experiment also complicates this matter since this gives more time for the ambient lighting values to change. More stable lighting conditions might be provided by more additional lighting and extra shades against sunlight.

With the new setup in Phase III, other properties of the cameras were sufficient for the job. The frame rate was sufficiently high, since the limiting factor was the vast amounts of data that had to be analysed, leading to only a fraction of the frames actually being used. The room left for improvement on the resolution part is also limited. The limiting factor in determining the border between the oil- and water phase actually becomes the size and shape of the interface instead of the resolution of the camera. The interface between the two phases is obviously three dimensional, something which can only be caught on a 2D image to a certain extent.

Another iteration of improvements on the video setup therefore might not bring the extra desired accuracy on the amount of oil that is flushed from the pipe. Nevertheless, video data analysis might be very useful for studying the flow phenomena in the pipe. As the shape and size of the interfacial waves can be caught on film, this might give access to more knowledge into the flushing process. This aspect has not been investigated further as it was outside the scope of this thesis, so it was added to recommendations for future research.

6.5 OLGA Simulations

6.5.1 Negative, Zero & Positive Inclinations

The OLGA simulations are very useful as a quick way to simulate the flow in an experimental setup. Some peculiarities popped up however, especially regarding the inclination angle. As seen in chapter 5, the OLGA simulation showed better flushing at slightly negative inclinations than in the horizontal case. This contradicts what is seen in the physical setup. This raised the question how the simulations would react to a minuscule negative or positive inclination of the setup. The two following figures 6.11 and 6.12 shed some light into this matter.

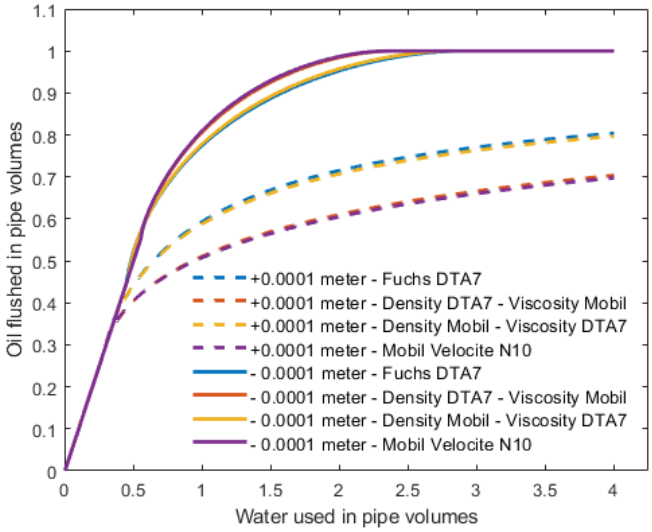

Figure 6.11: Amount of oil flushed per pipe volumes of water used, for a minuscule elevation increase or decrease on the downstream side of the setup. Results for the Fuchs Renolin DTA7 and Mobil Velocite No. 10 oils, and the two virtual oils.

Figure 6.11 shows the flushing curves for simulations on the regular straight pipe setup, with a superficial flushing velocity of 0.05 m/s. The figure displays eight curves. Because the values for the Fuchs Renolin DTA7 oil and the virtual oil with the density of Mobil and viscosity of Fuchs oil are so close together, the blue and yellow curves almost overlap. The same happens for the curves for the Mobil Velocite No. 10 oil and the virtual oil with the density of Fuchs and the viscosity of the Mobil oil. Because of this, it seems that there are only four curves in the figure, while in fact there are eight.

The first variation in this set of experiments is the elevation of the downstream end of the experimental section, being very slightly positive, and slightly negative. The values are chosen such that the difference is too minute to cause significant differences in flushing, just looking at the inclination angle. The second variation is the type of oil: all four types of oil mentioned in chapter 5. The figure displays the flushing efficacy for the oil variation as expected. There is however a vast difference between the flushing efficacy for the same types of oil, but a different elevation, although this elevation difference would be very difficult to even notice with the naked eye in a physical test. According to the OLGA simulation, the negatively inclined pipe sections would be flushed completely, while the positively inclined pipe sections would still have large amounts of oil in them after flushing. This is contrary to what is expected from the experiments.

Note that the horizontal case for each of the types of oil behaves almost exactly the same as the case for a slight positive inclination.

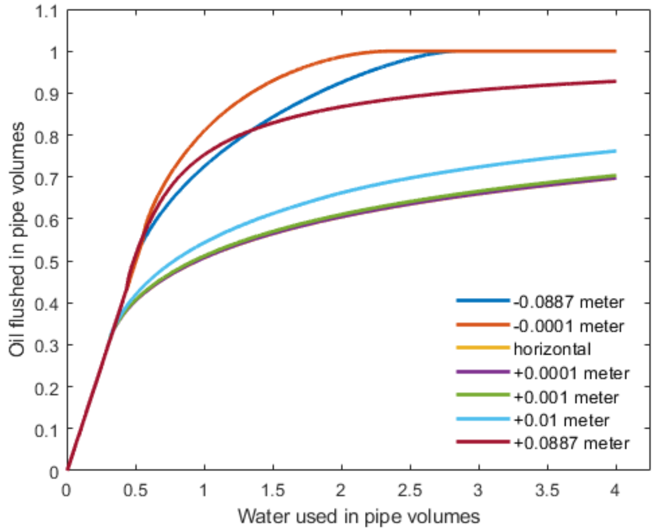

Figure 6.12: Amount of oil flushed per pipe volumes of water used, for a range of elevations of the downstream side of the setup. An elevation of ± 0.0887 meter corresponds with an angle of inclination of ± 1°.

A similar study is shown in figure 6.12. In these simulations the only variable is the elevation of the downstream end of the setup. The pipe is originally filled with Mobil Velocite No. 10 oil, and is flushed with a superficial water velocity of 0.05 m/s. An elevation of ± 0.0887 meter corresponds with an angle of inclination of ± 1°. What would be expected from the physical experiments is that the negatively inclined orientations flush the worst, which would get better when the orientation is turned horizontal, and successively positive. Unfortunately, this is not the result that OLGA presents.

The smallest negative inclination shows the best flushing, followed by the -1° inclination, according to the simulation. The curves for the horizontal, +0.0001 meter and +0.001 meter overlap, but all three show equally poor flushing. Moving from here, the more the downstream end of the pipe section elevates, the better the flushing becomes, something that indeed would be expected from the physical experiments.

These two previous figures (6.11 & 6.12) show that great caution is necessary when operating the flushing simulations at and around the horizontal plane. In trying to represent a physical problem in an equation, often correlations are used that are based on existing experimental data. The correlations might represent reality closely enough for specific conditions, but deviate for other conditions. It might be the case that in the OLGA simulation, one correlation is used for flows with negative inclinations, and another for flows with a positive inclination. These correlations don't necessarily overlap, which gives a discontinuity, in this case around inclinations of 0°. Although this reasoning seems plausible, there also might be other factors at play for the absence of a smooth transition zone.

6.5.2 Applicability of OLGA to Oil-Water Flushing

The modelling tool OLGA has been around since the 1980's, and has proven its value in many fields of practise, e.g. the formation of slugs in multi-phase oil pipelines. Because of this track record, OLGA is expected to be well applicable to oil-water flushing too.

In this flushing study mixed results were achieved with modelling oil-water pipe flushing. Details like the shape and size of the initial water front are represented correctly. The simulation trends are also very similar to what is observed in the physical experiments, like the effect of different superficial water velocities, and the effect of varying small negative inclinations.

There are some other points however where the modelling results produced in this thesis and the physical experiments disagree. OLGA shows a discontinuity in flushing results between minute variations of the inclination angle around 0°. In the case of individual parameters like density and viscosity, the results are mixed too. OLGA expects that for a density increase of the used oil, moving closer to the density of the flushing medium, the flushing efficiency increases too. The magnitude of the effect of the viscosity of the oil however seems to be overestimated. This causes the spread of the final flushing values determined with the other measuring methods in the experiments to be very large. Figure 6.4, earlier in this chapter, shows this spread between the values determined with the flow meters, and those determined using the modelling results. OLGA overestimates the flushing efficiency for negative inclinations to a certain degree for Fuchs Renolin DTA7 oil, but this overestimation is much larger for the viscous Mobil Velocite No. 10 oil.

OLGA simulations can be used to perform sensitivity studies, and in determining trends. Extracting exact flushing values for specific conditions has proven to be more complicated.

6.6 Influence of Oil Density and Viscosity on the Flushing Process

The individual effect of the density and the viscosity of the flushed oil remains unclear. Physical experiments cannot give a decisive answer, since in most oils, density and viscosity go hand in hand. For this reason, distinction between the two parameters is almost impossible in physical tests. By using OLGA simulations with oils with natural, and with modified characteristics, it was possible to get around this difficulty.

The OLGA simulations showed an overestimation for the amount of oil flushed from the experimental pipe section for both types of oil(figure 5.3). When looking at the results from the simulations with the virtual oils it appeared that OLGA gave the viscosity a far stronger weight factor than the density. The analysis on the OLGA results, collected in this study, concludes that a higher oil density increases the flushing efficiency slightly and that an increased viscosity increases the flushing efficiency majorly.

In a study by Kroes et al.(2013)[14], general crude oil-water flow was studied in horizontal pipes with two types of oil. They concluded that a higher oil viscosity causes more turbulent dispersion and therefore less stratification and more dispersed flows. For performed flow velocities of 0.64, 1.28 and 1.92 m/s, the differences between the two types of oil are most significant in the high velocity experiments, for which the dispersive forces are most prominent.

A higher degree of dispersion would be beneficial to the flushing process, so the conclusions of the study by Kroes et al.(2013) would support the claim that an increased viscosity is beneficial to the flushing process. The effect of higher velocities is harder to see in the case of flushing, since for the higher range of velocities, all oil is flushed from the pipe, regardless of the type of oil.

Folde(2017)[11] performed a sensitivity analysis using the dynamic pipeline simulation tool Ledaflow on the oil-water flushing process. This analysis showed that viscosity does not have that much of an effect, unless the viscosity of the displacing fluid is increased significantly. No significant changes were seen in the oil volume fraction when neither the water viscosity nor the oil viscosity was changed in an interval of ±40 % of the original value. Only when increasing the oil viscosity 50 times an increase in the displacement efficiency of 5 % was seen.

A frequently referred to equation in flushing is the effective bubble velocity in a pipe section, which uses findings of both Taylor(1950)[7] and Benjamin(1967)[8], $U_{\mathrm{E}} = U_{\mathrm{T}} \cdot sin(\phi) + U_{\mathrm{B}} \cdot cos(\phi)$. The only inputs in this relation are the bubble velocities for a vertical pipe($\mathrm{U_T}$) and a horizontal pipe($\mathrm{U_B}$), and the inclination of the pipe. These in turn are only a function of the density of the different fluids, the radius of the pipe and the gravitational constant. Both these studies arrive to their conclusions by ignoring the effects of viscosity and mixing of the fluids at the interface. Benjamin(1967) cites Zukoski(1966)[22] who states that "present work suggests that for Reynolds numbers greater than about 200, the propagation rates of air bubbles in inclined pipes are substantially independent of viscous effects". This value for the Reynolds number is reached in all flushing experiments treated in this thesis. Benjamin cautions readers that in practice, gravity currents are highly complex phenomena, generally featuring a great deal of turbulence and significant mixing of the two fluids.

A lot of studies agree with the conclusion that can be drawn from equation **??**, that when the oil density is higher, i.e. closer to that of the flushing medium, water, flushing efficiencies increase:

Folde(2017)[11] concluded their study that a higher oil density is beneficial to the flushing process.

Achmed et al.(2018)[13] found that for oil-water two-phase flow, a fluid with a higher momentum entrains a fluid with a lower momentum more effectively.

Kroes et al.(2013)[14] examined the effect of the salinity of water in two-phase flow with oil. The low salinity water they used had a concentration of 3g NaCL/l, the high salinity water had a concentration of 300g NaCL/l. The respective density values they reported for each of the solutions were $1.00 \cdot 10^3 kg/m^3$ and $1.15 \cdot 10^3 kg/m^3$. The mixture of high salinity water and oil showed more separation than that of low salinity water and oil. This increased separation has a negative effect on flushing. The higher the salinity of the water, i.e. the higher the density difference, the more pronounced this effect becomes.

A decisive conclusion on the effect of the oil viscosity on the flushing process remains to be found. The flow meter data suggests that the viscosity has a different effect on the flushing efficiency depending on the pipe inclination. As the four sub-figures in figure 4.17 in section 4.3 show, for a horizontal orientation the less dense, less viscous oil flushes more efficiently. The results for -2° and -5° show the opposite. Both the literature and the current experiments and simulations show that the closer the density of the oil is to that of the flushing medium, the more efficient the flushing process becomes.

7 | Conclusions

In this project multiple sets of experiments were performed to determine oil-water flushing efficiencies for various geometries, orientations, types of oil and superficial flushing velocities. Additionally simulations were performed using the dynamic multiphase flow simulation program OLGA.

In each of the experiments the experimental pipe section was filled with oil and subsequently flushed using four pipe volumes of water. Experiments were performed with two types of oil, Fuchs Renolin DTA7 oil having a density of 828.0 kg/m^3 and a kinematic viscosity of 12.16 mm2/s, and Mobil Velocite No. 10 oil having a density of 845.5 kg/m^3 with a kinematic viscosity of 44.79 mm2/s. These values were measured at a temperature of 20 °C.

Experiments in a straight pipe were performed with a superficial flushing velocity between 0.05 m/s and 1.5 m/s and an inclination between +2 ° and -5°. Another set of experiments was performed utilising two U-sections to determine the effect of the inclination of the pipe section in a range of 0° to -90° relative to the horizontal plane. These sets of experiments were performed for superficial water velocities of 0.05 m/s and 0.1 m/s. All pipes had an internal diameter of 56 mm. All experiments were performed at ambient pressure, at an ambient temperature between 15 °C and 20 °C.

The main conclusions that flowed from this project are:

- An increase in superficial water velocity is always beneficial to the flushing process. Less water is required, and the less time is needed to reach the same amount of flushing.
- At a velocity of 0.35 m/s, all oil is removed from the straight pipe at all considered inclinations. The bulk of the oil is flushed for velocities from 0.25 m/s upwards ($\geq$ 95%) for both types of oil and all considered orientations, leaving only a film of oil on the pipe walls.
- In a horizontal orientation, the lighter and less viscous Fuchs Renolin DTA7 oil is flushed more efficiently from the pipe compared to the Mobil Velocite No.10 oil. This effect diminishes for slightly negative inclined orientations and is reversed for an inclination of -5°.
- The critical pipe inclination for the oil-water flow to transition between stratified and mixed flow, occurs in a range of -7.5° to -20°, in a total range of 0° to -90° relative to the horizontal plane, for Mobil Velocite No. 10 oil flushed with a superficial water velocity of 0.1 m/s. In steeper inclinations, an increasing interfacial wave height induces mixing, increasing the flushing efficiency relative to the smaller inclinations.
- As used in this setup, the mass flow meter system gives superior data in comparison to the video data analysis. Video data could however still be of high value for calm flows, as well as for visual observations and for reference.
- Results obtained through the Coriolis mass flow meters are more accurate than results from the video data analysis. Disturbances at the oil water interface impede the video data accuracy, but the footage could still be valuable, e.g. by providing information on the wave frequency or height.
- The final flushing values are markedly underestimated for a horizontal inclination, and sharply overestimated for negative inclinations in the OLGA simulations. The OLGA simulations are useful however for e.g. sensitivity studies, where OLGA e.g. showed that the oil viscosity is of far greater influence on the flushing efficiency compared to the oil density.
- OLGA: For inclinations of -1°, -2° and -5°, increasing the viscosity of the oil, and increasing the density of the oil closer to that of the flushing medium, increases the flushing efficiency.

Next to these conclusions, the experimental data obtained in this work can be further used to validate tools for predicting oil flushing processes.

7.1 Recommendations for Future Research

Based on the work done in this project, several suggestions for future research arise, some of which are listed below.

- Extend the flushing study in the 0°- 90° range. Does the flushing transition point also lie around 10-15° for other superficial flushing velocities?
- A more theoretical approach was briefly looked into. Since the average oil velocity is relatively close to zero, certain relations for two phase flow are not valid, which makes applying closure relations for the holdup problematic. The possible relation of the water holdup to the Froude number could also be an interesting field of study. This could be the basis of a simple analytical model to predict oil-water pipe flushing.
- Extend the study on the property changes of oil mixed with water, on what kind of conditions cause the oil degradation seen in the current experiments, and measures to improve experimental conditions in future experiments.
- Extend the CFD study, possibly using another software tool to compare this to the already obtained flow meter-, video analysis- and OLGA simulation data. A suggestion would be: Is the influence that the oil viscosity have on the flushing efficiency, itself dependant on the superficial water flow velocity?
- Study the effects of transient flushing, stopping and starting halfway.
- As the shape and size of the interfacial waves are captured in the produced camera footage, this data can be used to study possible relations between the wave length or wave height and the flushing efficacy.

References

[1] *Net Zero by 2050*. Accessed: 06.2021. URL: iea.org/reports/net-zero-by-2050.

[2] Norway H.R. Skjoldal Institute of Marine Research Bergen. *Update report on North Sea conditions – 2nd quarter 2007*. Accessed: 05.2021. URL: na-basin.org/reports/NORSEPP.

[3] *Shell invests in PowerNap subsea tie-back in Gulf of Mexico*. Accessed: 06.2021. URL: shell.com/media/news-and-media-releases/2019/shell-invests-in-powernap-subsea-tie-back-in-gulf-of-mexico.html.

[4] H Mukherjee, JP Brill, and HD Beggs. "Experimental study of oil-water flow in inclined pipes". In: *Journal of Energy Resources Technology* (1981).

[5] P Vigneaux, P Chenais, and JP Hulin. "Liquid-liquid flows in an inclined pipe". In: *AIChE Journal* 34.5 (1988), pp. 781–789.

[6] P.V. Hemmingsen, A. Silset, and J. Sjöblom. "Emulsions of heavy crude oils. I: Influence of viscosity, temperature, and dilution". In: *Journal of dispersion science and technology* 26.5 (2005), pp. 615–627.

[7] R.M. Davies and G.I. Taylor. "The mechanics of large bubbles rising through extended liquids and through liquids in tubes". In: *Proceedings of the Royal Society of London. Series A. Mathematical and Physical Sciences* 200.1062 (1950), pp. 375–390.

[8] T. B. Benjamin. "Gravity currents and related phenomena". In: *Journal of Fluid Mechanics* 31 (2 1968), pp. 209–248. URL: http://journals.cambridge.org.

[9] "Hydraulic Guidelines - Part on Fluid - Fluid Displacement". In: *Restricted* ().

[10] M. Kazemihatami. *Experimental study of displacement of viscous oil in pipes by water*. Institutt for energi-og prosessteknikk - Master's Thesis, 2013.

[11] H. G. Folde. *Experimental and Numerical Study of Fluid Displacement in Subsea Pipe Sections Hanne Gjerstad Folde*. NTNU - Master's Thesis, 2017.

[12] L. Amundsen. *An experimental study of oil-water flow in horizontal and inclined pipes*. NTNU - PhD Thesis, 2011.

[13] S.A. Ahmed and B. John. "Liquid – Liquid horizontal pipe flow – A review". In: *Journal of Petroleum Science and Engineering* 168 (2018), pp. 426–447. ISSN: 0920-4105. DOI: https://doi.org/10.1016/j.petrol.2018.04.012.

[14] R. Kroes, L. Amundsen, and R. Hoffmann. *Crude oil-water flow in horizontal pipes*. NTNU - Master Internship Report, 2013.

[15] O. M.H. Rodriguez and R. V.A. Oliemans. "Experimental study on oil-water flow in horizontal and slightly inclined pipes". In: *International Journal of Multiphase Flow* 32.3 (2006). ISSN: 03019322. DOI: 10.1016/j.ijmultiphaseflow.2005.11.001.

[16] P. Abduvayt, R. Manabe, and N. Arihara. "Analisis of oil-water flow tests in horizontal, hilly-terrain, and vertical pipes". In: *SPE Annual Technical Conference and Exhibition* (2004). DOI: 10.2523/90096-ms.

[17] D. van Nimwegen H. Pereboom. *TNO 2021 R10838 - Experiments for oil flushing with water in a 2" pipe Phase I*. 2021.

[18] *Water hardheid Zuid-Holland*. Accessed: 12.2021. URL: perfectwater.nl/waterhardheid/zuid-holland/.

[19] *Water hardheid Rijswijk*. Accessed: 12.2021. URL: waterhardheid.nl/gemeente/rijswijk.

[20] D. van Nimwegen H. Pereboom. *TNO 2021 R11983 - Experiments for oil flushing with water in a 2" pipe Phase II*. 2021.

[21] *Surface roughness materials*. Accessed: 10.2021. URL: engineeringtoolbox.com/surface-roughness-ventilation-ducts-d_209.html.

[22] EE Zukoski. "Influence of viscosity, surface tension, and inclination angle on motion of long bubbles in closed tubes". In: *Journal of Fluid Mechanics* 25.4 (1966), pp. 821–837.

A| Appendix

A.1 Detailed Description of Performing of the Experiments

This section describes the steps that need to be taken in order to recreate an experiment. The level of detail is such that possible future experiments by others can be as close to the current experiments as possible.

Each experiment consists of three different flushing stages in sequence. The first stage is used as a benchmark and reference for the second stage. In the first stage the water-filled pipe is flushed with four pipe volumes of just water. In the second stage this water is removed from the pipe after which the pipe is filled with oil. After this filling the actual measurement is performed by flushing the pipe with the same flow of water that flushed the pipe in stage I. In the third stage the pipe, partly filled with remnants of oil and partly water, is flushed with four pipe volumes of water at a superficial water velocity of 1.5 m/s, which concludes one experiment.

Below this same process is elaborated in more detail. All parts of the setup referenced in the procedure below are presented in figure 3.2.

Stage I

Performing the reference measurement:

1. Set the inclination of the pipe section to the preferred value for this experiment.
2. Set the outflow three way valve at the end of the pipe section towards the flow meter.
3. Open the taps below the collection vessel to empty it.
4. With an open pneumatic inlet valve, adjust the circulation loop pump and flow control valve to such setting on the control panel that the preferred water flow velocity is reached.
5. After turning off the circulation loop pump and closing the pneumatic valve, wait until the collection vessel has emptied, and close the taps below the tank.
6. Set the timer on the control panel for a time such that, with the set superficial water velocity, four pipe volumes of water are flushed through the pipe.
7. Arm the Dewetron data acquisition system.
8. Trigger the Dewetron system by starting the video recording.
9. Start the circulation loop pump and start the timer.
10. Once the timer has reached its set value, the pneumatic valve will automatically close.
11. Stop the circulation loop pump.
12. Once the weight reading of the scale under the collection vessel has stabilised, stop the data collection on the Dewetron.
13. Read off the height of the water level in the collection vessel.

Stage II

Preparing the setup by emptying the pipe section and successively filling it with oil:

1. Raise the upstream part of the pipe section as high as possible(to a pipe inclination of -5°).
2. Open the taps below the collection vessel.
3. Direct the outflow valve at the end of the pipe section away from the flow meter.
4. Open the water outlet between the outflow valve at the end of the pipe section.
5. Aid the outflow of water by opening the pneumatic air supply at the upstream end of the pipe.
6. Once all water has exited the pipe section, close the water outlet.
7. Lower the upstream part of the pipe section as low as possible(to a pipe inclination of +5°.
8. Open the valve of the oil inlet and start the barrel pump.
9. As soon as oil flows out of the gooseneck at the end of the pipe section, stop the barrel pump and close the oil inlet valve.
10. Wait for any/all air bubbles to drift to the higher side of the pipe section and out of the gooseneck, adding some more oil to the pipe if necessary.

Performing the actual measurement:

1. Set the inclination of the pipe section to the preferred value for this experiment. In case of the straight pipe adjust the total length, in case of the U angle variation only adjust the second U section.
2. Set the outflow three way valve towards the flow meter.
3. Close the taps below the collection vessel once this has emptied fully.
4. Make sure the entries for the circulation loop pump, the flow control valve and the timer are the same as in stage I, step 4.
5. Arm the Dewetron data acquisition system.
6. Trigger the Dewetron system by starting the video recording.
7. Start the circulation loop pump and start the timer.
8. Once the timer has reached its set value, the pneumatic valve will automatically close.
9. Stop the circulation loop pump.
10. Once the weight reading of the scale under the collection vessel has stabilised, stop the data collection on the Dewetron. In case of the U angle variation, wait until the oil from the vertical pipe section has floated to the horizontal section before terminating the recording.
11. Read off the height of the surface level in the collection vessel.

Stage III
Performing the final flush:

1. Open the taps below the collection vessel.
2. Set the circulation pump and the flow control valve such that 1.5 m/s superficial water velocity is reached. Note that the water flow cannot be started at this moment as this will interfere with the experiment. The values that were used in this study with the stated setup were 87% of the circulation pump capacity and an orifice setting of 87% out of 100% for the flow control valve.
3. Set the timer such that four pipe volumes of water will be flushed at the superficial water velocity of 1.5 $m \cdot s^{-1}$.
4. Close the taps below the collection vessel.
5. Arm the Dewetron data acquisition system.
6. Trigger the Dewetron system by starting the video recording.
7. Start the circulation loop pump and start the timer.
8. Once the timer has reached its set value, the pneumatic valve will automatically close.
9. Stop the circulation loop pump.
10. Once the weight reading of the scale under the collection vessel has stabilised, stop the data collection on the Dewetron.
11. Read off the height of the surface level in the collection vessel, when reading of the levels of the separate phases is possible.

With this last stage the experiment for this angle of orientation and flushing velocity is performed. The pipe is completely filled with water again, without any oil left in the pipeline.